Translating nanotech inventions: Nanomaterial-based solutions for drinking water, human blood purification, and improved root canal fillers

Wendelin J Stark

Functional Materials Laboratory, Institute for Chemical and Bioengineering, Department of Chemistry and Applied Biosciences, ETH Zurich, CH.

What makes a laboratory-level invention or concept successfully go to the patient? The incredible pace of current discovery in biochemistry, medicine and biomaterials research stays in contrast to a more conservative change in clinical procedures and available materials to the treating/responsible surgeon.

After 7 spin-off companies were founded from our laboratory, we realized that commercial chances depend on rapid identification of clear, well-defined markets, rather than a pure scientific advance. This *a priori* trivial result, at least from a business perspective, is a hard learning for most young scientists. In this presentation, I would like to show how young (Ph.D.) scientists can became entrepreneurs, through rapid interaction with non-university topics.

Based on early work in nanotoxicology and safety (***Environ. Sci. Technol.***, 39 (2005): 9370; 40 (2006): 4373; 41 (2007): 4158) we defined precautionary principles for safe use of nanoparticles in products (***Angew. Chem.,*** 50 (2011): 1242; ***Nature Nanotechn.***, 7.8 (2012): 520). We discovered improved adhesion of plastics to human (wet) tissue when filled with nanobioglass (***Biomaterials***, 29 (2008): 1750; 31 (2010): 2806; 32 (2011): 8915) which lead to improved dental root canal fillers. Blood cleaning with biocompatible, ultrastrong nanomagnets (***Nano-scale***, 5 (2013): 8718), customized nanoparticles, clean water filters (Drinkpure) and ecosystem food web labels and product tagging (**ACS Nano**, 9 (2015): 9564) were results of knowing what is safe and what not.

Biography

Prof. W. J. Stark (1976) develops nanomaterial-based solutions for industrial and medical markets. He has commercialized over 20 products and cofounded seven companies: Turbobeads GmbH makes magnetic chemicals (partially distributed by Sigma-Aldrich) and diagnostic metal nanomagnets. Nanograde AG provides over 1 Million customized nanoparticles for organic photovoltaics, sensors, and the chemical industry. FlamePowders AG has made large scale oxide nanopowders (stopped operation in 2006). (Bio)medical companies include smartodont GmbH (bioactive polymer implants, e.g. root canal treatments, 3D printed model teeth), novamem GmbH (water purification, nanofiltration), and Zurich Biomaterials GmbH ("bone wool", an easy to shape dental and maxillofacial biomaterial). Haelixa GmbH provides encapsulated DNA tags for product identification and sub-micron size sensors.

Prof. Stark has formulated key mechanisms in nanomaterial/biology interactions that today support the regulatory basis for industrial nanotech products in Switzerland. He is inventor in > 30 patents and author of > 250 scientific articles. He is one of the most cited scientists globally (Thomson Reuters), and invited member of the New York Academy of Sciences.

From muscle to endothelium and back

Katrien De Bock

Laboratory of Exercise and Health, Institute of Movement Sciences (D-HEST), ETH Zürich

Skeletal muscle is a critical organ for the maintenance of glucose homeostasis. This glucose is delivered to the muscle via blood vessels, formed by nicely aligned endothelial cells (ECs). Whenever muscle activity or exercise is initiated, blood flow into the muscle is enhanced rapidly. Next, the formation of new vessels, a process termed angiogenesis, is initiated. Angiogenesis is an early adaptive event in the response to exercise, but the molecular mechanisms driving de novo blood vessel growth following exercise are not yet understood.

During my PhD in muscle metabolism and my postdoc in angiogenesis, I have gathered the expertise and knowledge to investigate this outstanding research question. During this lecture, I will give an overview about exercise, angiogenesis, my research career, and how some unexpected events have changed it forever.

Cell based therapies for the heart

SP Hoerstrup

Institute for Regenerative Medicine, University of Zurich, CH

Cardiovascular disease represents a major cause of morbidity and mortality worldwide accounting for the death of numerous patients. Cell-based therapy concepts comprising regeneration of damaged organs by e.g. transplanted stem cells and replacement of diseased/malformed structures by tissue engineered, living implants represent promising novel treatment modalities, ultimately aiming at “restitutio ad integrum” instead of repair. First successful clinical applications such as stem cell therapies for myocardial infarction have recently been demonstrated. To regenerate, the myocardium various cell sources including several categories of stem cells are being examined and the optimal cell delivery format using 3-D technologies as well as the most suitable route for cell delivery (intracoronary vs. intramyocardial) are currently under investigation. Next, cardiovascular tissue engineering has been demonstrated to be a promising concept to generate living, autologous cardiovascular structures with the ability to remodel and to grow which may be particularly beneficial for children. However, although these regenerative concepts have shown great potential in experimental studies, the safe and effective translation into a widespread clinical setting is still limited. Furthermore, the currently utilized ``classical`` approaches are still too complex with regards to logistical and financial effort. Therefore, significant simplification is needed and in particular, so called off-the-shelf concepts may represent an attractive option to overcome the current problems.

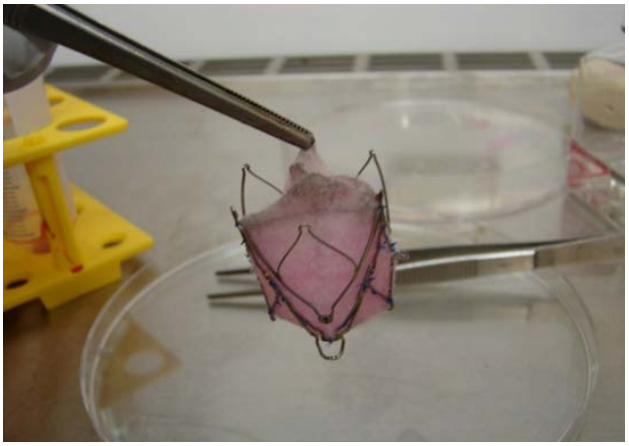

Fig. 1: Engineered, aortic heart valve for transcatheter implantation. (Emmert & Hoerstrup et al., Eur J Cardiothorac Surg. 2014 Jan;45(1):61-8)

Glycosaminoglycan-based polymer matrices for medical technologies

Carsten Werner

Leibniz Institute of Polymer Research Dresden, Max Bergmann Center of Biomaterials and TU Dresden, Center for Regenerative Therapies, Dresden, Germany

Sulphated glycosaminoglycans (GAGs) govern important functional characteristics of the extracellular matrix (ECM) in living tissues. Incorporation of GAGs into biomaterials opens up new routes for the presentation of signaling molecules, providing control over development, homeostasis, inflammation and tumor formation and progression. We report recent progress in the design of modular polymer networks made of multi-armed poly(ethylene glycol), GAGs and peptides by covalent and non-covalent conjugation schemes. Theory-driven concepts for the decoupling of biophysical and biochemical characteristics and advanced processing technologies will be highlighted. Approaches to the application of the resulting materials in regenerative therapies as well as in established medical technologies will be given.

Carsten Werner, Leibniz-Institut für Polymerforschung Dresden e.V., Hohe Str. 6, 01069 Dresden, Germany (phone: +493514658531; fax:+493514658533; e-mail: carsten.werner@tu-dresden.de). www.ipfdd.de

Carbon reinforced carbon: Its potential as material for orthopaedic applications

R Lerf[1], C Witt[2], D Delfosse[1],

[1] *Mathys Ltd Bettlach, Bettlach, CH.* [2] *Mathys Orthopädie GmbH, Mörsdorf, DE.*

INTRODUCTION: Pyrolytic carbon has been in clinical use for implants for decades. It exhibits favourable tribological behaviour combining low friction and low wear when articulated against itself. Therefore, pyrocarbon was first used in artificial heart valves and finger joint replacement [1, 2]. Recently, humeral head implants with articulating surface made from pyrocarbon were clinically introduced [3]. Due to its inherent brittleness, the use of pyrocarbon as bearing material is restricted to small joints. Aim of the present study was to evaluate if carbon reinforced carbon (C/C), owing to the mechanical reinforcement, could broaden the field of orthopaedic applications compared to pyrocarbon.

METHODS: The mechanical strength of the C/C material was characterised by a biaxial flexural bending test according ISO 6474-1 on C/C disk samples Ø 36 mm, H 2.1 mm. - Three C/C shoulder head samples, size 39/13, articulating against vitamin E stabilised, highly cross-linked UHMWPE (vitamys®) underwent a shoulder simulator study up to 10^6 cycles. Maximum force applied was 1.0 kN with diluted calf serum at 37°C as lubricant. Gravimetric measurements were done before start, at 0.1, 0.5 and 1 million. - The coefficient of friction (CoF) of C/C disks (R_a: 0.045 µm) against cartilage was analysed by a reciprocal cartilage wear tester. The test was conducted in cell culture medium at room temperature for 4 h and 12 h using bovine cartilage. Details of the test setup are published elsewhere [4]. - All test data is compared to the corresponding test results with Al_2O_3 ceramic [5].

RESULTS: The biaxial flexural strength of C/C was 294 ± 22 MPa compared to 422 ± 36 MPa for Al_2O_3 ceramic (Table 1). The fracture behaviour was brittle and similar to ceramic. The wear rate in the shoulder simulator compares as follows: C/C head against E-XLPE glenoid 13.6 ± 2.7 mg/10^6 cycles vs. Al_2O_3 – E-XLPE 9.97 ± 0.95 mg/10^6 cycles. After testing, only minor scratching of the C/C articulation surface was observed. The reciprocal wear test on cartilage yielded a CoF of 0.74 ± 0.01 and 0.72 ± 0.06 for C/C after 4 h and 12 h, respectively. The CoF of cartilage against Al_2O_3 was 0.35 ± 0.05 after 4 h.

Table 1. Results of the biaxial flexion test, the shoulder simulator study and the friction test against cartilage (Std Dev = standard deviation).

	Biaxial flexion		**Simulator study**	
Material	Strength [MPa]	Std Dev [MPa]	Wear rate [mg/Mcyc.]	Std Dev [mg/Mcyc.]
C/C	294	22	13.6	2.7
Al_2O_3	422	36	9.97	0.95
	Reciprocal cartilage wear test			
	CoF 4h	Std Dev	CoF 12h	Std Dev
C/C	0.74	0.01	0.72	0.06
Al_2O_3	0.35	0.05	n.a.	n.a.

DISCUSSION & CONCLUSIONS: C/C behaves as brittle as a ceramic material, but its mechanical strength is 30 % lower than that of Al_2O_3 ceramic. The wear rate of the C/C composite measured in the shoulder simulator against E-XLPE is similar, but not lower, compared to an Al_2O_3 ceramic head. The CoF against cartilage (0.74 ± 0.01) is twice as high compared to the same test with Al_2O_3 (0.35 ± 0.05) and also surprisingly high compared to other orthopaedic materials, e.g. CoCr alloy 0.37 ± 0.06, UHMWPE 0.40 – 0.59, PEEK 0.60 ± 0.02 or PCU 0.10 ± 0.05 [4]. Our results agree well with another cartilage study, comparing knee hemiprostheses made from different materials in a rabbit model [6]. No significant difference in comparison to CoCr and zirconia ceramic was found, but a large scatter in the pyrocarbon group and a tendency towards a higher CoF than CoCr. All in all, -C/C composites seem to have limited potential as material for orthopaedic application.

In vitro model for developing a 3rd generation ceramic dental implant surface

E Müller[1], M Rottmar[1], S Guimond[1], U Tobler[1], M Stephan[2], S Berner[2], K Maniura[1]

[1] *Biointerfaces, Empa, Swiss Federal Laboratories for Material Science and Technology, St. Gallen, CH,* [2] *Institut Straumann AG, Basel, CH*

INTRODUCTION: Materials surface characteristics such as roughness and chemistry are known to be decisive parameters for effective osseointegration of dental implants. Upon implantation, the implant comes in contact with the patient's blood and the cells from the surrounding tissue will interact with the adsorbed proteins. However, the impact of blood coagulation on surfaces on subsequent implant osseointegration is not considered as relevant parameter in most cell culture studies.

Titanium and to some extent titanium alloys have been the "gold-standard" for dental implant systems. Unfortunately, in case of thin gingival biotype or buccal bone loss a greyish region may appear through the gingiva. Ceramics of yttrium-stabilized zirconia are promising alternatives but current surface modifications fail to recreate the degree and dynamics of osseointegration of state-of-the-art titanium surfaces. Therefore, an *in vitro* model was developed to study the early interaction with blood and how this influences osteogenic fate decisions of human primary bone progenitor cells (HBCs). Furthermore, zirconia surfaces (ZLA) were evaluated with the *in vitro* model and compared with well-established titanium surfaces (SLA® and SLActive®).

METHODS: The concept of the *in vitro* model is described by Kopf et al.[1] In brief, whole human blood from healthy volunteers was partially heparinized (0.5 IU ml^{-1}). Material samples were placed into a custom device made out of polytetrafluoroethylene (PTFE) and incubated with blood under exclusion of air for 10 min at RT. Blood was carefully removed and samples rinsed with phosphate-buffered saline (PBS). The samples were fixed and stained for microscopy analysis or further used for cell experiments. HBCs were seeded onto samples with and without prior incubation in blood. After 21-28d of culture cell numbers were determined and osteogenic differentiation potential analysed via stainings for mineralization as well as quantification of Ca^{2+} normalized to cell number.

RESULTS: Independent of blood pre-incubation, significantly higher levels of Ca^{2+} were observed on SLActive® surfaces in comparison to SLA® (Fig. 1A). For SLActive® surfaces, blood incubation promoted an even stronger mineralisation of the HBCs. Comparing osteogenic differentiation of HBC on blood pre-incubated titanium and zirconia (ZLA) surfaces, higher levels of Ca^{2+} could be observed compared to standard titanium surface SLA® (Fig. 1B). All three surfaces are roughened and feature characteristic macro and micro topography, which differs in overall roughness and structural features between the ceramic and the titanium surfaces. The highest level of mineralization was observed for the super-hydrophilic SLActive® surface.

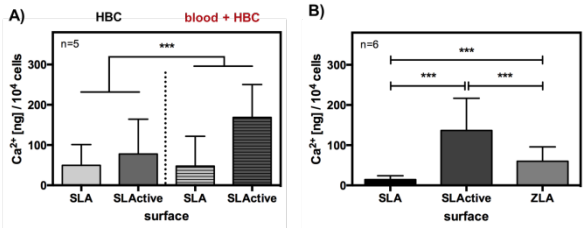

Fig. 1: A) Calcium concentration after 21d of culture on top of titanium surfaces with and w/o prior incubation in whole blood. B) Calcium levels of titanium and zirconia surfaces incubated in blood prior cell culture.

DISCUSSION & CONCLUSIONS: The established advanced *in vitro* model for osseointegration, encompassing a blood incubation step prior to HBC culture, mimics the *in vivo* situation during implantation and can be used to evaluate both titanium and zirconia surfaces. Interestingly, ZLA displayed the strongest blood coagulation but the osseointegration potential in in vitro studies was higher than SLA but lower than SLActive surfaces, which may be attributed to differential adsorption of key cytokines to the fibrin/sample surface.

ACKNOWLEDGEMENTS: The Commission for Technology "CTI Medtech" is acknowledged for financial support of the project under the contract 16873.2.

Macrophage polarization by titanium dioxide (TiO_2) particles: size matters

‡AD Schoenenberger[1,2], ‡A Schipanski[1], V Malheiro[1], M Kucki[3], JG Snedeker[2], P Wick[3], K Maniura-Weber[1,*]

[1] Biointerfaces, Empa, Swiss Federal Laboratories for Materials Science and Technology, St. Gallen, CH. [2] Department of Orthopaedics, Balgrist Hospital, University of Zurich, Zurich, CH.; Institute for Biomechanics, ETH, Swiss Federal Institute of Technology, Zurich, CH. [3] Laboratory for Particles-Biology Interactions, Empa, Swiss Federal Laboratories for Materials Science and Technology, St. Gallen, CH

INTRODUCTION: Life lasting stability of the implant bone interface is a clinical challenge. Aseptic loosening of total joint replacements associates with high health costs and reduced quality of life. Implant loosening originates from periprosthetic osteolysis, caused by the continuous release of wear particles that induce an inflammatory response driven by monocytes and macrophages. Macrophages, the surveillance cells of our immune system, are among the first cells in contact with foreign body/implant derived particles.[1] Several studies have documented the effect of polyethylene or PMMA particles in the micrometer range on macrophage polarization, observed to associate with an increased production of inflammatory cytokines.[2,3] Apart from the micrometer range, abundant TiO_2 wear particles in the nanometer range were observed in the peri-implant region[4], and their effect on macrophage polarization remains unknown. This study thus explored the effect of TiO_2 particle size on macrophage polarization.

METHODS: THP-1 monocytes previously differentiated to macrophages (M0), were exposed to different concentrations (4×10^4 - 4×10^6 particles/mL) and sizes (<100 nm, TiO_2-N & <5 μm, TiO_2-M (Fig.1A, B)) of TiO_2 particles, none of which were observed to significantly affect cell viability. Macrophage polarization from M0 towards either the pro-inflammatory (M1) or the anti-inflammatory (M2-like) phenotype was assessed based on differences in gene- and protein-expression levels, using qRT-PCR, e.g. surface markers CD197 (M1) and CD206 (M2-like), and ELISA.

RESULTS: The main finding of this study is the pronounced effect of TiO_2 particle size on macrophage polarization. Whereas micro-sized particles induced M1 polarization (suppression of CD206 & enhancement of CD197, Fig. 1C), although only at the highest concentration, nano-sized particles did not affect polarization at any of the applied concentrations.

Fig. 1: (A) SEM image showing the interaction of a macrophage with TiO_2-M particles (B) Magnification of

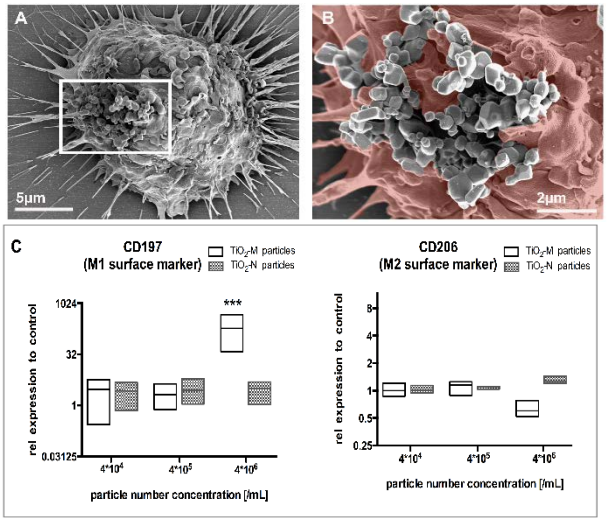

square in A (C) M0 macrophages were exposed to $4x10^6$ particles/mL of micro- (white bars, TiO_2-M) and nano-sized (grey bars, TiO_2-N) TiO_2 particles.

DISCUSSION & CONCLUSIONS: In this study, particle size was found to have a significant impact on their ability of TiO_2 particles to induce macrophage polarization. Our experiments show that only larger TiO_2 particles induce a pro-inflammatory M1 phenotype. This suggests that the micron-sized fraction of wear particles contributes to Ti implant loosening by promoting local inflammation through macrophage activation. In conclusion, TiO_2 particle size is a determinant factor in driving the biological response of macrophages, which can guide the design of new biomaterials, which aim to avoid wear-induced release of micron-sized particles.

ACKNOWLEDGEMENTS: The contribution of Liliane Diener (TEM) and is highly appreciated.

Deciphering hematopoietic stem cell niche factors in bioengineered human bone marrow models *in vivo*

Q Vallmajó-Martín[1,2], A Negro[2], M Lütolf[2], M Ehrbar[1]

[1] *Ehrbar Lab, Department of Obstetrics, UniversitätsSpital Zürich, CH.* [2] *Laboratory of Stem Cell Bioengineering, Institute of Bioengineering, École Polytechnique Fédérale de Lausanne, CH*

INTRODUCTION: Sufficient numbers of hematopoietic stem cells (HSCs) needed for bone marrow transplantations remains a major challenge in medicine today. HSCs expanded *in vitro* rapidly lose their regenerative capacity likely due to the lack of niche-derived signals comprising molecular and cellular components [1]. Identification of critical hematopoietic niche components necessitates both the generation of more tractable *in vivo* models and, in parallel, novel approaches for heightened throughput in screening such systems *in vivo*. We have previously reported on a blank biomaterial that can be decorated with different growth factors and cell types known to be present in the niche *in vivo* [2]. Here, we present a novel device, which allows the screening of multiple unique niche factor conditions in a single mouse with the aim to establish a minimalist human bone marrow model.

METHODS: Functionalized biomimetic polyethylene glycol (PEG) hydrogels were laden with human mesenchymal stem cells (hMSCs) and supplemented with or without bone morphogenetic protein-2 (BMP-2). These PEG gels were polymerized directly in the individual wells of novel multiplexing polydimethylsiloxane (PDMS) devices (Fig 1A). Next, the screening devices containing PEG hydrogels were subcutaneously implanted in immunocompromised mice (4x per animal). At 8 weeks, the devices were explanted and analyzed for bone and bone marrow formation by microCT, histology and FACS.

RESULTS: Screening devices featuring 2mm diameter wells were shown to be the minimal size for niche formation allowing 8 conditions to be screened per implantable site (32 different conditions per mouse). MicroCT analysis revealed mineralization in all wells containing gels with hMSCs and BMP-2 (Fig 1B, yellow circle), but not in those lacking the growth factor (green circle). Histological analysis corroborated these findings. Hydrogels containing hMSCs and BMP-2 developed into bone marrow-like constructs including a typical bone shell filled with marrow and trabecular bone structures (Fig 1C, yellow). Ultimately, long-term HSC enrichment in the constructs containing cells and BMP-2 was confirmed by FACS analysis on the recruited murine cell population. These results indicate the formation of a functional ectopic niche in BMP-2 and cells-laden gels.

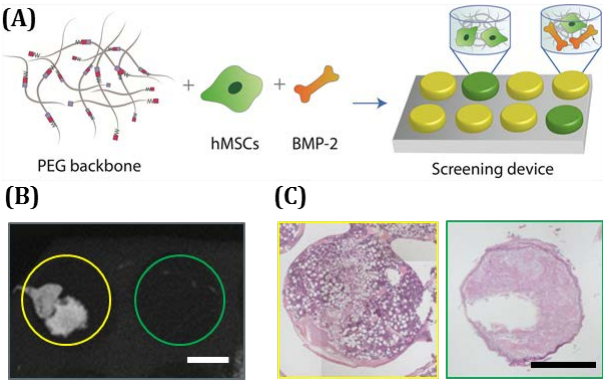

Fig.1: In vivo HSC niche model screening platform. (A) PEG precursors, different cell types, and growth factors are mixed inside the individual wells of the PDMS device. (B) MicroCT analysis depicts bone formation in wells with hMSCs and BMP-2 (yellow circle), and lack of mineralization in the wells without BMP-2 (green circle). (C) H&E stainings corroborate bone formation in cell-laden gels with BMP-2 (yellow) and fibrous tissue in absence of BMP-2 (green). Scale bars: 1mm.

DISCUSSION & CONCLUSIONS: An implantable screening device was developed to optimize hydrogel conditions, cell type, and soluble factors to support bone marrow niche formation *in vivo*. Up to 32 unique conditions could be tested per mouse. Results indicated the need for hMSCs and BMP-2 in hydrogel constructs for recruitment of murine HSCs. This device represents a powerful new tool for heightened *in vivo* screening of tissue engineering constructs with a broad range of applications.

ACKNOWLEDGEMENTS: This work was funded by the Swiss National Science Foundation grant 153316.

Steering electrospun fiber surface topography by use of Hansen solubility parameters and environmental conditions

G Yazgan, V Tyagi, G Rotaru, M Rottmar, RM Rossi, K Maniura-Weber, G Fortunato

Empa, Swiss Federal Laboratories for Materials Science and Technology, St. Gallen, CH

INTRODUCTION: The high surface to volume ratio of electrospun fibers facilitates many industrial and biomedical applications in the fields of tissue engineering, drug delivery, catalysis and sensors[1,2]. For surface sensitive applications it is even possible to change the fiber surface topography by adjusting the solution and process parameters used for electrospinning. However current approaches lack systematic understanding of such surface alterations. In the current study, we utilized Hansen solubility parameters (HSP)[3] to assess good and non-solvents for polycaprolactone (PCL) and we investigated these solution parameters at different relative humidity conditions with respect to morphological fiber evolution. We further aimed to understand the role of solvent evaporation rate, changes in the polymer solubilities due to solvent evaporation and the environmental conditions on the electrospun fiber surface topography.

METHODS: Hansen solubility parameters in practice (HSPiP) software[4] was utilized to evaluate the degree of solubility of PCL in dichloromethane (DCM), chloroform ($CHCl_3$), methanol (MeOH), dimethylsulfoxide (DMSO), ethanol (EtOH) and Acetonitrile in terms of the HSP distance (R_a) between the polymer and the solvent, which determines their compatibility.

$$R_a=(4(\delta^P_D-\delta^S_D)^2+(\delta^P_P-\delta^S_P)^2+(\delta^P_H-\delta^S_H)^2)^{1/2} \quad (1)$$

where dispersive interactions (δ_D), polar interactions (δ_P) and hydrogen bonds (δ_H) are in units of $MPa^{½}$ in the 3-D Hansen space. By electrospinning**,** solutions of 15% w/v PCL in $CHCl_3$:MeOH or $CHCl_3$:DMSO were processed into fibrous nonwovens at 12, 35 and 55% relative humidity (RH) and 20°C. WAXD and SEM allowed the characterisation of the fiber meshes. HSPiP was further used to explain the influence of MeOH and DMSO evaporation rate and the consequent solubility change in terms of thermodynamic instability of the polymer jet.

RESULTS: *Experimental results* - Average diameter of fibers electrospun from the mixture of $CHCl_3$:DMSO was smaller than $CHCl_3$:MeOH at each RH. At 12% RH, smooth electrospun fiber surfaces were obtained from both solution mixtures. With increasing RH, surface pits appeared on the fibers electrospun from $CHCl_3$:MeOH mixture whereas the ones electrospun from $CHCl_3$:DMSO mixture were obtained with irregular and more inter-connected surface topographies (Fig 1). The polymer crystallinity was found to be similar for all of the samples.

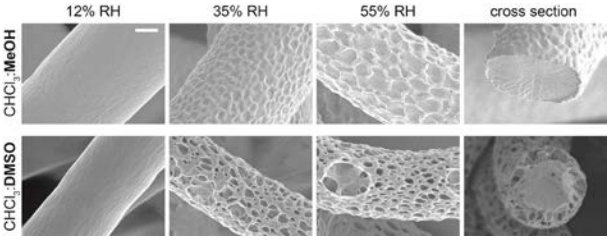

Fig. 1: SEM micrographs of electrospun fibers from mixtures of $CHCl_3$:MeOH (upper row) and $CHCl_3$:DMSO (lower row) at 12, 35 and 55% RH and the cross sections at 55% RH (scale bar 1μm).

Theoretical results - Based on the HSPiP calculations, DCM and $CHCl_3$ were good solvents whereas the remaining were non-solvents for PCL. Evaporation rate of $CHCl_3$ is closer to MeOH in comparison to DMSO. Upon evaporation, the mixture of $CHCl_3$:DMSO showed a higher decrease in PCL solubility with the increase in RH in comparison to $CHCl_3$:MeOH. This effect was pronounced by the increase of DMSO amount in the mixture.

DISCUSSION & CONCLUSIONS: Based on the evaporation rate of the non-solvent and the ratio between the solvent and the non-solvent, we were able to tailor the fiber morphology from smooth to porous with a gradient in the pore size and shape at controlled temperature and relative humidity. In future, steering surface topographies could be exploited for surface sensitive applications involving protein adsorption, drug delivery and cell-material interaction.

Mechano-sensitive liposome-containing hydrogel: towards an intra articular on-demand drug delivery system

E. Stalder[1], A. Zumbuehl[1]

[1] *Department of Chemistry, University of Fribourg, Fribourg, Switzerland*

INTRODUCTION: Osteoarthritis is a degenerative disease affecting the synovial joints and is the most common cause of chronic joint pain. Current treatments range from physical therapy to complete joint replacement. The core of the treatments consists of parenteral and/or oral administration of painkiller with all the known side effects.[1]

Here, we developed a mechano-sensitive *in situ* crosslinking hydrogel system containing liposomes. The aim is a local, on-demand release of a painkiller thus limiting side effects.

Periodate oxidized dextran makes a Schiff base formation reaction with both an amine bearing liposome (i.e. containing the aminolipid DPPE) and polyethyleneimine (PEI) to create a polymer network that contains covalently bound liposome. Upon compression, the network will deform and the active forces will break open the liposomes allowing them to release their cargo (see Fig 1).

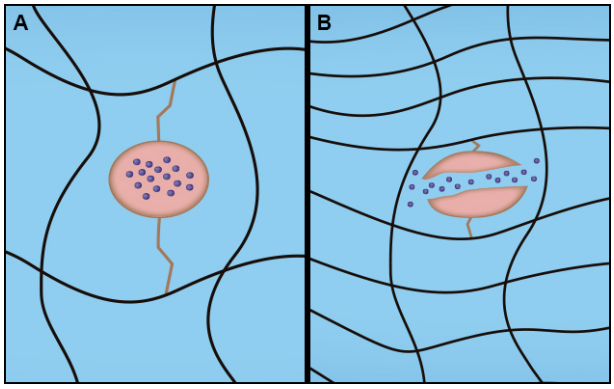

Fig. 1: Schematic representation of the liposome-hydrogel system. (A) In the relaxed state (no stress applied to the gel) the liposomes are linked to the polymer backbone and act as a drug reservoir. (B) In the stressed state (gel stressed by compression) the polymer network deforms leading to liposome disruption.

METHODS: Dextran was oxidized with sodium periodate according to a modified literature procedurel.[2] The degree of oxidation was determined by titration with hydroxylamine hydrochloride.[3]

Large unilamellar liposomes are formulated by extrusion.[4] The fluorescence marker sulforhodamine B in the outer buffer was removed by size exclusion column chromatography followed by dialysis.

The gel samples are prepared by mixing equal volumes of DextCHO (20% w/v) and liposome suspension (20 mg/mL) containing PEI (1.25% w/v). The gel samples were stressed using a tensile tester (Zwick Z010) in compression mode.

RESULTS: Preliminary results for $DextCHO_5$ (dextran with 5% of oxidized glucose units) compressed 20 times at a 30% crush show a large difference in the excess fluorescence release between inert liposomes (DPPC) and reactive liposomes containing 20% of reactive DPPE (see Table 1).

Table 1. Excess fluorescence for DPPC and DPPC/DPPE liposomal hydrogels.

	DPPC liposomes	DPPC/DPPE liposomes
Excess fluorescence	0.07%	14%

DISCUSSION & CONCLUSIONS: The preliminary results indicate that the concept works: inert liposomes are not affected by the stress put on the gel, contrary to contrary reactive liposomes are disrupted under stress and release a sulfo-rhodamine B marker. Following the promising initial results we will focus on studying the factors that influence the release of the fluorescent marker from liposomal hydrogels under conditions found in synovial joints.

ACKNOWLEDGEMENTS: The authors thank the Swiss National Science Foundation (PP00P2_138926/1) and the University of Fribourg for financial support.

Transferring 3D cell biology to synthetic environments: Microvascularization in PEG hydrogels

U Blache[1], S Metzger[1], Q Vallmajo-Martin[1], I Martin[2], M Ehrbar[1]

[1] *Laboratory for Cell and Tissue Engineering, Division of Obstetrics, University Hospital Zurich, Zurich, Switzerland*

[2] *Department of Biomedicine and Department of Surgery University Hospital Basel, Basel, Switzerland*

INTRODUCTION: Engineering tissue-like environments for the in vitro usage has become an important topic in cell biology due to the unique features of tissue that can not be recreated in 2D. Endothelial cells (EC), for instance, can self-assemble into real lumenized microvascular structures in a 3D environment but not on flat 2D surfaces. For the de novo formation of 3D vascular structures (vasculogenesis) extracellular matrix (ECM) derived protein hydrogels have been used and indeed brought tremendous knowledge to vascular biology Davis [l]. However, the drawback of ECM hydrogels is that they can trigger biological processes by themselves and are barley tunable. To overcome this limitations synthetic hydrogels such as poly(ethylene glycol) (PEG), which are engineered with fully defined functional modules can be used. Here, we combine a 3D PEG system with human endothelial cells (ECs) and human mesenchymal stem cells (MSCs) toward the establishment of a synthetic microvascularized tissue-like environment.

METHODS: TG PEG hydrogels are formed by the cross-linking of 8-PEG-MMPsensitive-Lys and 8-PEG-Gln precursors via FXIIIa transglutamination [2]. The cell adhesion peptide Lys-RGD is cross-linked into the gel at the same time. ECs and MSCs are 3D encapsulated in TG-PEG hydrogels during the gelation process at a 1:1 ratio and cultured for 14 days. The resulting microvasculature structures were analyzed in vitro or subcutaneously implanted into immunocompromised mice to evaluate their in vivo functionality.

RESULTS: In these synthetic hydrogels MSCs promote the in vitro formation of a stable microvascular networks by ECs (an example of microvascular structures is depicted in Fig.1). Moreover, the resulting microvascular networks are functional in vivo as they inosculate in the host vasculature when implanted subcutaneously in immunocompromised mice.

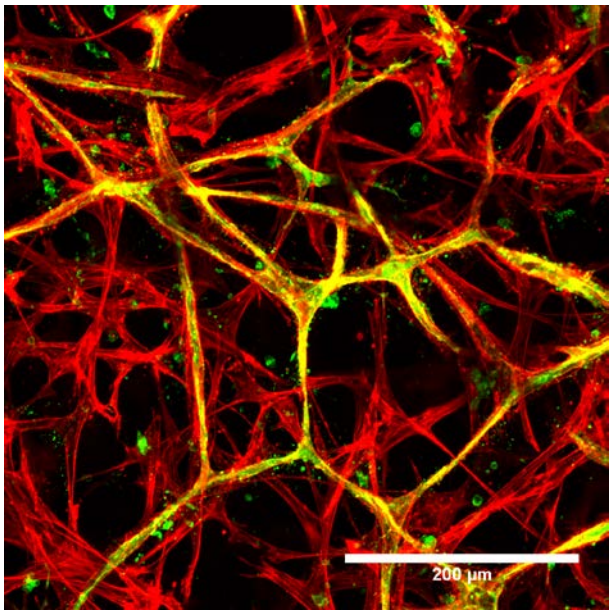

Fig. 1: Microvascularization in PEG hydrogels after 14 days of in vitro culture revealed by immunofluorescence of CD31 staining for ECs (green) and F-Actin staining for all cells (red), scale bar 200 µm.

DISCUSSION & CONCLUSIONS: We have established a 3D tissue model for the formation of microvascular tissues in a synthetic environment. In this set-up MSC support and promote ECs to self-assemble into microvascular structures. Moreover, by also making use of the stem cell potential of MSCs we envision to obtain specific vascularized tissue units in vitro.

ACKNOWLEDGEMENTS: This research has received funding from the People Programme (Marie Curie Actions) of the European Union's Seventh Framework Programme FP7/2007-2013/ under REA grant agreement No. 607868 (iTERM).

How surface wettability drives ligand assembly and stem cell osteogenic differentiation

T Razafiarison[1], U Silvan[1], M Jovic[1], JG Snedeker[1]

[1]*Department of Orthopedics, Balgrist University Hospital, University of Zurich, Zurich, Switzerland and Institute for Biomechanics, ETH Zurich, Zurich, Switzerland*

INTRODUCTION: Our current understanding of stem cell-extracellular matrix (ECM) interaction is based on studies that have explicitly considered the topological, mechanical and biochemical properties of a biomaterial substrate as the main factors driving stem cell fate[1]. While ECM ligand alone can play a decisive contextual role at the cell-material interface, we sought to specifically isolate the role of supramolecular ligand assembly on material surface as a potentially significant regulator of stem cell adhesion and osteogenic differentiation.

METHODS: Because surface wettability can affect protein deposition, folding, and ligand activity, we developed and characterized a PDMS-based platform with the ability to tune wettability of elastomeric substrates with otherwise equivalent topology, ligand loading, and mechanical properties. Human bone marrow stromal cells (hBMSCs) were cultured on hydrophobic and hydrophilic substrates of various stiffness covalently functionalized with collagen I. Difference in ligand conformation was assessed by scanning electron microscopy (SEM) and atomic force microscopy (AFM). Quantitative differentiation assays and molecular investigations were performed to evaluate effects on stem cell early signalling events. To evaluate the difference in cell mechanical coupling to the different substrates, we implemented a traction force microscopy to quantify the substrate deformation.

RESULTS: Atomic force and scanning electron microscopy both revealed markedly different assembly of covalently bound type I collagen monomers on atomically flat hydrophobic PDMS substrates with a layer of collagen aggregates compared to a smooth collagen layer on hydrophilic PDMS-PEO substrates (see Fig.1). When cultured for 24 hours, hBMSCs were fully spread on all hydrophobic substrates as previously reported[1] but spread according to stiffness on hydrophilic substrates (see Fig.2). Quantitative osteogenic differentiation assay after 1 week revealed a 3-fold lower ALP activity on soft PEO-PDMS compared to stiff PEO-PDMS.

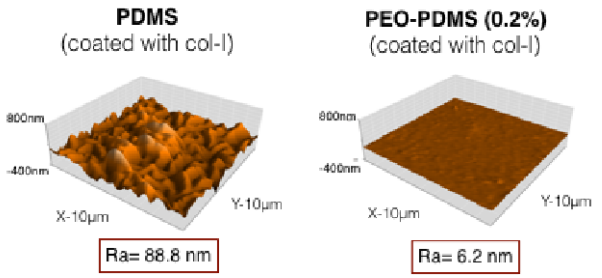

Fig. 1: Atomic Force Microscopy (AFM) images of PDMS and PEO-PDMS substrates coated with collagen I monomers.

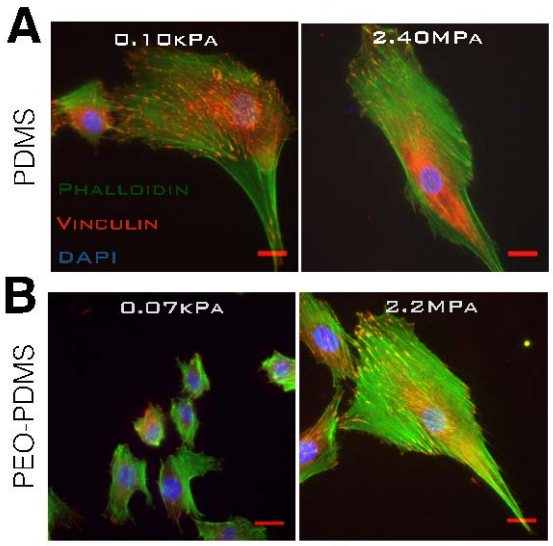

Fig.2: Morphology of hBMSCs on functionalized substrates seeded at 5'000 cells/cm^2 after 24 h culture on (A) PDMS and (B) PEO-PDMS (0.2%) substrates. Cells were immunostained with an antibody against vinculin (red), FITC-phalloidin (green) and DAPI (blue). Scale bar = 50 µm.

DISCUSSION & CONCLUSIONS: We demonstrate for the first time that surface driven ligand assembly on material surfaces, even on materials with otherwise identical starting topographies and mechanical properties, can dominate the biomaterial surface-driven cell response.

Bioprinting patient-specific auricular grafts

M Kesti[1], P Guillon[1,2], P Fisch[1,3], E Mazza[3], D Simmen[4], M Harder[4], T Linder[5], M Zenobi-Wong[1]

[1] *Cartilage Engineering + Regeneration, ETH Zürich, Switzerland.*
[2] *Sonova AG, Stäfa, Switzerland.*
[3] *Experimental continuum mechanics, Institute for Mechanical Systems, ETH Zürich, Switzerland*
[4] *Ear, Nose, Throat and plastic surgery centre, Klinik Hirslanden, Zürich, Switzerland.*
[5] *HNO-klinik, Luzerner kantonsspital, Luzern, Switzerland.*

INTRODUCTION: Bioprinting is an emerging technology in personalized medicine capable of producing complex grafts with patient-specific dimensions and autologous cells. The current autologous auricular reconstruction requires highly invasive costal cartilage harvest and the success of the shape reconstruction can be severely limited by the amount of available cartilage [1]. To improve the current clinical reconstruction we utilized 3D bioprinting technologies to manufacture patient-specific grafts with autologous cells. In vitro and in vivo tests were performed to characterize the bioink properties and the quality of the formed neocartilage.

METHODS: Newly introduced bioink consisting of gellan gum and alginate was used in the bioprinting process [2]. This bioink was mixed with human auricular chondrocytes ($6x10^6$ cell/ml) and characterized for rheological, mechanical (tensile) and biological tests (cell viability, DNA quantification and histological stains) when the grafts were cultured in chondrogenic medium supplemented with 10ng/ml transforming growth factor β3 (TGF-β3). Furthermore, an in vivo subcutaneous evaluation was carried out to assess the stability and the biocompatibility of the bioink following three week pre-culture and 8 week in vivo implantation.

RESULTS: Patient-specific auricular grafts were printed in high resolution replicating the anatomic dimensions of the current clinical reconstruction (Fig. 1). The tunable mechanical properties of the bioink ranged from 24kPa ± 3.2kPa to 228kPa ± 19kPa dependent on crosslinking parameters while high ductility (ultimate strain ~60%) was preserved for all conditions. The cell viability after printing was high (>95%) and after 3 weeks in vitro pre-culture the bioink grafts illustrated substantial cartilage specific extracellular matrix (ECM) deposition. The bioprinted grafts illustrated good stability in vivo, without significant changes in volume or shape.

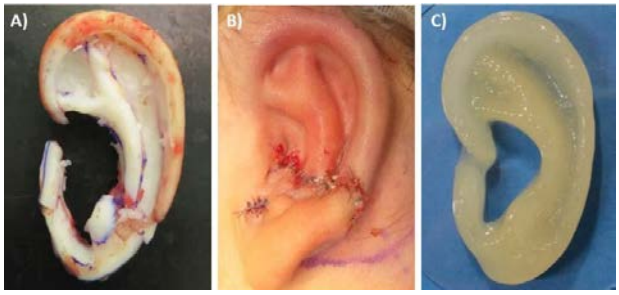

Fig. 1: Illustration of a clinical auricular reconstruction graft from costal cartilage A) and the implanted graft B). 3D bioprinted patient-specific graft C) can be manufactured to mimic the dimensions of the contralateral ear.

DISCUSSION & CONCLUSIONS: We present a bioink which allows fabrication of patient-specific anatomic structures in high resolution and high cell survival rate. These bioprinted cellular grafts are tunable in their mechanical properties, thus increasing the applicability of this approach. In vitro the cellular bioink promoted neocartilage formation after 3 weeks and in vivo the grafts retained stable dimensions over 8 weeks. Currently the bioink is being evaluated in vivo for its cartilage forming capabilities and neocartilage quality. This bioink represents an important step towards clinically-relevant 3D bioprinting where the patient-specific grafts can be manufactured with reproducible bioprinting. Furthermore, this bioink is composed of clinically used components, thus avoiding the extensive regulatory hurdles faced by many other bioinks.

ACKNOWLEDGEMENTS: The work was funded by the SNSF and FIFA\F-MARC. Authors would like to acknowledge Emma Cavalli, Ana Vukolic, Marco Pensalfini and Elia Guzzi for their help.

In situ photopolymerized composite hydrogels for implants: application to a nucleus pulposus replacement

ASchmocker[1], A Khoushabi[1], DA Frauchiger[2], C Schizas[3], B Gantenbein[2], PE Bourban[1], C Moser[1], DP Pioletti[1]

[1] Swiss Federal Institute of Technology (EPFL), Lausanne, CH, [2] University of Bern, Bern, CH, [3] Clinic Cécile, Lausanne, CH

INTRODUCTION: The nucleus pulposus (NP) is the core of the intervertebral disc (IVD). NP replacements have been subject to highly controversial discussions over the last forty years. Their utility seems to be eminent to treat herniated disc or degenerated disc disease (DDD). But, in practice not a single implant or tissue replacement was able to withstand the loads within an IVD. Hence, spinal-fusion remains the main treatment for DDD. The existing NP replacements suffer from extrusion and subsidence. To address such issues novel materials and placement methods are required.

METHODS: A composite hydrogel was developed by combining Poly-Ethylene-Glycol-Dimethacrylate (PEGDA) with Nano Fibril Cellulose (NFC) fibres[1,2]. The bio-composite was adapted to a range of native material properties including elastic modulus, water content or swelling pressure and evaluated using tests such as extrusion or confined compression experiments. A minimally invasive surgical device was developed[3] to inject the PEGDA-NFC hydrogel and activate it by light illumination in situ. To validate the approach the NP of bovine IVDs was removed and hydrogel samples were placed within the degenerated IVD disc model. After surgery the IVDs were cyclically loaded in a bioreactor over more than 0.5 million cycles and the change of organ height was compared between healthy, degenerated, repaired and cyclically loaded states (fig. 1).

RESULTS: The developed hydrogel could be tuned according to native material properties and was able to reach similar material properties in terms of swelling pressure, extrusion and confined compression strength. It was successfully implanted[4] and photopolymerized within the IVD model and was able to resist cyclic loading over 0.5 million cycles (fig. 1). The post-operative disc high increase was 33.4 % and was significant between degenerated/repaired state ($p < 0.0025$ and between degenerated and loaded state ($p < 0.025$). Histology of the samples showed a continuous interface between native tissue and implanted hydrogel.

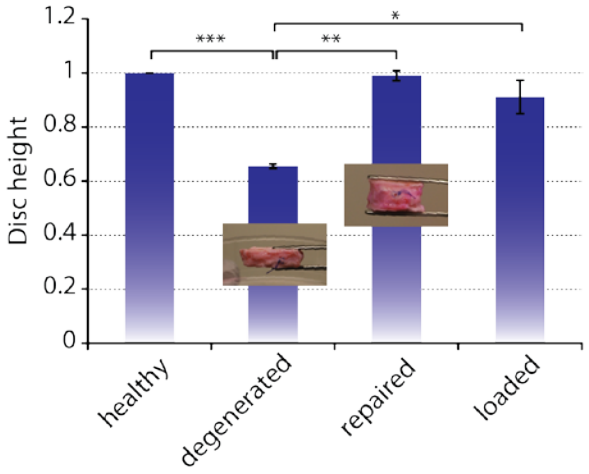

Fig. 1: The disc height significantly increased after implantation of the PEGDM-NFC composite hydrogel (repaired state) and could be maintained after 0.5 million cycles of compressive loading (loaded state).

DISCUSSION & CONCLUSIONS: The minimally invasive implantation by in situ photopolymerization is a unique feature to control the surgery and provide optimal tissue integration. The restauration of disc height over 0.5 million loading cycles suggests that the orthopedic implant could also be functional in humans.

ACKNOWLEDGEMENTS: Funding for this work was provided by the two SNF grants #10024003165465 and #310030_153411.

Biocompatibility and MRI imaging of radiation microdosimeter

MD Dominietto[1], G Verona-Rinati[2], C Verona[2], B Müller[1] and G Magrin[3]

[1]*Biomaterials Science Center, University of Basel, Switzerland.* [2]*Dipartimento di Ingegneria Industriale, Università di Tor Vergata.* [3] *EBG MedAustron, Wiener Neustadt, Austria.*

INTRODUCTION: The use of microdosimeters for the specification of radiation quality has a fundamental role in the framework of cancer therapy performed with ion-beam [1].
The rationale is the accurate determination of the characteristics of the radiation beams that, together with the absorbed dose, allow the forecast of the biological effects. Microdosimeter allows determining the lineal energy spectra, which describe the release of the energy to the cells. Such parameter is correlated to the cellular damage and varies drastically at the end of particle path.
Among several microdosimeters based on gaseous or solid-state sensitive volume, synthetic diamonds where chosen in the first studies for their high tissue equivalence and capability of being reduced in both, overall size and sensitive volume (see Tab. 1). [2] A first prototype of miniaturized diamond based microdosimeter, 1 mm^2 in size, has been developed (see Fig.1(a)). The goal of this experiment was to test the compatibility of the device with MRI scanner for future in-vivo measurement. Such results will be used as input for the study of biocompatibility in living small animals.

METHODS: A first version of the detector has been implanted post-mortem in nude BALB/C mice (N=3) at the following positions: on the skin surface (right flank), subcutaneously (left flank) and in brain following the opening of the skull.
For each position, T1 and T2-weighted MRI images have been acquired using an animal MRI scanner (4.7T Bruker, Ettlingen) to evaluate the presence of artifact determined by the components of the detector: diamond sensor, metallic electrodes and wire. Acute damage of the tissue due to potential over-heating has been also visually inspected.

Table 1: Physical characteristics of the microdosimeter

sensitive volume	≥0.003 mm^3
detector area	1÷3 mm^2
electrode diameter	100µm÷2mm
electrode thickness	50 nm
wire diameter	25 µm

RESULTS: The images acquired with MRI scanner showed a substantial compatibility of the device at each position of the detector in the mouse body. The sensible volume (diamond plate) was well visible in all images and did not produce artefacts. Metallic elements, as electrodes and wires in our case, are extremely critical since they can produce artefacts and heating the surrounded tissue due to the interaction with MRI radio-frequency. In both cases we did not detected any kind of artefacts. This unexpected, but good results, is due to the reduce thickness and diameter of the electrodes (the largest 2mm-diameter was used) and wire, respectively (see Table 1).

No macroscopic tissue damaged due to overheating has been detected.

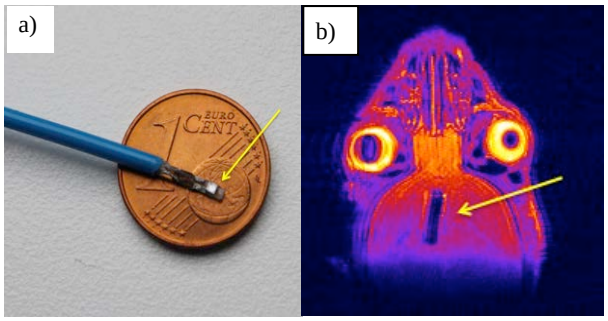

Fig. 1: a) Picture of the smallest microdosimeter (marked by the yellow arrow) compared to 1cent. b) MRI image of the mouse head showing the presence of the microdosimeter and the absence of artifacts.

DISCUSSION & CONCLUSIONS: the detector did not show any issue regarding the measurement in MRI scanner. Based on this preliminarily result, we are planning to use MRI to test biocompatibility during in-vivo experiments also considering miniaturized, silicon and gaseous detectors. Moreover, we are evaluating the possibility to substitute metallic wire with liquid metals (Ga-In alloy).

Biomimetic implants based on smart materials for severe incontinence treatment

VYF Leung[1], M Karapetkova[1], T Brusa[3], D Abler[3], B Osmani[1], T Töpper[1], FM Weiss[1], E Fattorini[1], L Brügger[4], C Gingert[5], P Büchler[3], B Müller[1,2]

[1]Biomaterials Science Center, University of Basel, 4123 Allschwil, CH. [2]University Hospital Basel, 4031 Basel, CH. [3]Institute for Surgical Technology and Biomechanics, University of Bern, CH. [4]University Hospital Bern, CH. [5]Kantonspitäler Schaffhausen, CH.

INTRODUCTION: As a much-needed alternative to conventional fluid-filled sphincter implants [1], one may fabricate biomimetic adaptive sphincters for treating severe incontinence (Fig. 1). Dielectric elastomer actuators (DEA) offer key advantages for the construction of an artificial sphincter, such as millisecond response times and power-to-mass densities similar to natural muscles. The realization of stacked, sub-micrometer thin DEA operating at medically acceptable voltages will open the way for smart implants that utilizes the ability of DEA to operate as actuator and sensor. Such a sphincter implant can actively monitor and adapt the closing pressure to the patient's activities.

METHODS: Molecular beam deposition (MBD), electrospray deposition, and spin-coating were used to fabricate single- and multi-layer DEAs from silicones. A layer of DMS-V05 in the sub-micron range (for MBD and electrospray) is deposited between two gold layers. These layers were typically 30 nm thick and fabricated by either sputtering or MBD onto a 50 µm-thick PEN substrate. The resulting asymmetric cantilevers (Fig. 1, top left) are tested for actuation properties. Alternatively, the sub-micron layer of DMS-V05 is replaced by a spin-coated 5 µm-thick layer of Elastosil. The electrode-elastomer-electrode units were stacked to create multilayer DEAs.

RESULTS: We have observed reliable actuation in spin-coated multilayer DEA, showing that at an elastomer layer thickness of above 1 µm a functional actuator can reliably be fabricated [2]. Below 1 µm, the surface microstructure of each layer plays a critical role in determining electrical conductivity and material adhesion, making it a challenge to achieve reliable actuation with both MBD and electrospray in this regime [3]. For MBD fabricated samples, we have observed initial indications of an actuation response, however the failure rate is still high. One key to success appears to improve the compatibility between the metallic and polymeric, i.e. mechanically stiff and soft layers of the actuator, so as to preserve the structural and mechanical integrity of the stacked structures.

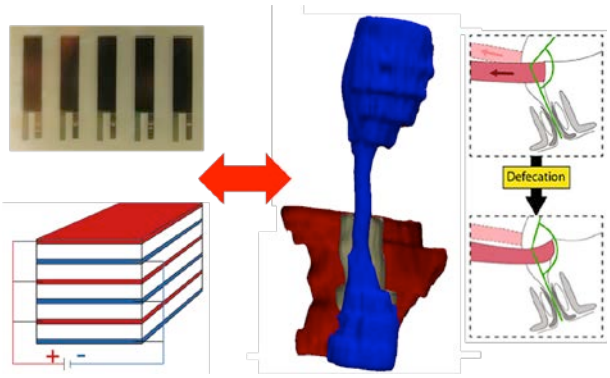

Fig. 1: Stacked actuators prepared from silicones with sensing capabilities (left) offer a biomimetic solution to treat severe incontinence. In this manner, the new implant actively adapts to the complex anatomy and function of the natural sphincter (right). A functional lumen imaging probe (FLIP) image shows the irregular shape of the internal (yellow) and external (red) anal sphincters. Defecation is accompanied by an angular modification of the rectum by the puborectal sling.

DISCUSSION & CONCLUSIONS: Biomimetic sphincter implants require engineered smart materials with actuation and sensing capabilities. The use of sub-micron stacked silicones and conducting layers for sphincter implants relies on a combination of sophisticated fabrication methods. The most effective means of fabrication depends on parameters including deposition rates, structural integrity, conductivity and above all mechanical stiffness.

ACKNOWLEDGEMENTS: Financial support from the nano-tera.ch initiative (project SmartSphincter) and the Swiss National Science Foundation (project 200021-135496) are gratefully acknowledged.

Direct induction of endochondral ossification of human bone marrow- derived mesenchymal stromal cells in a functionalized hydrogel system

C Stüdle[1], A Barbero[1], M Centola[1,2], S Metzger[3], M Ehrbar[3], I Martin[1]

[1] Department of Biomedicine, University hospital Basel, Basel, CH. [2] Musculoskeletal Department, NIBR, Basel, CH. [3] Department of Obstetrics, University hospital Zurich, Zurich, CH

INTRODUCTION: Endochondral ossification encompasses the process during long bone development that starts with the condensation of embryonic mesenchymal cells forming the cartilage anlagen which then is remodelled into bone. Earlier, we have shown that adult human bone-marrow derived mesenchymal stromal cells (BMSCs) have the capacity to form bone upon ectopic implantation through endochondral ossification. Usually, for efficient production of ossicles, the process requires several weeks of in vitro culture to produce a mature hypertrophic tissue, prior to implantation[1,2]. Here, the goal was to develop a system where the in vitro step can be omitted and the BMSCs were instructed to undergo chondrogenesis directly in vivo.

METHODS: An enzymatically cross-linkable poly(ethylene glycol) based hydrogel containing the adhesion peptide RGD and metalloproteinase cleavage sites[3] was used to be functionalized with TGFβ3. For functionalization streptavidin was incorporated in the gel backbone[4] and biotinylated TGFβ3 was added to the pre-polymerized hydrogel mix. BMSC after expansion in presence of FGF-2 were encapsulated at a density of 20-25x10^6 cells/mL in functionalized or non-functionalized hydrogels cultured in vitro with serum-free medium (to assess their chondrogenic capacity) or immediately implanted in the subcutaneous pocket of nude mice in order to assess their potential to undergo endochondral ossification. In vitro culture was stopped after 2 weeks and in vivo constructs were explanted after 2-12 weeks and analysed by histology.

RESULTS: In vitro, BMSCs underwent chondrogenic differentiation in presence of immobilized TGFβ3- functionalized hydrogels to a similar extent than if stimulated with soluble TGFβ3. In vivo after two weeks functionalized hydrogels showed Safranin-O-positive areas with cells of a round morphology. At later time points, the cartilaginous constructs underwent matrix remodeling leading finally after 12 weeks to ossicles consisting of a rim of cortical bone surrounding a host-derived hematopoietic compartment. In contrast in non-functionalized hydrogels, the cells remained in an undifferentiated fibroblastic-like stage throughout all time points. In bi-layered gels in which only one part contained TGFß3, cartilage and bone formation strictly occurred only in the functionalized layer, whereas the cells in the other part remained undifferentiated.

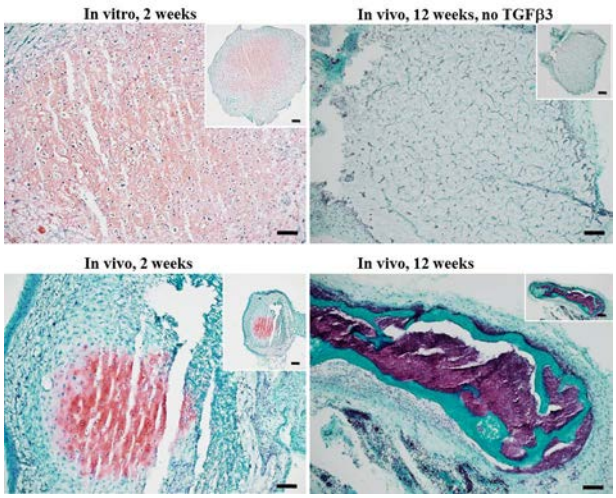

Fig. 1: Safranin-O staining of an in vitro cultured TGFβ3-functionalized hydrogel and of explants after 2 and 12 weeks upon implantation. Big scale bar 100 μm and small scale bar 200 μm.

DISCUSSION & CONCLUSIONS: Our findings suggest that the BMSCs are induced to take the endochondral route by the presentation of TGFβ3 in the gel and that this bypasses the otherwise needed in vitro priming step. Aiming at generating a properly integrated cartilage-bone interface in the context of osteochondral repair, in an ongoing study the TGFβ3 functionalized gel is extended by a second layer containing nasal chondrocytes.

ACKNOWLEDGEMENTS: This work was supported by the AO foundation.

Biomimetic sulfated hydrogels suppress IL-1β-mediated inflammation in human articular chondrocytes

E Öztürk[1], Ø Arlov[2], G Skjak-Braek[2], M Zenobi-Wong[1]

[1] Cartilage Engineering+Regeneration, ETH, Zurich, CH. [2] Department of Biotechnology, Norwegian University of Science and Technology, Trondheim, Norway.

INTRODUCTION: Damage of articular cartilage from aging or trauma is often coupled with inflammation that further accelerates cartilage matrix degradation. Autologous cell-based therapies for cartilage regeneration require implantation of a high number of chondrocytes which demands their 2D expansion and causes loss of phenotype. Therefore, scaffolds for cartilage engineering should both provide biological cues that induce re-differentiation of chondrocytes and act as a protective microenvironment against the inflammatory effects from the defect site. Here we show that biomimetic alginate sulfate hydrogels induce cartilage matrix production and suppress IL-1β-induced inflammation in chondrocytes.

METHODS: Sulfation of alginate was carried out as previously described.[1] Human articular chondrocytes were isolated and encapsulated in alginate (Alg), alginate sulfate (S-Alg, ds: 0.32 sulfates/monomer) or mixtures of alginate/alginate sulfate (ds: 0.9) hydrogels at passage 4. For inflammatory induction, the cells were serum starved overnight and treated with 1 ng/ml IL-1β for 24h or 48h. The gels were collected at given time points and assessed for cell viability and morphology, gene and protein expression and immunohistochemistry.

RESULTS: Alginate and alginate sulfate hydrogels support viability and growth of encapsulated chondrocytes after 7 days (Fig. 1).

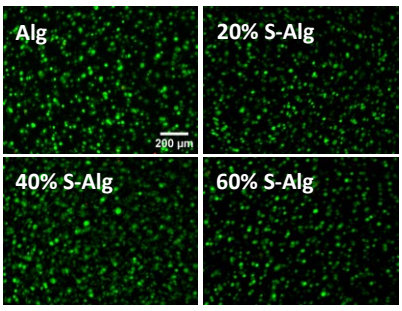

Fig. 1: Live(green)/dead(red) staining of human chondrocytes encapsulated in Alg/S-Alg hydrogels.

IL-1β-induced gene expression of inflammatory (IL-6, IL-8, COX-2) and catabolic markers (ADAMTS-5, MMP-13) was significantly reduced in the sulfated hydrogels compared to unmodified alginate (Fig. 2).

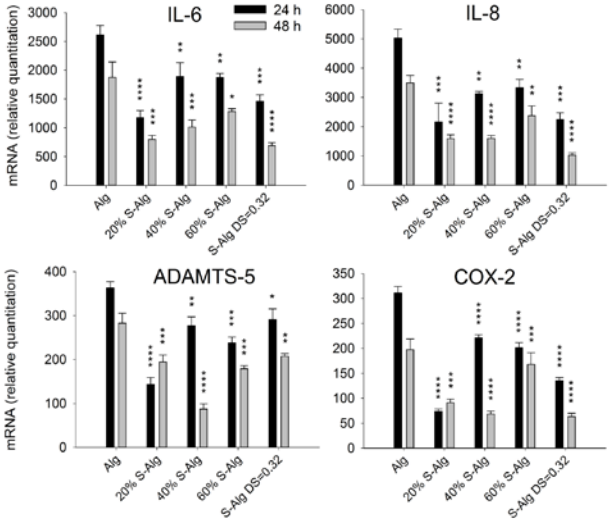

Fig. 2: Gene expression of inflammatory markers in Alg/S-Alg hydrogels after induction with IL-1β.

Furthermore, sulfated hydrogels suppressed the protein expression of COX-2 and NF-κB as well as the phosphorylation of NF-κB and upstream activator p38-MAPK in response to IL-1β treatment (Fig. 3).

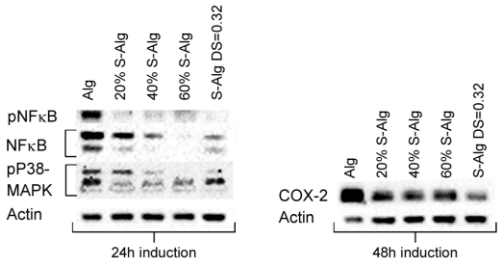

Fig. 3: Western blots showing the expression of inflammatory markers in IL-1β induced cells.

DISCUSSION & CONCLUSIONS: Here we show that alginate sulfate hydrogels promote the growth of human chondrocytes and prevent induction of inflammation by IL-1β. This protective gel microenvironment, likely through entrapment of cytokines, exhibits an important role of biomimetic sulfate moieties for chondrocytes.

ACKNOWLEDGEMENTS: This project was funded by SNF (315230_159783).

Exploiting enzymatic-visible light dual-gelation for 3D printing of tyramine-modified hyaluronan

D Petta[1,2], CM Sprecher[1], DW Grijpma[2], D Eglin[1], M D'Este[1]

[1] *AO Research Institute Davos, Davos, CH* [2] *Department of Biomaterials Science and Technology, University of Twente, Enschede, NL*

INTRODUCTION: 3D printing (3DP) offers peculiar possibilities in biofabrication. However, in order to fully exploit this potential, bioinks with good printability, supporting high cell viability and function are needed [1]. Here we introduce a dual gelation for 3DP of tyramine (Tyr)-modified hyaluronic acid (HAT) consisting in 1) enzymatic pre-crosslink for optimal extrusion and 2) visible light crosslink for shape retention.

METHODS: HAT with Tyr substitution of 14.5% was prepared by amidation of Tyr to hyaluronan [2]. HAT was dissolved at 2.5%, 3.5% or 5% w/v in PBS solution containing horseradish peroxidase (HRP) 0.1 U/ml and Eosin 0.02 % w/v. Enzymatic crosslinking was triggered by adding H_2O_2. Rheology (Anton Paar MCR-302 rheometer) was performed to evaluate the viscosity at different shear rates and the tan δ. 3D constructs of 10 mm diameter and 3 mm height with a criss-cross structure were produced with a 3D Discovery® system from RegenHU Ltd. After optimization, the following parameters were used: pressure (4 bar), layer height (0.14 mm), needle inner diameter (0.25 mm). Visible light photocrosslink was carried out between each layer.

RESULTS: An estimated shear rate between 10-25 s^{-1} (grey area in the Fig. 1) is applied to the bioinks during 3DP. Fig. 1 illustrates the influence of HAT concentration and enzymatic crosslinking on the viscosity at different shear rates. For all compositions viscosity was below 45 Pa·s in the printing region. HAT 2.5% w/v displays the highest viscosity at low shear rate (= 3.6 kPa·s at 0.01 s^{-1}), whereas without crosslinking (black line) viscosity was 8 Pa·s. Printed struts of HAT 2.5 and 3.5% w/v with 0.17mM H_2O_2 displayed the best shape fidelity. Compositions with tan δ >0.6 or <0.5 are too tacky, fluid or brittle. The HAT 2.5% w/v with 0.17mM H_2O_2 composition was employed for the fabrication of a 3D structure (inset Fig. 1).

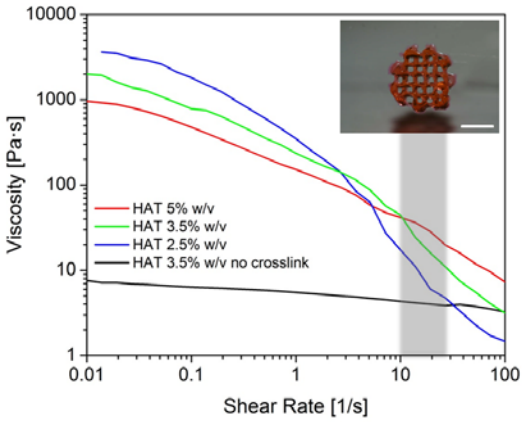

Fig. 1: Viscosity curves for different HAT compositions. Inset: 3D printed construct (scale bar = 5 mm)

Table 1. Influence of tan δ on the printability.

HA-Tyr [% w/v]	H_2O_2 [mM]	Tan δ	Printability
2.5	0.17	0.54	Good
3.5	0.17	0.58	Good
5	0.17	0.81	Good (but tacky)
2.5	0.50	0.02	Poor (too brittle)
3.5	0.90	0.001	Not printable
3.5	0.10	2.20	Poor (liquid state)
3.5	0.17	0.18	Light crosslink

DISCUSSION & CONCLUSIONS: The two crosslinking mechanisms of HAT allow the independent tuning of the HAT bioink rheological properties for optimal extrusion/plotting and shape retention. Both crosslinking methods and their combination have allowed the viable encapsulation of cells in HAT [3]. Thus, future work is now directed toward the fabrication of cell-laden HAT 3DP constructs.

A hyaluronic acid / platelet rich plasma hydrogel for mesenchymal stem cells delivery to the intervertebral disc: rheological and biological characterization

G Vadalà[1], M D'Este[2], F Russo[1], M Alini[2], D Eglin[2], R Giordano[3], V Denaro[1]

[1] *Department of Orthopaedic and Trauma Surgery, Campus Bio-Medico University of Rome, Italy*

[2] *AO Research Institute Davos, AO Foundation, Davos, Switzerland* [3] *Cell Factory, Fondazione IRCCS Ca' Granda Ospedale Maggiore Policlinico, Milan, Italy.*

INTRODUCTION: Intervertebral disc degeneration is a major source of pain and associated social costs [1]. Mesenchymal Stem Cells (MSC) were proven to induce regeneration *in vivo* [2]; however their clinical translation requires suitable delivery. Starting from clinically-approved materials, here we characterise a hyaluronan (HA) / platelet rich plasma (PRP) hydrogel as delivery carrier for MSC to the nucleus pulposus.

METHODS: A pooled platelet concentrate of 1.8 x10^6 cells/ml was obtained from healthy donors after informed consent (PRP). HA was mixed 6:1 with batroxobin (BTX) at 5 BU/ml. The gel obtained by mixing HA/BTX and PRP 1:1 was rheologically characterised. Human bone marrow-derived MSC harvested from iliac crest after informed consent (3 donors, each experiment in triplicate) were encapsulated in PRP/HA/BTX hydrogels and cultured in growing medium (control) and chondrogenic medium with or without TGF-β1 up to day 21. Viability was assessed via live/dead assay, sulphated glycosaminoglycans (GAG) with DMMB assay. The constructs were fixed in 4% paraformaldehyde, cryosectioned and stained with Alcian blue and Safranin-O. Quantitative gene expression evaluation for collagen type II and aggrecan (HACAN) were performed. A p-value<0.05 was considered statistically significant.

RESULTS: PRP/HA/BTX gelled in 15 minutes at 20°C, whereas at 37°C gelation time drops to 3 minutes (fig 1 A). The composite without HA 1) sets within seconds (fig 1A) and 2) displayed rheological features of a more rigid matrix (fig 1 B). MSCs cultured in the PRP/HA/BTX hydrogel maintained high cell viability. The proliferation was significantly higher in hydrogels cultured with TGF-β1 compared to the other groups at all-time points. MSC encapsulated in PRP/HA/BTX hydrogel cultured in chondrogenic medium with or without TGF-β1 showed a 1.5 fold increase in GAG production compared to control media. MSCs embedded in the PRP/HA/BTX hydrogel, in presence of TGF-β1 showed high metachromatic staining of Alcian Blue and the red staining with Safranin-O (not shown), as well as significantly higher gene expression levels of collagen type II and HACAN compared to controls (fig 2).

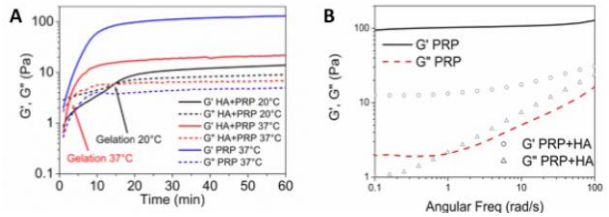

Fig. 1: (A) Viscoelasticity PRP/HA/BTX gels as a function of time; blue lines represent PRP/BTX without HA. Continuous lines: storage moduli; dotted lines: loss moduli. (B) Mechanical spectra of PRP/BTX and PRP/HA/BTX.

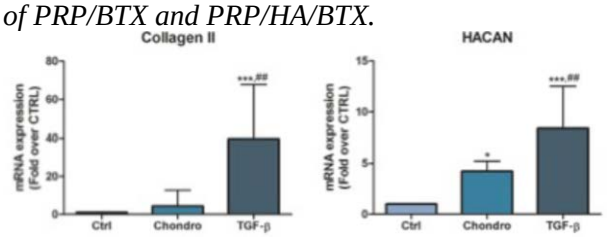

Fig. 2: Quantitative Real Time PCR for collagen type II and HACAN gene expression in the construct after 3 weeks in each culture condition.

DISCUSSION & CONCLUSIONS: Our composite is prepared from products already approved for human use, eliminating an important barrier towards clinical translation. Interestingly, with HA the gelation time and therefore handling are drastically improved over PRP/BTX hydrogel. In addition, MSC within the gel displayed high viability and the ability to differentiate towards nucleus pulposus cell-like phenotype. PRP/HA/BTX is therefore a promising and directly translatable carrier for the delivery of MSC to the intervertebral disc.

Adipose-derived stem cell seeded biominerizable nanocomposite for chest wall repair: suppression of inflammatory response in a murine model

J Buschmann[1], E Balli[1], SC Hess[2], WJ Stark[2], P Cinelli[3], S Märsmann[1,3], M Welti[1,4], W Weder[4], W Jungraitmayr[4]

[1]*Plastic Surgery, University Hospital Zürich, Zürich, CH.* [2]*Institute for Chemical and Bioengineering, ETH, Zürich, CH.* [3]*Trauma Surgery, University Hospital Zürich, Zürich, CH.* [4]*Thoracic Surgery, University Hospital Zürich, Zürich, CH.*

INTRODUCTION: Defects to the chest wall can occur after tumour resections or trauma caused by accidents, and appropriate chest wall reconstruction is therefore needed. Stability and integrity of the repaired chest wall should reach similarity to natural physiology. Addressing the treatment of critical size full-thickness chest wall defects, the ideal graft should be stable, fluid- and air-tight, biocompatible inducing no inflammatory reactions, biodegradable during the healing with non- toxic degradation products as well as rapidly integrating into the surrounding tissue. Here, we present the implantation of a biocompatible, biodegradable and easily vascularizable nanocomposite seeded with adipose-derived stem cells (ASCs) as a chest wall graft in a murine model. The cellular response towards this graft is compared to the cell-free graft.

METHODS: An electrospun poly(lactic-co-glycolide)/amorphous calcium phosphate (PLGA/aCaP) nanocomposite was seeded on both sides with murine ASCs and cultivated for two weeks before implantation as a chest wall graft. In addition, a cell-free analogous PLGA/aCaP scaffold was implanted on top of the cell-seeded scaffold towards the skin in order to be able to study not only direct cell-to-cell contact-based effects, but also to address paracrine effects caused by ASCs (control: cell-free scaffold alone). Histomorphometric analysis was performed at 4 and 8 weeks post-operation, respectively, to assess cell density of macrophages, lymphocytes and foreign body giant cells (Figure 1).

RESULTS: Inflammatory response towards the graft material was significantly reduced for macrophages, lymphocytes and foreign body giant cells in the presence of ASCs compared to cell-free scaffolds. Moreover, this anti-inflammatory action caused by ASCs was not only found on the side where direct cell-to-cell contact between seeded ASCs and local cell population was enabled and studied, but also on the scaffold side where predominantly diffusible factors secreted by ASCs were active (paracrine function).

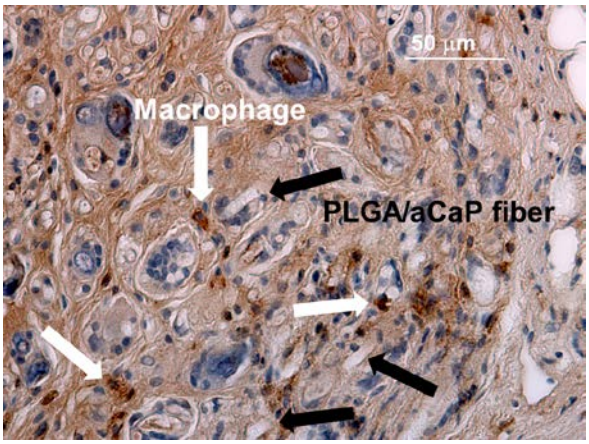

Fig. 1: F4/80 stained histological section at 8 weeks post-operation showing selected macrophages (white arrows) and electrospun PLGA/aCaP fibers of the degrading chest wall graft.

DISCUSSION & CONCLUSIONS: In clinics, the state of the art of repairing critical size chest wall defects is to use inert materials such as Goretex® which are not easily vascularizable and not biodegradable. Here, we present a biocompatible, biodegradable and well vascularizable nanocomposite for chest wall repair. In order to enhance integration of this graft material and accelerate wound healing, ASCs were seeded. A beneficial effect of these ASCs was that the inflammatory response towards the implant was significantly reduced. Therefore, such cell-seeded nanocomposites may be applied as chest wall grafts in clinics in the future.

ACKNOWLEDGEMENTS: We thank Gabriella Meier Bürgisser for her help with analysis of histological sections and Pia Fuchs for histological staining.

Bioactive, elastic and biodegradable double – layered emulsion electrospun DegraPol tube delivering PDGF-BB for tendon rupture repair: *in vitro* and *in vivo* assessment

O Evrova[1,2], GM Bürgisser[1], M Calcagni[1], C Scalera[3], E Bachmann[4], J Snedeker[4], P Giovanoli[1], V Vogel[2] and J Buschmann[1]

[1] Division of Plastic Surgery and Hand Surgery, University Hospital Zürich, CH. [2] Laboratory of Applied Mechanobiology, ETH Zürich, CH. [3] Ab Medica, Lainate, Milan, Italy,[4] Laboratory for Orthopaedic Biomechanics, Uniklinik Balgrist/ ETH, CH.

INTRODUCTION: Healing of tendon ruptures represents a major challenge in musculoskeletal injuries. Approaches of repair by conventional suture may lead to re-rupture. A new, highly elastic polyester urethane (DegraPol® (DP))[1,2] was explored as a delivery device for platelet derived growth factor – BB (PDGF-BB) to promote tendon healing.[3] Morphological, mechanical and delivery properties of the bioactive DP scaffolds were studied. Assessment of double-layered emulsion electrospun DP was performed *in vivo*, in a rabbit Achilles tendon rupture model.

METHODS: Water-in-oil emulsions were produced by dropwise addition of aqueous phase with biomolecules to the polymer solution, stirred, ultrasonicated and electrospun using in-house built electrospinning device. Changes in fiber morphology and diameter as a function of different electrospinning parameters were determined from SEM images. Mechanical properties of bioactive DP scaffolds were determined from stress/strain curves and compared to pure DP scaffolds. The delivery of rhPDGF-BB was analysed by ELISA. Bioactivity of the released PDGF was tested on rabbit tenocytes *in vitro* by analysing cell proliferation (EdU assay). Performance of bioactive scaffolds in a form of double-layered tube, with inner layer delivering PDGF-BB at the site of tendon rupture (Figure 1A) was assessed in an *in vivo* rabbit model where biomechanical and histomorphological analysis of the regenerating tendons was performed 3 weeks post – surgery. t – test and one-way ANOVA were used to test differences between groups (*$p < 0.05$, **$p < 0.01$, *** $p < 0.001$).

RESULTS: Emulsion electrospinning resulted in significantly smaller fiber diameters, compared to single electrospinning. PDGF-BB was released in a sustained manner within a period of 30 days. No differences were observed in Young's modulus, but bioactive scaffolds had decreased strain at break [%], however still high enough for proper surgeon handling. Tenocyte proliferation was higher on them and significantly different from pure DP scaffolds (Figure 1B)[3]. *In vivo* results revealed the positive impact of PDGF-BB by significant higher failure stress (MPa) and stiffness (N/mm) of the regenerated tendons, when compared to conditions with only pure DP electrospun tubes.

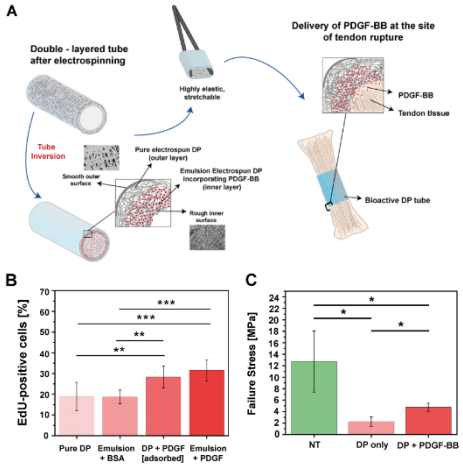

Fig. 1: A) Scheme of double-layered DP tube. B) B) Bioactivity of incorporated PDGF-BB in DP scaffolds. C) Failure stress (MPa) of tendons 3 – weeks post-surgery.

DISCUSSION & CONCLUSIONS: The data suggests that emulsion electrospun DP tubes deliver bioactive PDGF-BB, thus increasing tenocyte proliferation and leading to enhanced biomechanical properties of regenerating tendons *in vivo* 3 weeks post-surgery, presenting a promising application in aiding tendon regeneration after rupture.

ACKNOWLEDGEMENTS: This work was supported by the EMDO foundation and fellowship by *ab medica*, Lainate, Milan, Italy for O.E.

Mussel-inspired chemistry for long-term *in vitro* maintenance of human pluripotent stem cells

M Lee, H Lee

Bio-inspired NanoEnergy Materials Labs, Department of Chemistry, Korea Advanced Institute of Science and Technology (KAIST), Republic of Korea

INTRODUCTION: Towards practical utilization of human pluripotent stem cells as regenerative medicine, *in vitro* expansion of isolated stem cells is crucial [1]. Here, we report that mussel-inspired catechol chemistry [2] enables facile immobilization of a non-adherent polysaccharide on the culture dishes to support long-term, feeder-free culture of human embryonic stem cells (hESCs). This approach provides the chemically-defined, scalable and stable method for *in vitro* expansion of hESCs.

METHODS: Mussel-inspired adhesive dopamine was conjugated onto heparin via EDC coupling between amines of dopamine (16 mg/ml) and carboxylate of heparin (4 mg/ml) under the slightly acidified (pH ~4) aqueous solution to give dopamine-g-heparin. For the surface modification, a cell culture dish was coated using solutions of dopamine-g-heparin (2 mg/ml), sodium periodate (1 mg/ml) and collagen type I (2 mg/ml). The prepared substrates were analysed by X-ray photoelectroscopy and surface plasmon resonance. H9 hESC lines were cultured on matrigel, collagen type I, dopamine-g-heparin, or dopamine-g-heparin /collagen type I – treated culture dishes using conditioned medium prepared as described previously [3]. The cultured hESCs were analysed by qRT-PCR and immunostaining.

RESULTS: When dopamine was conjugated to heparin (Fig. 1a), the dopamine-g-heparin was readily coated on the surface, whereas heparin itself barely adsorbed on the surface (Fig.1b). In addition, the surface-immobilized heparin effectively recruited vitronectin onto the surface (Fig. 1c). Dopamine-g-heparin coating was able to support undifferentiated growth of hESCs under the feeder-free condition up to 4th passage. Furthermore, when collagen type I was co-immobilized with dopamine-g-heparin, long-term (18 passages) maintenance of hESCs was achieved (Fig. 1e). Interestingly, we observed that hESCs underwent spontaneous differentiation on collagen type I-coated substrate after 6 passages (Fig. 1d), which strongly implied that surface-immobilized

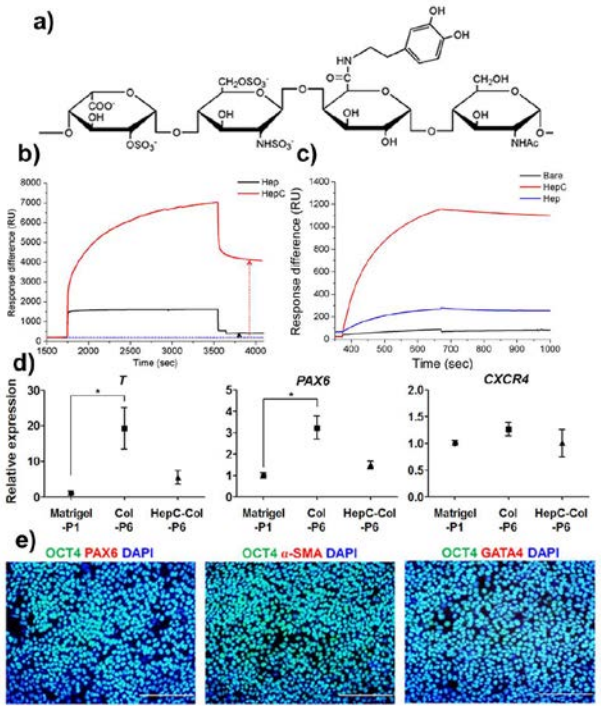

Fig. 1: preparation of dopamine-g-heparin (HepC) and culture of hESCs for mid and long term on various feeder-free substrates.

dopamine-g-heparin efficiently supressed differentiation of hESCs under the feeder-free condition and thus enabled long-term undifferentiated growth of hESCs. hESCs maintained normal karyotype and pluripotency after such a long-term culture on dopamine-g-heparin/collagen I coating.

DISCUSSION & CONCLUSIONS: In this study, we demonstrated that dopamine-g-heparin was effectively immobilized on the surface and recruited proteins to support long-term, undifferentiated growth of hESCs. This approach suggests that the use of polysaccharides can be a new, alternative design principle for 2-dimensional culture materials for hESCs.

Alginate-sulfate nanocellulose bioinks for cartilage bioprinting application

M Müller[1], E Öztürk[1], Ø Arlov[2], P Gatenholm[3], M Zenobi-Wong[1]

[1]Cartilage Engineering +Regeneration Laboratory, ETH Zürich, Zürich, Switzerland. [2] Department of Biotechnology, Norwegian University of Science and Technology, Trondheim, Norway. [3]Wallenberg Wood Science Center and Biopolymer Technology, Departement of Chemical and Biological Engineering, Chalmers University of Technology, Gothenburg, Sweden.

INTRODUCTION: The lack of available materials for biopritnting applications is currently what is holding this promising technology back. A good bioink should not only be biologically active but also have the proper rheological properties. A combination of materials is often superior over single materials and necessary to fulfil both the biological and rheological requirements. Here we present a combination of the biologically active biopolymer alginate sulfate, which was shown to be chondrogenic and induce cell proliferation and spreading [1], and the viscosity modifying agent nanocellulose (NC).

METHODS: Rheological measurements were performed to assess the flow behaviour and gelation properties of alginate sulfate when mixed with NC. Bovine chondrocytes were encapsulated in alginate and alginate sulfate with or without NC and the viability and cell morphology was investigated at day 1, 14 and 28. Cells were also printed using the alginate sulfate-NC bioink with different needle diameters and shapes and cell viability and morphology were evaluated. COMSOL simulations were performed to see if differences between the printed and the encapsulated cells arise from differences in maximum and average shear stresses occurring in the different printing geometries.

RESULTS: Rheological measurements revealed that, despite the lower viscosity of alginate sulfate solutions compared to unmodified alginate, the flow properties of the final bioink with NC were only slightly influenced. Mechanical properties of alginate sulfate-NC were equal to alginate NC after increasing the alginate sulfate concentration in the bioink. Cells showed a round morphology at every time point in the alginate and alginate-NC gels, whereas in the alginate sulfate and alginate sulfate-NC samples the cells started spreading after 14 days in culture. Only when the printing geometry was optimized was the ability of cells in alginate sulphate to spread and proliferate maintained. Simulations revealed differences in the average and maximum shear stress between conical and straight needles of different diameters which might explain the differences in the cells ability to spread or not in the printed samples.

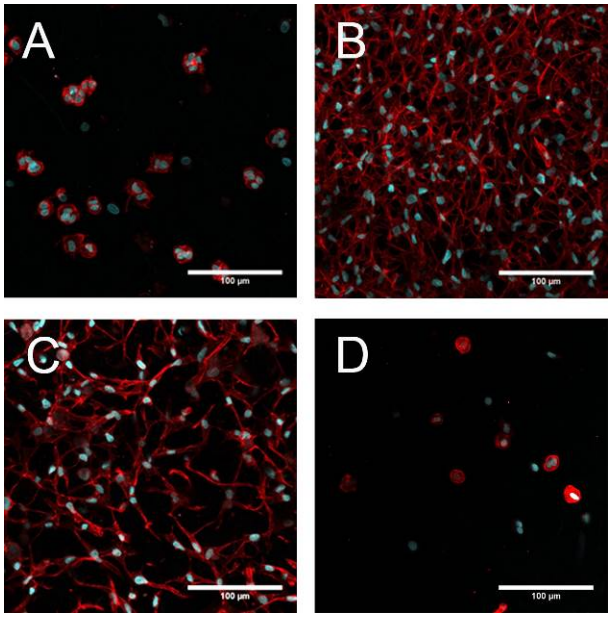

Fig. 1: Chondrocyte morphology at day 28 encapsulated in alginate-NC (A) or alginate sulfate-NC (B) or printed with alginate sulfate-NC with a straight 413 µm (C) or 159 µm (D) needle. Scale Bar is 100 µm.

DISCUSSION & CONCLUSIONS: Alginate sulfate maintained its mitogenic properties and effects on cell spreading in the presence of NC. The NC addition made alginate sulfate a printable material, but restrictions remain in regards to usable inner needle diameters and shapes for cells to survive and show the spreading behaviour.

.

ACKNOWLEDGEMENTS: This work was supported by ETH Research Grant ETH-23 14-1, FIFA/F-MARC and EU program Eureka and Vinnova.

Efficacy of a thermo-responsive hyaluronan based hydrogel containing gentamicin in an *in vivo* fracture model with plating osteosynthesis and *S. aureus* contamination

GA ter Boo[1,2], T Schmid[1], I Zderic[1], DW Grijpma[2], RG Richards[1], D Eglin[1], TF Moriarty[1]

[1] *AO Research Institute Davos, AO Foundation, Davos, CH.* [2] *Department of Biomaterials Science and Technology, University of Twente, Enschede, NL.*

INTRODUCTION: The infection rate can exceed 30% in grade III open fractures. Antibiotic loaded biomaterials (ALBs) may offer improved protection against infection by delivery of high concentrations of antibiotics locally [1]. Flowing thermo-responsive hydrogels might be beneficial over conventional ALBs. However, tuning the lower critical solution temperature (LCST) of thermo-responsive hydrogels is required for gelation in open wounds. Here, the LCST of a hyaluronic acid-poly(*N*-isopropylacrylamide) (HApN) hydrogel with gentamicin was assessed as a function of sulfate content. Furthermore, healing with or without the presence of the HApN hydrogel was investigated in an *in vivo* model.

METHODS: *Tayloring the LCST*: HApN [2] was dissolved in PBS with increasing concentrations of gentamicin sulfate (0.0, 0.5, 1.0 and 2.0% w/v) or potassium sulfate (stoichiometrically matched). Storage and loss moduli were recorded as a function of temperature.

Post-mortem evaluation: Rabbits included in the healing study were euthanized 4 weeks post-operatively. Quantitative bacteriology was performed on tissue + hardware. A four-point bending test was used to determine humerus strength and stiffness.

RESULTS: Control over LCST by the 'hofmeister effect' was verified by the rheology of HApN in presence of K_2SO_4 (not shown). For HApN with 2.0 % w/v gentamicin-sulfate, the shift towards lower LCST was -1.7 °C (Fig 1). Quantitative bacteriology showed all gentamicin-loaded HApN hydrogel treated rabbits cleared the $2x10^6$ CFU *S. aureus* load. The HApN hydrogel without antibiotics did not significantly decrease bone stiffness compared to humeri of rabbits that only had surgery without application of the hydrogel (Fig 2). Humeri of rabbits that did not receive treatment after bacterial inoculation of the wound site had decreased bone stiffness. Although rabbits receiving the HApN hydrogel with gentamicin killed all bacteria, humeri from these rabbits had a decreased stiffness potentially due to interference of dead bacteria on the healing process (Fig 2).

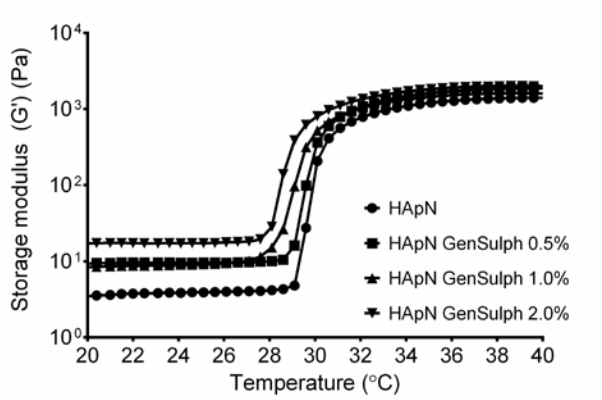

Fig. 1: Elastic moduli of HApN hydrogels with increasing gentamicin sulfate content

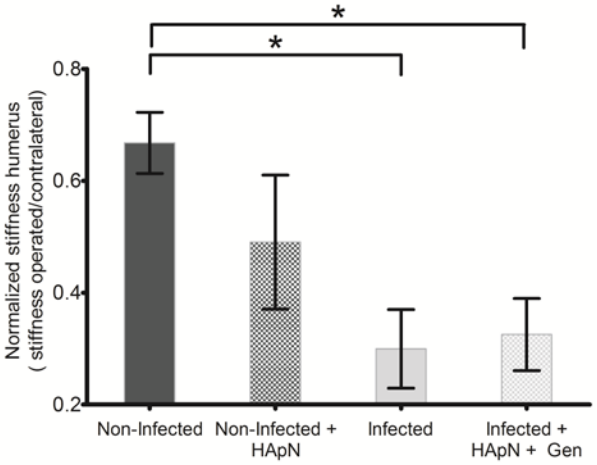

*Fig. 2: Stiffness of rabbit humeri expressed as ratio compared to contralateral, *P≤0.05*

DISCUSSION & CONCLUSIONS: Control over LCST of the HApN hydrogel has been shown. The HApN hydrogel with gentamicin prevents infection *in vivo*. The HApN hydrogel itself does not significantly affect fracture healing, however presence of dead bacteria appears to delay healing.

Scaffold architecture influences the outcome of dynamic bone tissue engineering cultures

M Rubert[1], JR Vetsch[1], I Lehtoviita[1], M Sommer[2], A R Studart[2], R Müller[1], S Hofmann[1,3,4]

[1] Institute for Biomechanics and [2] Complex Materials, ETH Zurich, Zurich, Switzerland.
[3] Department of Biomedical Engineering and [4] Institute for Complex Molecular Systems, Eindhoven University of Technology, Eindhoven, The Netherlands.

INTRODUCTION: Bone tissue engineering (BTE) aim at providing tissue constructs with structural and mechanical characteristics closely mimicking natural tissue. Bioreactors are attractive because they enable a controlled and reproducible environment that mimics the one of bone *in vivo*. Spinner flask bioreactors provide a dynamic environment that supports bone-like tissue formation as shown by increased cell proliferation, expression of bone-related genes and calcium deposition [1]. A new method for the fabrication of silk fibroin scaffolds (SFSC) with a highly homogeneous structure, namely inverse opal scaffolds (IOSC), has been developed. IOSC enhanced the formation of extracellular matrix (ECM) mineralization by human mesenchymal stem cells (hMSC) compared to salt leached silk fibroin scaffolds (SLSC) under static conditions. IOSC and SLSC differed in some architectural properties, notably pore geometry (PG), pore diameter distribution (PDD) and the porosity. The increase in the mineral content was attributed to differences in the PDD or in the PG. Nevertheless, the effect of scaffold architecture on cell behaviour in dynamic cultures, closely mimicking the natural environment, has not been studied yet. Here we study the influence of the scaffold architecture on mineralized ECM formation by hMSCs cultured on SFSC either under static or dynamic culture conditions.

METHODS: SLSC were produced as described by [2]. IOSC were prepared by assembling monodisperse and spherical pore template micro-particles into a crystalline lattice before infiltration with aqueous silk fibroin solution. hMSCs were cultured on IOSC and SLSC either under static or dynamic (spinner flask bioreactor) conditions for up to 49 days with osteogenic supplementation. Mineralized ECM formation was evaluated using micro-computed tomography. Collagen deposition was assessed by sirius red (SR) staining. Gene expression was determined by real-time RT-PCR.

RESULTS: While dynamic culturing did not induce significant differences in mineralized ECM volume fraction (BV/TV) in IOSC compared to static conditions, a 35% increase (p=0.013) in BV/TV was observed for SLSC cultured under static compared to dynamic conditions (Fig 1A). In addition, dynamic culture induced differences in collagen formation between IOSC and SLSC, showing more pronounced collagen deposition especially at the edge of SLSC (Fig 1B) as revealed by SR staining and Coll-I gene expression (data not shown). Furthermore, mineralized tissue was homogeneously distributed in both scaffold types under dynamic compared to static culture.

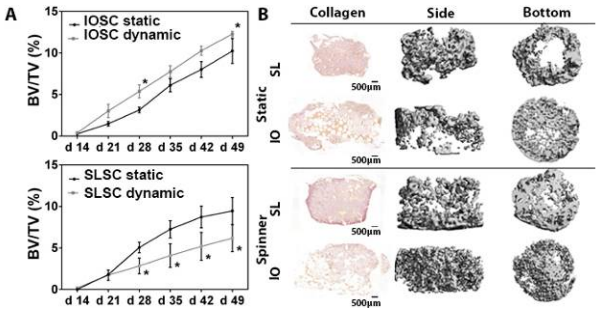

Fig. 1: (A) Mineralized ECM volume fraction of IOSC (top) and SLSC (bottom). (B) Collagen and 3D mineralized ECM distribution.

DISCUSSION & CONCLUSIONS: Dynamic culture supports a more regular mineralized ECM distribution for both scaffold types. However, the influence of dynamic culture on the mineralized ECM formation depends on the scaffold architecture. These results suggest that IOSC provides a more homogenous environment for the cells that better supports mineralized ECM formation and distribution compared to SLSC when cultured in more physiological conditions.

ACKNOWLEDGEMENTS: This project has been funded by EU Seventh Framework Programme (FP7/2007-2013); grant agreements no. 329389, 262948 and 618603.

Influence of swelling on the fatigue behaviour of composite hydrogel for disc implant

C Wyss[1], A Khoushabi[1], B Caglar[1], D Pioletti[2], PE Bourban[1]

[1] *Laboratory of Polymer and Composite Technology*, [2] *Laboratory of Biomechanical Orthopedics*

Ecole Polytechnique Fédérale de Lausanne (EPFL), Station 12, CH-1015, Lausanne

INTRODUCTION: One of the most recent treatment proposed for disco-genic low back pain is to permanently replace the core of the Inter Vertebral Disc (IVD), so-called Nucleus Pulposus (NP), through minimally invasive surgery. Recently Poly(Ethylene Glycol) Dimethacrylate (PEGDM) hydrogel reinforced with Nano-Fibrillated Cellulose (NFC) fibres is proposed as an appropriate Nucleus Pulposus Replacement (NPR)[1,2] material. In addition to the tuneable properties, that mimic those of the native tissue, it can be injected directly into the degraded disc in the liquid form and cured *in situ* via UV-light irradiation. However, reliability of the proposed material under long-term fatigue loading has to be investigated in view of clinical applications.

METHODS: The photopolymerizable hydrogels were synthesized as described previously[2]. The fatigue behavior of the composite hydrogel was investigated in cyclic unconfined compression. The hydrogel without cellulose was also evaluated as a representative of the composite matrix. The fatigue behaviour of the composite hydrogel is examined thoroughly via an extensive parametric study incorporating the influence of swelling, applied strain amplitudes and fibres concentration. In order to better understand the fatigue results, the microstructure of the composite hydrogel was analyzed with the aid of the confocal microscopy.

RESULTS: The microstructure of NFC fibres located in PEGDM matrix is shown on Fig.1a. The NFC fibres are randomly dispersed in the 3 space directions and exhibit a large size distribution.

The swollen composite hydrogel resists the high cycle fatigue test (10^7 cycles) in physiological condition of the human IVD (max 20% strain). However, elastic modulus decreases by 10% in the first cycle and stays constant throughout the rest of the test. Such softening behaviour is not present in the hydrogel without cellulose. A detailed study reveals that the composite hydrogel behaviour under cyclic loading resembles to the so-called Mullins effect[3]. A significant influence of swelling on the fatigue behaviour of the composite hydrogel is observed. As shown on Fig.1b, when a strain of 70% is applied, softening of 40% is observed in swollen samples (92 wt.% of water content), whereas a stiffness reduction of only 14% could be noted in the as-prepared state (water content of 90 wt.%). Moreover, composite hydrogels exhibit larger modulus in their swollen state contrary to the neat hydrogels.

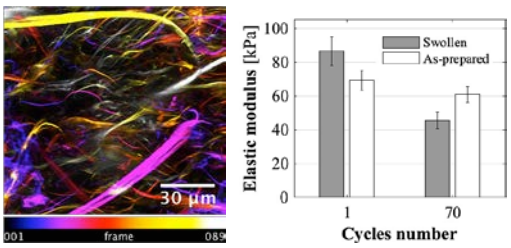

(a) (b)

Fig. 1: (a) Colour coded hyperstacks image of NFC in the hydrogel taken with fluorescence confocal microscopy (b) Influence of swelling on the elastic modulus under cyclic compression test at 70% strain.

DISCUSSION & CONCLUSIONS: The long-term fatigue study results indicate that the proposed composite hydrogel is reliable for the targeted application of NPR.

The current data suggest that the change of the 3 dimensional NFC network during swelling and cyclic deformation is responsible for observed behaviours. When the hydrogel matrix is swollen, the NFC network is pre-strained, which results in a formation of a more elastically active network and stiffening of composite hydrogel. The softening of the composite hydrogel under cyclic loading can be therefore explained by the degradation of pre-strained NFC network in the swollen state. To confirm this hypothesis, microscope imaging and modelling are currently thoroughly investigated.

ACKNOWLEDGEMENTS: The authors appreciate the support of Swiss National Science Foundation and the collaboration with EPFL-BIOP, EPFL-LBO, EPFL-LAPD and EMPA.

A study for the optimization of hyaluronan-based eye drops

A La Gatta, R Salzillo, L Corsuto, A D'agostino, M De Rosa, C Schiraldi

Department of Experimental Medicine, Second University of Naples, Via L. De Crecchio,7 80131 Naples, Italy

INTRODUCTION: One of the main challenges associated to the use of topical ophthalmic formulations is the short retention time of the components on the ocular surface. Introduction of mucoadhesive polymers in the preparation represents the most used strategy to prolong the contact time with the corneal/conjunctival epithelium [1]. Hyaluronan (HA) is frequently incorporated in eye drops to extend precorneal residence time exploiting its viscosifying and mucoadhesive properties.

A hydrodynamic and rheological characterization of several marketed HA-based eye drops was firstly provided here. Starting from this, a study aiming at optimizing HA-based eye drops efficacy, by maximizing mucoadhesiveness and viscosity (within limits suitable for the intended application) was performed. In particular, polymer molecular weight and concentration were the parameters exploited. Efficacy of the set formulations in the protection of corneal epithelium from dehydration was also investigated. A comparison with marketed products is provided.

METHODS: Hydrodynamic analyses (molecular weight, molecular size and intrinsic viscosity distributions) were accomplished using a SEC-TDA (Size Exclusion Chromatography-Triple Detector Array) equipment by Viscotek (Lab Service Analytica, Italy). The system and the analytical conditions are described in the literature [2].

Rheological measurements were performed using a Physica MCR301 oscillatory rheometer (Anton Paar, Germany) equipped with a coaxial cylinders geometry. Mucoadhesiveness was evaluated by means of viscosity measurements as previously described [3]. Mucin from porcine stomach type II was used.
Biological evaluation was performed using a primary culture of porcine corneal epithelial cells.

RESULTS: Characterization of marketed products provided data on the range of HA molecular weight and concentration used confirming literature data. Additionally, viscosity data were acquired revealing that most of the available preparations are not optimized. The effect of polymer molecular weight and concentration on viscosity and mucoadhesiveness of the formulations was studied and molecular weight/concentration pairs maximizing performance were identified. Rheological results proved that, compared to marketed products, the formulations set here performed better since exhibiting higher but still suitable viscosity and enhanced capacity to interact with mucin especially in conditions simulating *in vivo* blinking. Results from the biological experimentation proved set preparations overperforming also in terms of protection of corneal epithelial cells against desiccation.

CONCLUSIONS: Results allowed to predict for the developed formulations a longer retention on the ocular surface and, therefore, higher efficacy. In this respect, the study presented is thought to be valuable for the set up of topical ophthalmic formulations including HA to extend the precorneal residence time of the active ingredient. Biological results indicate the preparations set as promising medications for the treatment of dry eye disorders.

Correlation between viscosity and 3D printing quality of polylactide structures

J Pasquale[1], MGM. Marascio[1], JA Månson[1], D Pioletti[2], PE Bourban[1]

[1] *Laboratory of Polymer and Composite Technology*,

[2]*Laboratory of Biomechanical Orthopedics*,

Ecole Polytechnique Fédérale de Lausanne (EPFL), Station 12, CH-1015 Lausanne

INTRODUCTION: Cartilage damage leads, if left untreated, to pre-mature early arthritis affecting daily living activities. Cartilage has a really low healing potential. Its repair represents a challenging research area. Tissue engineering using biodegradable polymer scaffolds to induce regeneration is an alternative solution to conventional surgical approach having limited efficiency in the long term. While many methods exist to process biomaterials, the unique combination of 3D printing (FDM) and foaming in an integrated process constitutes a promising approach to produce scaffolds with controlled properties. Polymer viscosity is a key parameter controlling 3D printing and foaming quality. A model combining experimental data from capillary rheometer with a theoretical model (1) is proposed to assess viscosity variations for different 3D printing conditions and to define the process viscosity for foaming the printed filaments.

METHODS: PLA Natureworks D2002 grade was used as a model material to validate both the processing window of filament extrusion for 3D printing and the viscosity model. Filament extrusion processing window was built using a Noztek Touch extruder, selecting the temperature and motor speed of the extruder to produce filament diameter closer to the setpoint (1.75mm) without degrading the material. The power law coefficients of the viscosity model n and κ of PLA D2002 were extracted from isothermal capillary flow measurements using a twin-bore capillary rheometer RH7 (Rosand Precision Ldt, Sturbridge, UK). Knowing the relationship between the flow rate Q resp. with the viscosity η (eq.1) and the printing speed V_{print} (eq.2), $\eta = f(V_{print})$ plots for given temperatures were established:

$$\eta = \kappa \left[\frac{4Q}{\pi (w/2)^3} \left(\frac{3n+1}{4n} \right) \right]^{n-1} \quad \text{(eq.1)}$$

$$Q = h.w.V_{print} \quad \text{(eq.2)}$$

, where h and w are respectively the nozzle size and deposited layer height.

RESULTS: PLA D2002 filaments of constant diameter were successfully produced, validating the extrusion processing window for this model material. The viscosity model shows the influence of the input parameters split in 3D printer design parameter (nozzle size) and deposition parameters (deposition speed and temperature, layer height) on the viscosity of the printed material (Fig.1). Depending on the input parameters, viscosity ranges from 4500 to 50 Pa.s were obtained.

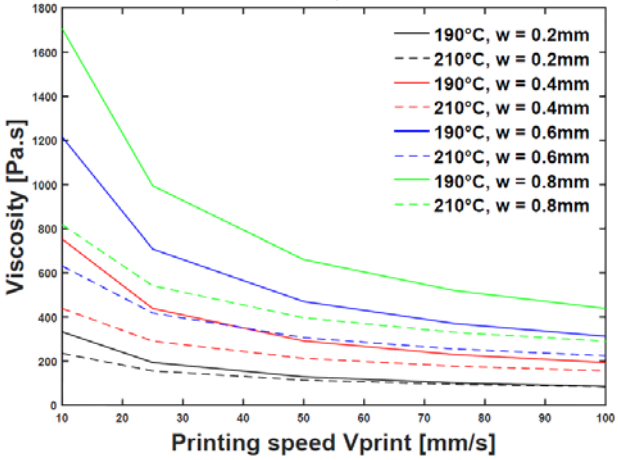

Fig.1: *Effect of the deposition speed and temperature of PLA2002D on the material viscosity at the exit of the nozzle for h=0.1mm.*

DISCUSSION & CONCLUSIONS: Following the idea of combining 3D printing with supercritical foaming technology in an integrated process, this model allows to understand the influence of the printing input parameters on the viscosity, a key material property controlling 3D printing and foaming efficiency and final scaffold properties. The developed model is applied to different biopolymers used in cartilage tissue engineering.

ACKNOWLEDGEMENTS: The Swiss National Science Foundation (grant 200021_150190) supports this research.

Using laboratory µCT for assessing peripheral nerve regeneration

C Bikis[1], L Degrugillier[2], H Deyhle[1], G Schulz[1], G Schweighauser[3], J Hench[3], B Müller[1], S Madduri[2]*, SE Hieber[1]*

*Shared senior authorship

[1]*Biomaterials Science Center, Department of Biomedical Engineering, University of Basel, CH.*
[2]*Center for Bioengineering and Regenerative Medicine, Department of Biomedical Engineering, University of Basel, CH* [3] *Institute of Pathology, Department of Neuropathology, University Hospital Basel, CH*

INTRODUCTION: Peripheral nerve injuries are increasing in number, with approximately 300,000 cases reported annually in Europe. With the existing therapeutic interventions, axonal regeneration frequently remains challenging and the functional outcome is unsatisfactory.[1] Research on biodegradable nerve conduits (NC) gained increasing importance. Thus, different materials are used with or without growth promoting agents. To assess various approaches, the nerve regrowth must be visualized inside the NC at different time points[2] This task is usually performed after standard histological preparation and immunohistochemistry, requiring dedicated equipment and considerable expertise. Resulting data are two-dimensional, consequently volume measurements are associated with sampling error and often require time-consuming serial sectioning. We thus tested a micro computed tomography (µCT) laboratory system as a complementary approach for fast and reliable imaging and quantification of nerve regeneration through the NC. Additionally, µCT is a powerful tool to select the histology cutting plane for validation purposes.

METHODS: The µCT laboratory system used was the phoenix nanotom®m (phoenix|x-ray, GE Sensing & Inspection Technologies GmbH, Wunstorf, Germany), operating at the Biomaterials Science Center at the University of Basel. It is equipped with a 180 kV source and a 3072×2400 pixels detector. The test specimen was prepared from a collagen NC implanted in a rat sciatic nerve gap model. Following formalin fixation and paraffin embedding, the NC-nerve complex was scanned. A voltage of 60 kV and a current of 310 mA were selected for the X-ray beam. In a range of 360º, 839 projections were acquired. Scanning time was less than 15 minutes. The reconstructed dataset had an effective pixel size of 27.6 µm. It was filtered with a median filter and a histogram-thresholding segmentation was then performed, using the VGL Studio Software (Volume Graphics GmbH, Germany).

RESULTS: A time-efficient scan reveals all structures of interest. Before filtering, NC and nerve dimensions can be measured manually. After filtering, the collagen tube, the nerve inside it and the surrounding paraffin have sufficient contrast for fully automatic intensity-based segmentation and volume measurements, as indicated in Figure 1. Scanning parameters will be optimized so that the entire nerve can be correctly segmented.

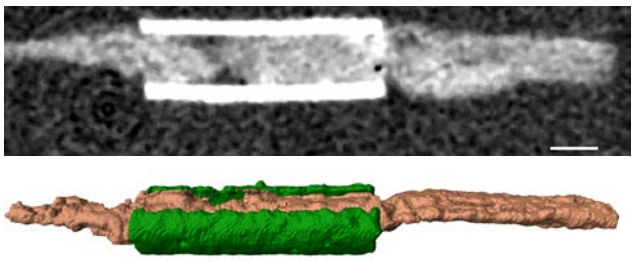

Fig. 1: The µCT scan results indicate the possibility of quantifying the growing nerve inside the collagen tube. A virtual slice of the initial, unfiltered dataset (top). The scalebar is 1 mm in length. A three-dimensional rendering of the same dataset after filtering (bottom). Region-growing segmentation allows for the three-dimensional visualization of the rat sciatic nerve (brown) inside the collagen tube (green). The surrounding paraffin has been made transparent.

DISCUSSION & CONCLUSIONS: The µCT laboratory system nanotom®m is a potent tool for the quick, non-destructive imaging of specimens and retains absolute compatibility with the established protocols. Parameters need to be adjusted for each application, after which, high automation is possible. Currently, the critical step for the full integration of such laboratory µCT systems is the increased collaboration of imaging specialists with groups working on the field of biomedical engineering and regenerative medicine.

Studying shear-stress sensitive liposomes using microfluidics

M Buscema[1], H Deyhle[1], T Pfohl[1], SE Hieber[1], S Matviykiv[1], A Zumbuehl[2], B Müller[1]

[1]*Biomaterials Science Center, University of Basel, Gewerbestrasse 14, 4123 Allschwil, Switzerland;* [2]*Department of Chemistry, University of Fribourg, Chemin du Musée 9, 1700 Fribourg, Switzerland*

INTRODUCTION: Heart diseases are among the top causes of death worldwide [1]: up to 50 % of people struck by heart attack die before arriving at the hospital. A shear-stress sensitive liposome [2] loaded with a vasodilator is a valid tool to overcome the high risk of mortality. To investigate the morphology and the mechanical properties of such promising phospholipid liposome, small angle X-ray scattering (SAXS) technique has been combined with microfluidics.

METHODS: The shear-sensitive artificial liposome 1,3-diamide Pad-PC-Pad has been synthesized [2]. The natural and no shear-stress sensitive 1,2-diester DPPC (Lipoid, Zug, Switzerland) has been used as control. Both lipid formulations were prepared by the thin lipid film hydration method and the extrusion technique [3]. Polycarbonate membranes were used to achieve liposomes of around 100 nm in diameter. The microfluidic devices were built using soft lithography combining poly(di-methylsiloxane) (PDMS), UV-curable adhesive material, and polyimide films [4]. The technique allows for building flexible and reproducible microfluidic channels mimicking diseased blood vessels [5]. SAXS measurements were carried out at the beamline ID02 (ESRF, Grenoble, France) using a photon energy of 12.4 keV and a beam size of 20×60 µm^2. The liposomes were measured both in conventional glass capillaries and in microfluidic devices. Flow simulations were performed to predict the suitable range of shear stress values, where the liposomes properties as to be studied [5].

RESULTS: Figure 1 shows a simplified scheme of the mechano-sensitive liposome based on the phospholipid Pad-PC-Pad. The inner cavity is designed to incorporate a vasodilator such as nitroglycerin (a). Flow simulations of micro-channels (b) are a valuable tool to test a wide range of shear rate values according to those one found in healthy and diseased human coronary arteries [6]. The SAXS data, which are still under evaluation, reflect the structural properties of the liposomes. Potential structural changes due to the applied shear rates can be revealed.

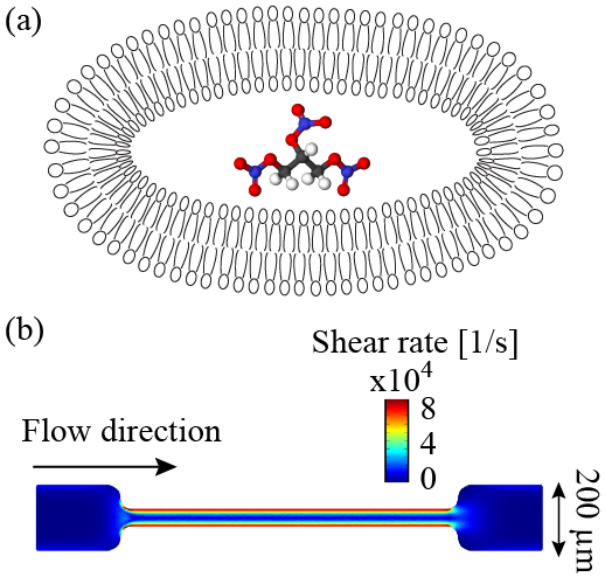

Fig. 1. Pad-PC-Pad mechano-sensitive liposome containing nitroglycerin (a); shear rate profile of a micro-channel setting the flow rate at 1 µL/s (b).

DISCUSSION & CONCLUSIONS: The optimization of the local release of a vasodilator using a phospholipid liposome is not trivial. SAXS combined with microfluidics is a precious tool to determine the structural changes due to the enhanced shear stress, as present in the diseased, stenosed human artery.

ACKNOWLEDGEMENTS: The support of Dr. T. Saxer and the financial contributions of the Swiss National Science Foundation in the frame of NRP 62 “Smart Materials”/NOstress are gratefully acknowledged. Beamtime at ESRF was granted (MD-977).

Nickel-free P558 stainless steel processed from metal powder – PHA biopolymer feedstocks

E Carreño-Morelli, M Zinn, M Rodriguez-Arbaizar, M Bassas

University of Applied Sciences and Arts Western Switzerland, 1950 Sion, Switzerland.

INTRODUCTION: Nickel-free stainless steels are used in prosthetics to avoid the harmful effect of nickel-ion release in the human body [1-2]. Metal powder injection moulding (MIM) allows net-shape processing of complex parts from metal-polymer feedstocks [3]. The feasibility of a novel binder formulation using biosourced polymer produced by bacterial fermentation [4] is explored.

METHODS: The starting powder (Fig. 1) was gas atomized P558 steel (PANACEA, Sandvik Osprey Ltd, UK, median particle size Dv50 = 6.05 µm). Polyhydroxalkanoate (PHA) binders from dried biomass (P. putida GPo1 and R. eutropha) were extracted with CH_2Cl_2 and polymer solutions were recovered using a pressure-filtration unit. Then, the extracted polymer was purified by precipitation in ice-cold MeOH. The selected binder was P(3HB-co-3HV) copolymer.

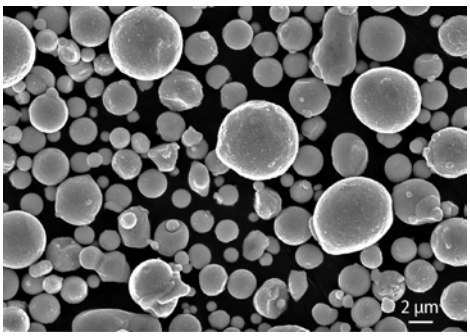

Fig. 1: P558 steel gas atomized powder

Feedstocks for MIM were prepared with a binder consisting of 45 wt% P(3HB-co-3HV), 45 wt% paraffin wax and 10 wt% stearic acid. The solids loading was 60 vol.%. Tensile test specimens were shaped using a Boy XS injection moulding machine with a mould thermalized at 40°C and a nozzle temperature of 120°C. Green parts were solvent debinded in heptane at 50°C for 20h, then thermal debinded at 500°C for 1h under argon. Steel parts were sintered at 1270°C for 3h under nitrogen in a Nabertherm VHT08-16MO furnace. Some samples were solution annealed at 1150°C 1h and water quenched. The density was measured by the Archimedes method. Tensile tests were performed according to DIN EN ISO 6892-1 method B in a Zwick 1445 machine.

RESULTS & DISCUSSION: Sintered P558 parts (Fig.2) exhibit a density of 7.45±0.05 g/cm^3 and a linear shrinkage of about 15%. The specimens are non-magnetic and the metallographic observation reveals a microstructure of twinned austenitic equiaxed grains with rounded porosity typical of MIM materials. Measured values for yield stress (YS), ultimate tensile strength (UTS) and elongation (A5) are summarized in Table 1 and compared with reference P558 commercial steel [1]. The carbon and nitrogen contents were measured by melt extraction with LECO devices as 0.15% and 0.90% respectively, with negligible increase between as sintered and annealed conditions. Both tensile strength and ductility are improved after solution annealing and quenching, which is due to the effective dissolution of Cr_2N precipitates present in the as-sintered material [5].

Fig. 2: Green (top) and sintered (bottom) parts.

Table 1: Mechanical properties of P558 steel

	YS [MPa]	UTS [MPa]	A5 [%]
MIM P558 as sintered	640	800	16
MIM 558 solution annealed	600	900	25
Böhler P558 solution annealed	≥ 520	≥ 850	≥ 45

CONCLUSIONS: Nickel-free austenitic stainless steel with good mechanical properties has been processed by MIM technology. The feasibility of using PHA natural polymers as a backbone binder constituent has been assessed.

ACKNOWLEDGEMENTS: This project was funded by HES-SO EcoSwissMade BioMIM grant.

Increased screening throughput for cell recruitment into growth factor modified PEG-hydrogel

YR Devaud[12], MP Lutolf[2], V Milleret[1], M Ehrbar[1]

[1]Laboratory for Cell and Tissue Engineering, University Hospital Zurich, Switzerland. [2]Institute of Bioengineering, Ecole Polytechnique Fédérale de Lausanne (EPFL), Switzerland.

INTRODUCTION: The healing of tissues is a complex process in which recruitment of cells into the wound and matrix deposition play essential roles. In order to better understand the underlying biological processes and to test elements influencing regeneration, it is important to dissect the problem into separate approachable questions and develop in vitro assays for each of them. Here we present a poly(ethylene glycol) (PEG) hydrogel-based 3D-in vitro model that allows to test the recruitment of cells into a healing-inducing material in a relatively high-throughput manner. In this case, we evaluate the effects of the concentration of platelet-derived growth factor (PDGF), known to trigger cell migration.

METHODS: PEG-hydrogels were made in 96-well plates using electrochemistry in order to inhibit hydrogel polymerization on the top of the gel[1]. This inhibition creates a gradient of gel density permitting cells to be seeded on top and migrate into the gel if triggered by the right growth factors.

MSCs were seeded on top of the hydrogel and standard culture media was added with different concentration of PDGF. Each experimental group had five samples. The cells were kept in culture for 3 days without changing medium until fixation of the samples.

Cells were stained with Rhodamin-Phalloidin for actin cytoskeleton and DAPI for nuclear bodies. After that, confocal imaging of 500µm stacks was automated and done on each sample. A lateral view was generated using Fiji 3D-viewer software and signal intensity at each depth was averaged. This enabled to assess the presence MSCs into the gel and evaluate recruitment efficiency depending on the growth factor concentration.

RESULTS: We were able to reproducibly form PEG-hydrogels with density gradients by electro-chemical inhibition of polymerization in a 96-well plate. MSCs showed migration into the hydrogel in a dose dependent manner. The analysis showed that MSCs don't migrate at all into the gel if not activated by any growth factor. However, the penetration depth of the cells increased significantly depending on the concentration of PDGF present in the medium.

Both the fabrication of the gel and the analysis were automated, enabling to significantly increase the throughput of the experimental procedure and its analysis.

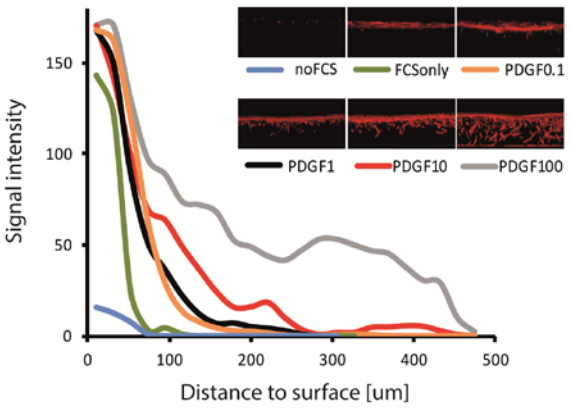

Fig. 1: Side view of 500µm gel stack showing cell ingrowth depending on the PDGF concentration (concentration in ng/ml). The graph represents the averaged signal intensity over the length of each depth depending on the depth (surface is taken as depth = 0). The more PDGF the deeper the cells migrate in.

DISCUSSION & CONCLUSIONS: The combination of advanced biomaterials with confocal imaging enabled us to advance one step towards a faster assessment of cell recruitment. In the more precise context of wound healing, this platform offers a very powerful way to screen for factors and help finding their best dose to optimise recruitment. This is absolutely necessary to understand part of the biological process of healing as well as to build the next complex material triggering wound healing

ACKNOWLEDGEMENTS: Swiss National Science Foundation for funds; Ivan Martin for providing cells; University and University Hospital Zurich.

A bioinspired nanofiber-hydrogel mimic of the cartilage extracellular matrix

FA Formica[1], E Öztürk[1], M Rottmar[2], SC Hess[3], WJ Stark[3], K Maniura-Weber[2], M Zenobi-Wong[1]

[1]Cartilage Engineering + Regeneration, ETH Zürich, Switzerland. [2]Laboratory for Biointerfaces, Empa St Gallen, Switzerland. [3]Functional Materials Laboratory, ETH Zürich, Switzerland

INTRODUCTION: Today, cartilage injuries remain a major challenge due to the lack of a stable scaffold that favors cartilage matrix production. Like most extracellular matrices (ECM) throughout the body, articular cartilage is a composite tissue made of a fibrillar collagenous network embedded in a hydrophilic environment. In cartilage, the swelling of the negatively charged glycosaminoglycans puts the collagen network under tension and gives the tissue an exceptional resistance to compressive forces. Here we report on a biomimetic of this composite structure based on electronspun fibers, polyanionic hydrogel and articular chondrocytes.

METHODS: Poly(ε-caprolactone) was dissolved at 12% w/v in $CHCl_3$/EtOH 4:1 and electrospun on a dry ice-filled mandrel (EC-CLI, IME Technologies). This porous membrane was further treated with O_2 plasma. Ultrapure alginate 1% w/v or alginate sulfate (ds 0.2) 2% w/v was mixed with a human articular chondrocyte cell suspension to obtain cell densities from 0.1 to 100x10^6 cells/ml. This solution was infiltrated onto the fibrous membrane prior to calcium cross-linking.
Ø 6 mm punches were cut and compression testing was performed to 20% strain. For the in vivo studies, alginate sulfate was used at 2% w/v. After an *in vitro* pre-culture time of 3 weeks in a TGFβ-containing media, the PCL-alginate sulfate hybrid was implanted subcutaneously in a nude mouse model and kept for 3 additional weeks.

RESULTS: Electrospinning on a dry ice-filled mandrel allowed the preparation of an ultraporous membrane. After plasma treatment, this hybrid system could be seeded with chondrocytes up to a thickness of 2 mm with tunable cell density (up to 100x10^6 cells/ml) (Fig. 1). The fibrillar component reinforced the weak alginate sulfate hydrogels, doubling their compression modulus. It allowed them to withstand an *in vivo* implantation and preserved a collagen type II-rich scaffold (Fig. 2).

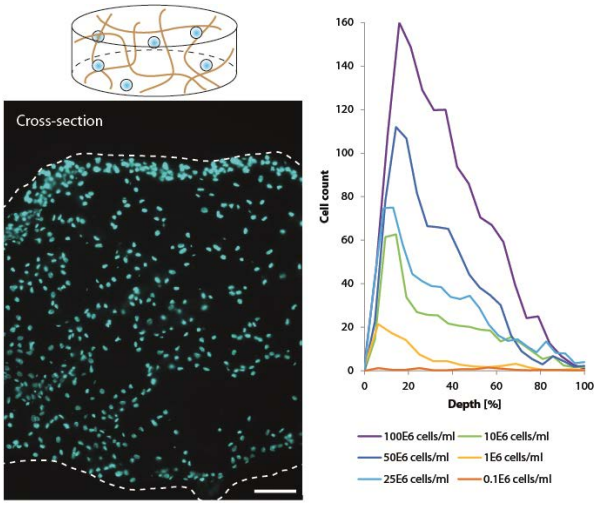

Fig. 1: (left) DAPI staining of chondrocyte-seeded electrospun scaffolds,25x10^6 cells/ml, at day 3. (Scale bar: 100 µm) (right) The total cell content could be tuned by changing the seeding density.

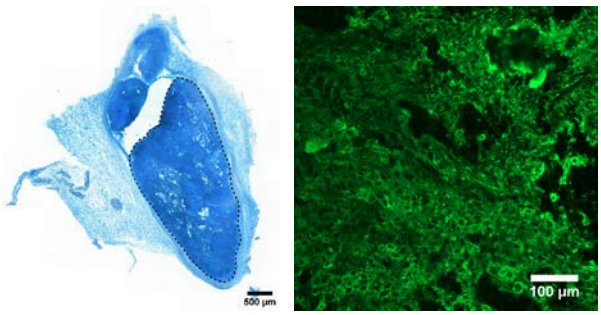

Fig. 2: After 3 weeks in vivo, the scaffolds showed a high concentration of glycosaminoglycans (left) and collagen type II, characteristic of cartilage (right). The intensity of the staining was similar to 6 weeks in vitro. Gel and fibrous scaffold (dashed line) are still visible.

DISCUSSION & CONCLUSIONS: Hydrogels by themselves do not possess all the required characteristics for successful cartilage regeneration. We here report the design of a composite cartilage ECM biomimetic, stable *in vivo*, with a high cell content and expression of chondrogenic markers.

ACKNOWLEDGEMENTS: This work was funded by the Swiss National Science Foundation (Grant 315230_159783 and 315230_143667).

Differentiation of human mesenchymal stem cells towards intervertebral disc-like cells on genetically-engineered silk

DA Frauchiger[1], S Heeb[1], LM Benneker[2], M Wöltje[3], B Gantenbein[1]

[1] *Institute for Surgical Technology and Biomechanics, University of Bern, Bern, CH.* [2] *Department of Orthopaedic Surgery and Traumatology, Inselspital, University of Bern, CH* [3] *Institute of Textile Machinery and High Performance Material Technology, TU Dresden, Dresden, DE.*

INTRODUCTION: An increasing number of people are affected by low back pain. Possible reasons are trauma and intervertebral disc (IVD) degeneration. Here we want to assess the differentiation ability of human mesenchymal stem cells (hMSC) on genetically engineered silk [1]. The silk was modified to either present GDF-6 or TGFβ_3 [2].

METHODS: Larvae of *Bombyx mori* were infected with a baculovirus to produce silk protein functionalized with either GDF-6 or TGFβ_3 (Spintec Engineering GmbH, Germany) [1]. In addition to these growth factor carrying silks unmodified silk was used as a control. The silk was harvested directly from the silk glands of *B. mori*. For the purpose of an annulus fibrosus seal the silk was designed to form a fleece-membrane composite. To test its differentiation potential hMSCs from five different donors were seeded at a density of 120,000 cells per 5x5mm^2 silk scaffold. As a control unmodified silk (cSilk) with and without exogenous GDF-6 (exGDF6, 100ng/ml) was used. Samples were cultured for three weeks in high glucose (HG)-DMEM supplemented with 2% fetal calf serum (FCS), ITS+ and vitamin C. Additionally, hMSC were cultured in monolayer with α-MEM supplemented with 10% FCS as an undifferentiated control. At defined points day 1, 7, 14, and 21 mitochondrial activity (alamar blue), glycosaminoglycan (GAG) and DNA content were determined. Additionally, gene expression of anabolic and catabolic IVD marker genes (aggrecan (ACAN), versican (VCAN), collagen 1 and 2 (Col1 and Col2), matrix metalloproteinase 3 and 13 (MMP3 and MMP13)) were assessed on day 21 relative to day 0.

RESULTS: Over the culture period of three weeks hMSC activity was in the range of monolayer control independently of the growth factor present in the silk or exogenously added to the media. Gene expression revealed that hMSC cultured on GDF-6 silk expressed more ACAN relative to Col2 (Figure 1). This indicated a differentiated MSC phenotype after culture on the silk, which was close to an NP phenotype [3]. Furthermore, catabolic genes like ADAMTS5, MMP3 and 13 showed a trend towards down-regulation compared to monolayer control while ACAN and Col2 tended to be up-regulated or stay in the range of the control like for the gene VCAN.

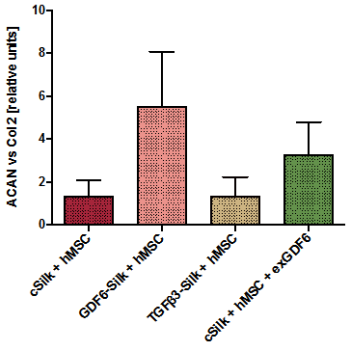

Fig. 1: Aggrecan to collagen 2 expression ratio on day 21 relative to day 0 for hMSC cultured on unaltered silk (cSilk), engineered silk with present GDF-6 (GDF6-Silk) and TGFβ3 (TGFβ3-Silk) and cSilk with exogenous GDF-6 (exGDF6) (n=5, mean plus SEM).

DISCUSSION & CONCLUSIONS: The silks' good biocompatibility assessed in previous assays could be confirmed by an increasing DNA content over the culture period. hMSCs cultured on the different scaffolds, especially GDF-6 silk, showed a favourable ACAN/Col2 ratio. Furthermore, catabolic genes were down-regulated while ACAN and Col2 showed a trend towards up-regulation, while Col1 was not up-regulated. This was suggesting that cells did not differentiate towards a fibroblastic or osteogenic but indeed towards an NP-like phenotype. Hence, it would be a good possible candidate for AF closure and regeneration.

ACKNOWLEDGEMENT: This project is supported by the Gebert Rüf Stiftung project # GRS-028/13.

Advanced 3D skin wound healing model for the study and development of materials

C Griffoni, S Chan, M Rottmar, K Maniura-Weber

Laboratory for Biointerfaces, Empa Swiss Federal Laboratories for Materials Science and Technology, St Gallen, CH.

INTRODUCTION: Due to the increasing occurrence of chronic wounds in the aging society, preclinical investigation of novel wound healing therapies is of growing relevance. One of the major issues in wound care is the absence of models enabling to assess novel treatments designed to improve healing. The need to establish reliable *in vitro* skin equivalents to be used as test systems for evaluating the effectiveness of newly developed materials is of interest for both clinicians and industry. Indeed, the involved biological mechanisms are still not completely understood and the models used so far poorly translate to the human physiology[1]. Our aim was to establish a method for the creation of a full thickness skin model (FTSM) including wound integration and healing assessment.

METHODS: FTSM was established encompassing a dermal compartment consisting of primary human fibroblasts in compressed bovine collagen 1, and an epidermal compartment consisting of primary human keratinocytes differentiated with air-lift culture (Fig. 1). Excisional wounds were created with a biopsy puncher of 2mm diameter. After wounding, a fibrin hydrogel was applied to the wound site, and the effects of fibrin on the healing process was evaluated assessing wound closure rate, imaging of keratinocyte migration and ELISA quantification of inflammatory cytokines (IL-6, IL-8).

RESULTS: After fibrin hydrogel inclusion in the wound the area appeared transparent, becoming opaque by day 7 due to epithelial cells infiltration (Fig. 2). By measuring the rate of wound closure over time, a decrease of 40% in the wounded area was detected at day 7, calculated as a percentage of day 1 (Fig. 3).

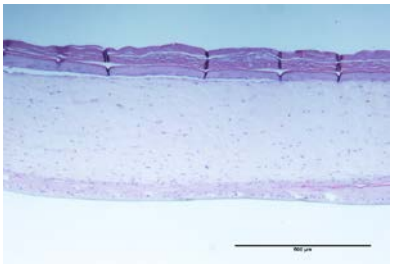

Fig. 1: Histology of one of the in vitro skin equivalents after 21 days of air-lift culture.

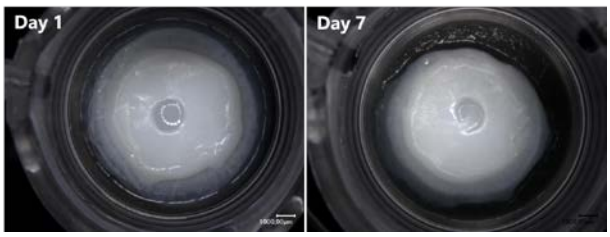

Fig. 2: Top view of the wounded FTSM created by a 2mm biopsy puncher and filled with a fibrin hydrogel, at day 1 and 7 after wounding.

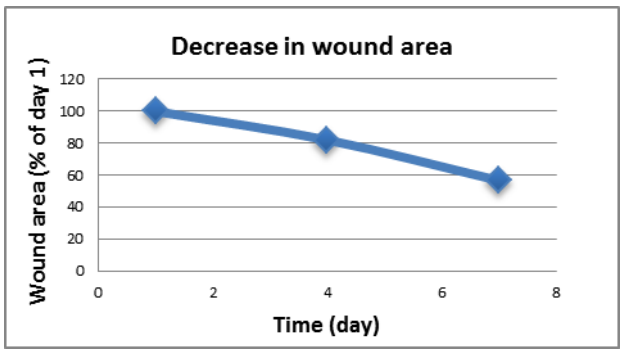

Fig. 3: Quantification of decrease in wound area with fibrin clot over time. N =2.

DISCUSSION & CONCLUSIONS: A FTSM with an excisional wounding method was established, which allow the quantification of the rate of healing in response to different wound filling materials. After the supplementation of a fibrin hydrogel, a decrease in wound area was detected over time. Since immune cells are crucial elements in wound healing, highly influencing the outcomes[2], the presence of an immune component has a high relevance when evaluating novel healing treatments. Hence, the integration of macrophages, which are the most represented cell type in wounds, in the model is currently under investigation.

ACKNOWLEDGEMENTS: This study was supported by the Commission for Technology and Innovation (KTI 16302.2 PFNM-NM).

Poly(trimethylene carbonate)-hydroxyapatite printed scaffolds for bone healing: *in vitro* and *in vivo* characterization

O Guillaume[1], M Geven[2], K Kluge[1], U Eberli[1], S Zeiter[1], D Grijpma[2], M Alini[1], D Eglin[1]

[1]*AO Research Institute, AO Foundation, Davos, CH.*
[2]*Department of Biomaterials Science and Technology, University of Twente, Enschede, NL*

INTRODUCTION: Stereolithographic process of scaffolds with controlled internal structure and degradation, and with incorporation of osteoinductive ceramic has seldom been achieved. Poly(trimethylene carbonate) (PTMC) based resin loaded with nano-hydroxyapatite (nHA) were recently produced to create implants using stereolithography (SLA)[1]. In this study, 3D macroporous scaffolds were fabricated and assessed for their osteopromotive effect *in vitro* and *in vivo*.

METHODS: PTMC-methacrylate resin mixed with nHA at 0, 20 and 40% w/w were prepared and scaffolds with 500 µm pores were fabricated by SLA. Human bone marrow stromal cells (hMSCs) were seeded at 150x103 cells/scaffold and cultivated for 4 weeks in osteogenic media. At the end of the cultivation, cell proliferation and viability was assessed using DNA quantification and Live-and-Dead staining and collagen deposition was evaluated histologically using Safranin O Fast Green. Subsequently, in vivo experiment were conducted by creating 4 calvarial defects of 6 mm Ø on 8 rabbits (agreement 19A/2015) using Codman perforator device (DePuy Synthes). After cleaning and washing, the defects were either left empty (control group) or PTMC and PTMC/nHA at 20 and 40% w/w scaffolds (Ø 6 mm x H 3.5 mm) were inserted in the cavities (Figure 1D). Following 6 weeks of implantation, osseointegration was assessed by X-ray scan and by histology (Giemsa-Eosin staining).

RESULTS: *In vitro* hMSCs were able to proliferate similarly in all SLA scaffolds (Fig 1A and B) and deposit collagen-rich matrix (Fig 1C). Following implantation (Fig 1D), the incorporation of 40% w/w of nHA in PTMC significantly increased the amount of bone formation in scaffolds in comparison to PTMC with 20% nHA (Fig 1E and F) and the osseointegration of PTMC 40% was improved compared to PTMC 20% (quantified at 70% *vs* 45% respectively).

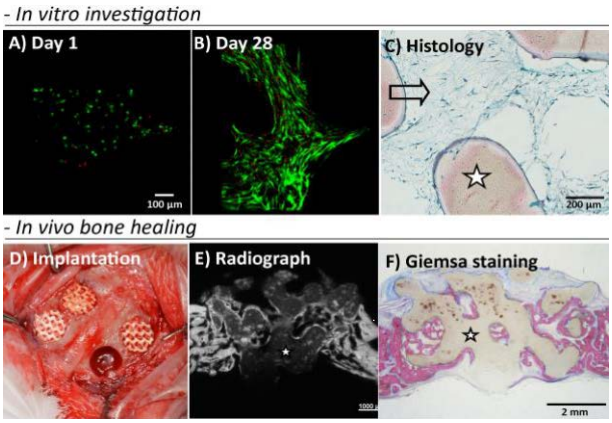

Figure 1: In vitro assessment of cells viability at Day 1 and 28 (A and B) and collagen deposition (C, in blue) on PTMC 20%. In vivo bone healing of the osteotomy filled with scaffolds (D) investigated by radiography (E) and histology (F) on PTMC 40%, stars denoted the scaffolds 'cross-section.

DISCUSSION & CONCLUSIONS:
For the first time, we reported the fabrication of PTMC/nHA-based SLA scaffolds for bone repair. This composite biomaterial exhibited excellent biocompatibility and osteopromotive effect.

ACKNOWLEDGEMENTS: NSFC-DG-RTD Joint Scheme (Project No. 51361130034) and the European Union's 7th Framework Program under grant agreement n° NMP3-SL-2013-604517.

Recycling supernumerary digits: a new source of chondrocytes

M Hertl[1], E Cavalli[1], A Gerstenberg[2], D Weber[2], M Zenobi-Wong[1]

[1]Cartilage Engineering + Regeneration, ETH Zürich, Zürich, Switzerland. [2]University Children's Hospital, Zürich, Switzerland

INTRODUCTION: This study aims to characterize a novel source of chondrocytes for cartilage regeneration therapies. We used chondrocytes from the supernumerary joints of infants who underwent surgical correction of their polydactylies. The hypothesis is that the young age of the donors means cells with a more potent chondrogenic ability (e.g. producing type II collagen and aggrecan) than sources from older patients. Chondrocytes from 1-year-old children with polydactylies on hands and feet were isolated and cultivated in order to assess their characteristics and suitability for potential cartilage defect treatments. Ongoing studies will compare the infant chondrocytes to adult chondrocytes in terms of their ability to produce cartilage-specific matrix in different concentrations of the hyaluronic acid-transglutaminase (HA-TG) gel system via histological staining and gene expression assays.

METHODS: Chondrocytes (ethics approval number KEK-ZH 2013-0097) were isolated from samples via collagenase digestion and passaged three times before suspending in gels. Three different seeding densities and three different gel densities were assayed. Gels were crosslinked in PDMS molds (8mm outer diameter, 4mm inner diameter) and cultured in TGFβ-containing chondrogenic media for three weeks. Levels of chondrogenic markers (collagen II and aggrecan) as well as markers of chondrocyte de-differentiation (collagen I) were measured via RT-qPCR and visualized via immunostaining.

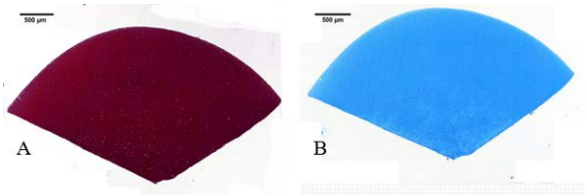

Fig. 1: Native cartilage from 7-month-old female with polydactyly stained with Safranin O (A) and Alcian Blue (B).

RESULTS: The native cartilage samples were stained with Safranin O (Fig. 1A) and Alcian Blue (Fig. 1B) and showed high levels of glycosaminoglycans indicating the presence of large amounts of chondrogenic markers. Collagen II production was increased the most in 2% gels seeded with 15 million cells (Fig. 2B, E) with a 20,000-fold increase in production over day 0 (Fig. 2, I), but for all other seeding densities 1% gels performed best (Fig. 2A, D) and 3% gels the worst (Fig. 2C, F). The levels of collagen I were relatively low for all conditions (Fig. 2H).

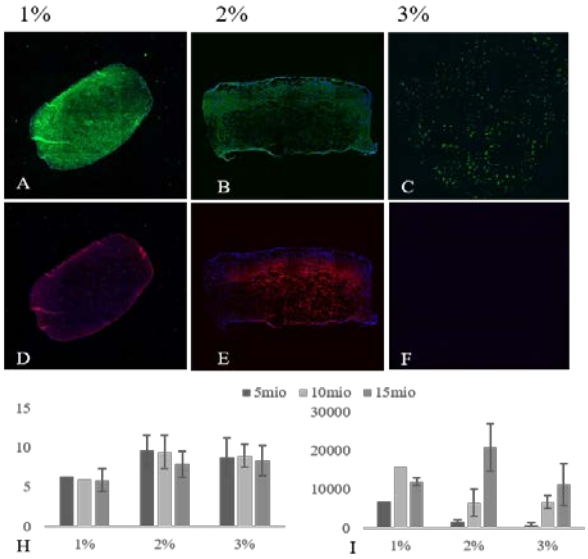

Fig. 2: 1%, 2%, and 3% HA-GT gels seeded with 15 million cells. Collagen II + DAPI (A-C) and Collagen I + DAPI (D-F). Fold increase in Collagen I (H) and Collagen II (I) RNA over a Day 0 sample of all gel conditions with standard error. (n=1 for 1% 5 and 10 million, n=3 otherwise).

DISCUSSION & CONCLUSIONS: The results from this study indicate that infant chondrocytes from polydactylies appear to be a promising source of cells for cartilage regeneration. High levels of desirable collagen II are produced with relatively low levels of undesirable collagen I present. Future experiments should focus on specific gel and seeding density conditions (1%, 15 million), comparison with adult chondrocytes, and test growth kinetics, as well as mechanical and proliferation properties of the cells.

ACKNOWLEDGEMENTS: This project was funded by the ETH Foundation (Grant ETH-50 13-1).

Bone evaluation of stem cell treatments in jaw bone

SE Hieber[1], C Jaquiery[2], C Kunz[2], B Ilgenstein[1], B Müller[1]

[1]*Biomaterials Science Center, University of Basel, Allschwil, Switzerland.* [2]*Department of Cranomaxillofacial Surgery, University Hospital Basel, Basel, Switzerland*

INTRODUCTION: Distraction osteogenesis proved to be powerful for correcting craniofacial deformities, especially in younger patients. The simultaneous expansion of the bone and the surrounding soft tissue promises an enhancement of further growth and stability[1]. The time effort is a main drawback of the procedure resulting in high costs and the risk of disturbed healing during the consolidation period. Therefore, the current challenges are the increase of the distraction rate and the acceleration of osseous consolidation while preserving the bone quality.

METHODS: The effect of additional stem cell supply was studied on 4 nude rats (CR) in a pilot study. Human stem cells were injected at the beginning of the protocol into two rats. Two rats served as control. After a latency period of five days, linear distraction was performed at a regular rate of 0.5 mm/day up to a distance of 6 mm. The specimens were harvested 40 days after distraction before full consolidation[2].

The three-dimensional (3D) imaging of the extracted jaws was carried out post mortem using nanotom®s (GE, Wunstorf, Germany). The nanotom is a 180-kV nanofocus scanner, that accommodated the entire jaw with a maximal length of 16 mm (pixel size 6.9 µm). After decalcification, the rat mandibles were scanned at the beamline BW 2 (HASYLAB, DESY, Hamburg, Germany). Synchrotron radiation- based µCT (SRµCT) measurements in absorption contrast mode were performed using a photon energy of 14 keV with a pixel size of 2.5 µm. VG Studio Max 2.1 (Volume Graphics, Heidelberg, Germany) served for the 3D representations and their slices.

RESULTS: Fig. 1 shows the results of the CT scans of the mandibles before de-calcification. The 3D representations and the 2D slices above show the differences in the mineralization with stem cells injection (left) and without one (right). Complete osseous bridging of the distraction gap is observed after stem cell treatment, whereas osseous healing remains incomplete otherwise. The SRµCT measurements confirms the findings and enables the comparison to histological slices.

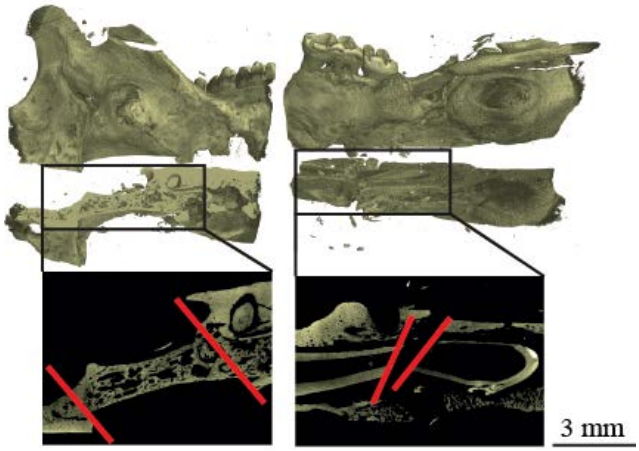

Fig. 1: The quantity of the newly formed bone can be evaluated in the 3D representations and virtual cuts of the mandibles after regular distraction with injection of stem cells (left) and without injecting stem cells (right) scanned by the nanotom® s before de-calcification.

DISCUSSION & CONCLUSIONS: The combination of high-resolution µCT with dedicated histology permits the optimization of distraction osteogenesis incorporating stem cells before starting the distraction. The CT scans revealed the enhancement of bone formation with complete bridging of the interzone, whereas in the control animal an unmineralized interzone remained. CT-analysis is a non-destructive tool to identify the mineralization complementary to histological slices and to determine regions and cutting directions for histology.

ACKNOWLEDGEMENTS: The authors thank Nunzia Di Maggio for the preparation of the stem cells and Gernot Jundt for the histological results. Beamtime was granted through the project proposals I-20110780 EC and I-20110555 EC (HASYLAB at DESY, Hamburg, Germany).

Gel-phase 3D bioprinting of a physical hydrogel to create cell-laden scaffolds perfused by a channel network

B Kessel[1], R Wieduwild[1], Y Zhang[1]

[1] *B CUBE Center for Molecular Bioengineering, Technische Universität Dresden, Dresden, Germany.*

INTRODUCTION: In this study we present gel-phase bioprinting [1] of a novel bioink. The ink is based on a physical hydrogel containing starPEG-peptide conjugates. Peptides need to consist of multiple repetitions of B (basic residue lysine or arginine) and A (alanine) built up in a $(BA)_n$ scheme. Electrostatic interactions, as well as heparin-induced α-helix formation of these peptides play an important part in the assembling process [2] (Fig. 1). Utilizing this bioink we could realize bioprinting of stable matrices with incorporated channel networks and embedded cells with high cell viability.

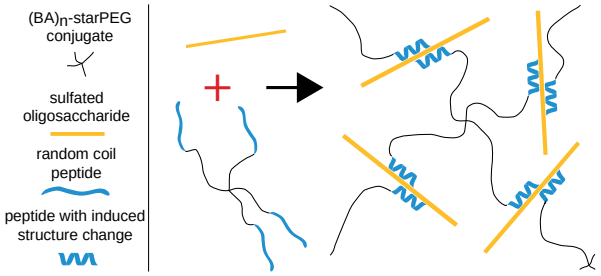

Fig. 1: Scheme of non-covalent hydrogel formation based on peptide oligosaccharide interaction [2].

METHODS: For bioprinting, an in-house built microextrusion based 3D printer was used consisting of a piston driven syringe with a 200 µm needle for extrusion. A solution of starPEG-RGDSP-$(KA)_5$ together with neural precursor cells (NPCs) and growth factors (FGF2 and EGF) was prepared in neural basal media. Solution was mixed with dextran sulphate and transferred into 250 µl borosilicate syringes. Mixture gels within 5 min and hardens over time. After 1 hour the hydrogel with embedded cells was printed into 35 µm well dishes. For this task, we created 3D models containing channel networks with openSCAD and generated viable G-code with Slic3er. Printer control was done with RepetierHost. Printing speed was at 30 mm / s.

RESULTS: StarPEG-RGDSP-$(KA)_5$ mixed with dextran sulphate yields hydrogel with a stiffness above 10 kPa after 1 hour of gelation time. Stiffness can be adjusted by changing the length and amino acids of the $(BA)_n$ part of the peptide conjugates. During printing, bulk hydrogel is pushed into the steel needle and gets fragmented in microscopic particles in the process. These particles stick together and fuse again, which results in bulk hydrogel rearranging into a filament shape. This way, a continuous gel filament can be created (Fig 2a). Printed structures consisted of up to 10 layers (layer height: 200 µm) with channels completely surrounded by gel. Gel filaments are stable enough to support subsequent layers without any collapse of filaments or channels (Fig. 2b + c). Cell viability assays of printed structures showed a cell survival rate above 90%.

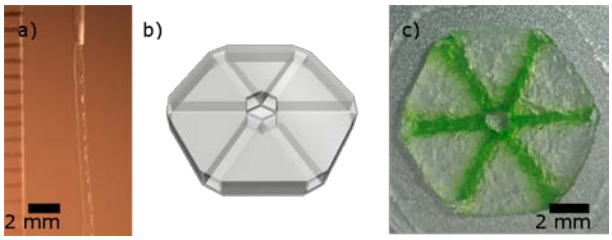

Fig. 2: a) Bioink extruded through a needle in gel-phase results in a consecutive filament that can be deposited. b) 3D model of a hexagonal structure pervaded by a channel network. c) Bioprinted realization of the hexagonal model. Channels are flushed with food colour for better visualization.

DISCUSSION & CONCLUSIONS: We present gel-phase printing of a stiff, physical hydrogel that can be used to print channel perfused structures. No sacrificial material is needed to create channels and no additional crosslinking is required to ensure long term stability of the cell-laden scaffolds. The sticky behaviour of the hydrogel allows for a workflow similar to conventional plastic or paste 3D printers. Hardware as well as software can be adopted with minimal adjustments and efforts, resulting in an easy to use bioprinting solution.

ACKNOWLEDGEMENTS: We thank the BMBF for financial support (grant 03Z2EN12 and 03Z2E511).

Single grating X-ray phase-contrast tomography for evaluation of brain tissue degeneration on cellular level

A Khimchenko[1], G Schulz[1], I Zanette[2], M-C Zdora[2,3], A Hipp[4], H Deyhle[1], S E Hieber[1], C Bikis[1], G Schweighauser[5], J Hench[5], P Thalmann[1], B Müller[1]

[1] *Biomaterials Science Center, Department of Biomedical Engineering, University of Basel, Allschwil, CH.* [2] *Diamond Light Source, Didcot, UK.* [3] *Department of Physics and Astronomy, University College London, London, UK.* [4] *Helmholtz-Zentrum Geesthacht, Geesthacht, DE.* [5] *Institute of Pathology, Department of Neuropathology, Basel University Hospital, Basel, CH.*

INTRODUCTION: Three-dimensional (3D) characterization of brain tissues on cellular level is attractive for neurodegenerative studies as it can improve understanding of such diseases that cause a progressive deterioration as Alzheimer's or Parkinson's diseases. Grating-based X-ray phase-contrast micro tomography (PCμCT) is a non-destructive 3D imaging modality that allows simultaneous reconstruction of absorption, phase and scattering (dark-field) data [1], which is suitable for visualization of soft and hard tissues [2] with cellular resolution, and which can be implemented into a laboratory environment. The aim of the present study is to evaluate performance of the single-grating interferometry for a brain tissue investigation, using a human cerebellum block as an example.

METHODS: A human cerebellum extracted from a 73 year-old male was visualized *post mortem*. The tissue was formalin-fixed, dehydrated and paraffin-embedded. Cylindrical specimens were 4 mm in diameter and 23 mm in height. The imaging data was acquired using a single-grating setup at Diamond Manchester imaging beamline I13-2 (Diamond Light Source, Didcot, UK). The tomography was performed over 180º with a step of 0.15º, at a mean photon energy of 19 keV, using Ni grating with a periodicity of 10 μm and structure height of 10 μm, effective pixel size of 2.3 μm, at a grating-detector distance of 72 cm, corresponding to a 1st Talbot order.

RESULTS: As demonstrated in the selected slice in Fig. 1, PCμCT data reveals a variety of tissue types including *stratum granulosum* (1), *stratum moleculare* (2) and white matter (3), individual blood vessels and a diversity of cell types. These presumably include Purkinje cells (white arrow), granule cells in the *stratum granulosum*, and stellate cells in the *stratum moleculare*. The phase images reveal inner structures of the tissue with high contrast while the absorption data provides a complementary edge enhancement.

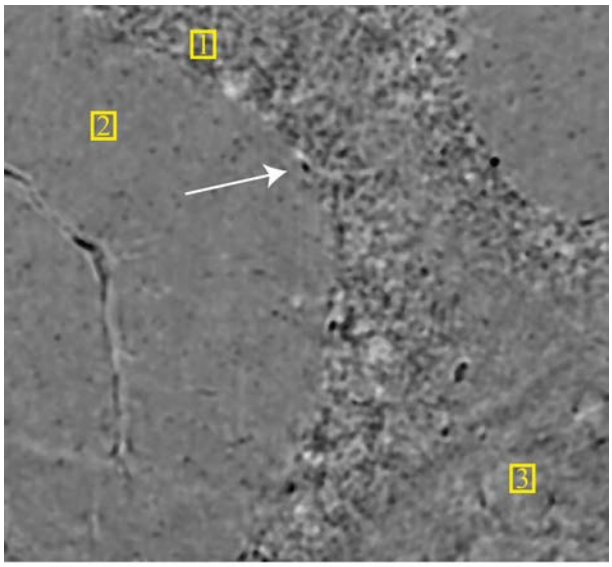

Fig. 1: Combined slice of the absorption- and phase-contrast data of a human cerebellum showing the variety of cell types. 1: stratum granulosum; 2: stratum moleculare; 3: white matter; white arrow: Purkinje cell.

DISCUSSION & CONCLUSIONS: PCμCT is well suited for 3D characterization of physically soft tissues as it provides a superb price-performance ratio between spatial resolution, density contrast, and required time. PCμCT bears the potential to become an important auxiliary modality in neurodegenerative disorders research.

ACKNOWLEDGEMENTS: The financial support of the SNSF project 147172 and the beamtime proposal MT13164-1 is acknowledged. The support of P. Thibault, C. Rau and J. Vila-Comamala is highly appreciated. Grating was kindly provided by HZG, G eesthacht, Hamburg.

Targeting selective cell response by topographical structuring of resorbable polymer implants

J Koeser[1], U. Bruggisser[2], S Beck[3], PM Kristiansen[2]

[1]FHNW University of Applied Sciences and Arts Northwestern Switzerland, School of Lifesciences, Institute of Chemistry and Bioanalytics, Muttenz, CH. [2]FHNW University of Applied Sciences and Arts Northwestern Switzerland, Windisch, CH. [3]DePuy Synthes, Oberdorf, CH.

INTRODUCTION: Resorbable plates and screws based on poly(lactide-co-glycolide) (PLGA) are increasingly used in facial restorations. Such implants require special properties since they interact on one side of the implant with bone tissue while the other side is in contact with connective/fibrous tissue. Here we investigate and compare the interaction of osteoblasts with subcellular sized feature (5-20 µm) patterned substrates in order to identify specific effects on cell morphology and proliferation.

METHODS: A 4 inch silicon wafer master harbouring 13 regions (2 x 2 cm) with different subcellular sized features (5-20 µm, 5 µm height) was successfully replicated into PLGA films by hot embossing. MC3T3-E1 pre-osteoblastic cells were cultured on the microstructured PLGA substrates and their morphology and nuclear shape subsequently analyzed by fluorescent staining of the actin cytoskeleton with rhodamine-phalloidin and DNA with DAPI. The proliferation of MC3T3-E1 cells on the different pattern was determined by a metabolic resazurin assay on cut samples in 48 well plates.

RESULTS: It was observed that on substrates with regular or irregular shaped well structures cells preferred to grow on top of the structures whereas on pillar structures the majority of their cell bodies were found squeezed in between the elevations as evidenced by the deformed nuclei in between individual pillars (Fig. 1 c, c'). To assess influences of certain substrate patterns on cell proliferation MC3T3-E1 osteoblast cells were grown on structured PLGA substrates and quantified using the metabolic stain resazurin. All patterns examined reduced cell metabolism/ proliferation as compared to flat PLGA substrates, with the strongest effects being an inhibition of more than 40% (structures marked in red in Fig. 1b).

DISCUSSION & CONCLUSIONS: Here we present data on the influence of micropatterned PLGA substrates on adhering osteoblast cells.

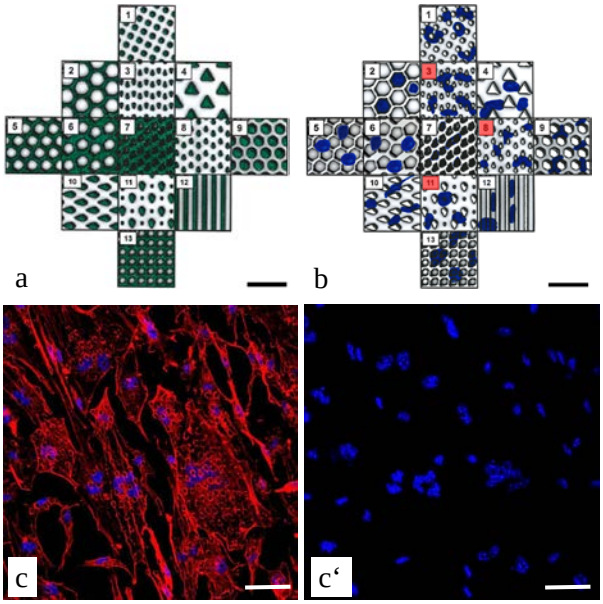

Fig. 1: Cellular responses to different substrate patterns. Scheme of the multi-patterned PLGA substrate indicating the top of the embossed structures in green (a), as well as the nuclear morphology of attached MC3T3-E1 osteoblasts (b). Pattern reducing cell metabolism/proliferation most are marked in red. (c, c') fluorescently stained sample images of cells on pattern 3. Scalebars: 50 µm.

Both, the cell cytoskeleton and the nuclear morphology were largely influenced by the analysed subcellular sized features. Furthermore cell metabolism on protruding patterns was reduced by up to more than 40% which makes them suitable target structures for PLGA implants were reduced osteoblast cell metabolism/ proliferation is desired as e.g. on areas which face the connective tissue. Thus microstructuration represents a simple approach towards the modification of specific cell proliferation on non load-bearing resorbable PLGA implants used in facial restorations.

ACKNOWLEDGEMENTS: The presented research was kindly funded by the Swiss Nanoscience Institute under the Nano Argovia program.

Activation of ligamentocytes from the anterior cruciate ligament on 3D collagen patches with platelet rich plasma (PRP)

A Krismer[1], R Cabra[1], S Kohl[2], A Tekari[1], DA Frauchiger[1], RD May[1], SS Ahmad[2], B Gantenbein

[1] *Institute for Surgical Technology and Biomechanics, University of Bern, CH,* [2] *Department of Orthopaedic Surgery and Traumatology, Inselspital, University of Bern, CH*

INTRODUCTION: Rupture of the anterior cruciate ligament (ACL) is the most common ligament injury with high complication rates [1]. The current treatment strategy is the replacement with a local autograft because of the poor healing capacity of the ACL. Therefor we investigated the biological healing potency of ACL ligamentocytes (LCs) comparing two different protocols producing platelet rich plasma (PRP) and their potential to "activate" ACL-derived LCs in an *in vitro* co-culture set-up on clinically FDA-approved 3D collagen patches. Thus, we hypothesized that primary LCs can be stimulated for increased wound healing potential by the application of allogeneic PRP, which releases multiple different growth factors.

METHODS: PRP was produced from fresh whole blood samples (N = 3 donors) according to two different protocols: i) instructions of the Platelets Matter/GPS® III commercial Kit, and ii) according to Yoshida *et al.* [2]. ~30k LCs (N = 3 donors) were seeded on the rough side of collagen patches (⌀ 8mm, ChondroGide™, Geistlich, Wohlhusen) [3]. LCs were seeded in 12-well plates in duplicates and stimulated with allogeneic 2.5% and 20% PRP in medium, separated by co-culture inserts with a high-density PET membrane (0.4 µm pore size, BD, Belgium). PRP was freshly produced from fresh blood samples and refreshed every 2-3 days (ethically approved). Culture medium was serum-free high glucose (HG)-DMEM (Gibco, Basel). DNA content, cellular activity (resazurin red assay for 3h), collagen content (hydroxyproline = HYP content) was quantified at day 7, 14 and 21.

RESULTS: The results of the PRP protocols demonstrated that both protocols significantly enriched platelets (Fig. 1A). However, Biomet also contains a higher level of white blood cells compared to Yoshida (Fig. 1B). For both, 2.5 and 20% PRP, DNA and cellular activity showed a significant up-regulation after exposure of 14 and 21 days relative to seven days. No such effects were found using PRP produced by Yoshida *et al.*'s protocol or using medium with 10% fetal calf serum (FCS) as a control.

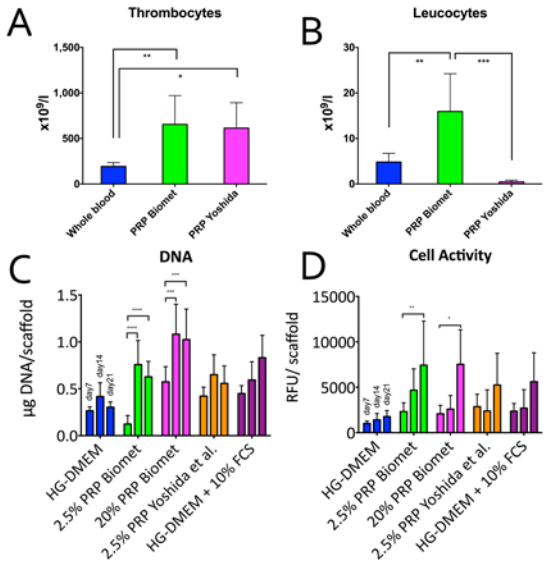

*Fig. 1: Comparison of **A**. Thrombocytes (N = 8, mean ± SD) and **B**. Leucocytes concentration (N = 8, mean ± SD) in PRP according to the protocols by Biomet™ and Yoshida et al. and whole blood **C.** DNA content of PRP stimulated LCs (N = 3, mean ± SD) on 3D collagen matrices **D**. Cellular activity of LCs (N = 3, mean ± SD) (One-Way ANOVA * = P < 0.05, ** P < 0.01, *** = P < 0.001).*

DISCUSSION & CONCLUSIONS: LCs are responsive to PRP produced by Biomet's protocol, which contains about four times more leucocytes than whole blood. It cannot be excluded that the leucocytes released additional factors, which might have led to the increase of cell proliferation and activity of the LCs on collagen patches. These intercellular effects can be addressed by increasing pore size to 5 or 8 µm, enabling cell migration in future experiments. Regenerative effect of PRP can be confirmed, however, in a clinical setting the PRP can only be used once, at the time of surgery.

ACKNOWLEDGEMENTS: This project was funded by the Insel Grant support to SS Ahmad**.** Eva Roth assisted in biochemical assays.

Synthesis of Monetite platelets for composite bone graft substitutes

B Le Gars Santoni[1,2], C Stähli[1], N Döbelin[1], L Galea[1], P Bowen[2], M Bohner[1]

[1]RMS Foundation, Bettlach, Switzerland. [2]EPFL, Department of Materials, Lausanne, Switzerland.

INTRODUCTION: The self-healing ability of bone is limited to small defects. If too large, surgical intervention and implantation of a bone graft may be required. However, auto- and allografts are associated with donor site morbidity or disease transmission respectively, thus highlighting the importance of developing synthetic bone graft substitutes[1]. The main challenge is to combine in one material biocompatibility, resorbability and load-bearing properties[2]. Hence, current approach consists in composites made from biodegradable polymers and reinforced with bioactive inorganic materials (e.g. CaP ceramics) which should be non-agglomerated, have a large aspect ratio, be monodisperse and have a uniform shape[2]. Recently, a composite made with a chitosan matrix reinforced with calcium phosphate platelets was developed in our group[1,2]. Nonetheless, although monetite ($CaHPO_4$) platelets were found to be a promising reinforcement due to their good adhesion to chitosan and their large aspect ratio[2], reproducible synthesis of such platelets is still challenging and a better understanding of the relationship between synthesis parameters and the platelet geometry is required.

METHODS: Monetite platelets were synthesized by precipitation from ethylene glycol reagents containing $CaCl_2$ and H_3PO_4. The pH was adjusted with a NaOH solution, and the temperature was kept at 100°C to 170°C during 90 min. Platelet shape and dimensions were assessed by scanning electron microscopy (SEM).

RESULTS: Several reaction parameters were studied in order to examine their influence on monetite platelets. The NaOH concentration involved in the reaction had mainly an effect on the platelet morphology. Namely, with a low concentration of NaOH, the pH of the solution was too acidic and high amounts of three-dimensional (3D) monetite clusters were obtained, whereas if the NaOH concentration was too high, the pH was too basic and mainly beta-tricalcium phosphate (β-TCP, $Ca_3(PO_4)_2$) hexagonal platelets were obtained. Hence, a NaOH concentration of 19 mM was found to be a good compromise in order to obtain uniform monetite parallelepiped platelets. The temperature was also found to influence the particle shape (Fig. 1): at 100°C, thick sheet-like particles were obtained. Increasing the temperature to 130°C led to monetite 3D clusters whereas more defined parallelepiped monetite platelets exhibiting high aspect ratios (up to 30) were obtained at 160-170°C along with a complete elimination of the 3D clusters. Experiments with variable Ca/P ratio conducted at 19 mM and 150°C showed that the Ca/P ratio had no effect on the dimensions of the monetite platelets. Only the size dispersion seemed affected by the ratio and was increased by 36% by reducing the Ca/P ratio from 1.5 to 1.0.

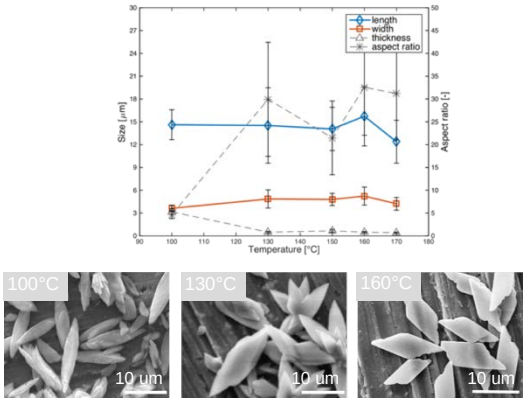

Fig. 1: Influence of Temperature on the geometry of monetite platelets produced by precipitation.

DISCUSSION & CONCLUSIONS: In order to obtain uniform monetite parallelepiped platelets with a high aspect ratio, no clusters and no secondary phases, the effect of several reaction parameters were investigated. From these results, the best reproducibility and suitable geometry were found at 160°C, with a NaOH concentration of 19mM, a total precursor concentration of 32mM and a Ca/P ratio of 1.5. These new monetite platelets are consequently promising reinforcements in load-bearing composite bone substitutes.

ACKNOWLEDGEMENTS: Swiss National Science Foundation (SNF; 200021_13758).

Developing strategies to promote chondrocyte outgrowth in 3D scaffolds

CSJ Levinson[1], E Cavalli[1], G Salzmann[2], M Zenobi-Wong[1]

[1]*Cartilage Engineering + Regeneration, ETH, Zürich;* [2]*Schulthess Clinic – Musculoskeletal Center, Zürich*

INTRODUCTION: Articular cartilage has a very low healing capacity upon injury and no optimal surgical procedure exists. Cartilage autograft implantation system (CAIS) is a promising treatment in which non-load-bearing cartilage is removed from the patient, minced, and placed together with a biomaterial in the defect [l]. However, the conditions which optimally promote outgrowth of chondrocytes from the cartilage chips are still unknown. A custom hyaluronan (HA)-derived hydrogel was shown previously to preserve the chondrogenic properties of immature chondrocytes [2]. Its biomimetic properties led us to hypothesize that functionalized, it could be used to enhance outgrowth of chondrocytes. Specifically, we hypothesized that non-covalent binding of growth factors (GFs) through addition of heparin could augment cell outgrowth.

METHODS: Human knee articular cartilage was minced and digested with collagenase (1 mg/ml). Cartilage chips were embedded in fibrin glue for the screening of conditions. The samples were cultured in medium containing 10% FBS, at 37°C, 5% CO_2. Staining with DAPI and phalloidin was done on 2 mm thick cartilage rings filled with HA gel and cultured 6 weeks in complete medium, fixed in PFA. Images were acquired with a Zeiss Apotome microscope and analyzed with Fiji.

HA gels were obtained by grafting lysine- or glutamine- donor peptides, which can be crosslinked by activated factor XIII, to the HA polymers [2]. Glutamine-donor peptides were covalently bound to heparin to crosslink it to the HA backbone (1 mg/ml of heparin in HA). BSA release was studied by quantifying the mean intensity of fluorescence of a fluorescein-tagged BSA loaded in the gels. FGF2 release was monitored with Elisa (R&D Systems).

RESULTS: To systematically compare the different conditions, we first established a method to quantify outgrowth. The number of migrating cells was determined by counting the number of nuclei stained with DAPI (Fig. 1A, 1140 nuclei),the fraction of the perimeter of the explant and the fraction of the area of the gel, respectively 31.6% and 24%, were calculated using the phalloidin staining (Fig. 2B).

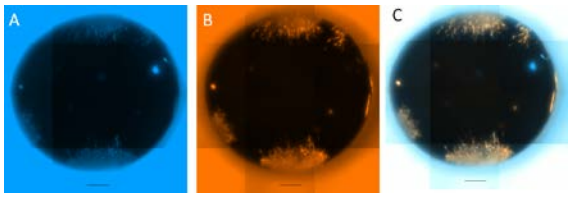

Fig. 1: DAPI (A) and phalloidin (B) staining with overlay (C). Scale bar: 500 µm.

Using fibrin as a gel, we observed that digestion shortened the time before onset of outgrowth from 10 to 7 days. Interestingly, 70% of non-digested samples displayed outgrowth after 10 days. This underlines the importance of serum to drive outgrowth, probably due to the high GFs content. We subsequently tested FGF2 release in HA gels. HA alone did not bind proteins, but showed a burst release (Fig. 2A). The addition of heparin resulted in a prolonged binding of FGF2 (200 ng/ml in the gel initially) (Fig. 2B).

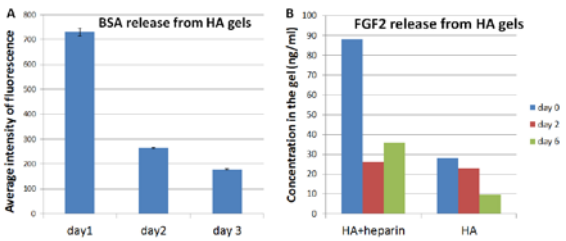

Fig. 2: Protein release studies with (A) BSA (3 gels per condition) and (B) FGF2 (1 gel per condition).

DISCUSSION & CONCLUSIONS: We present a novel system to determine the optimal parameters (digestion method, active molecules) which favour cell outgrowth. These findings represent an important step before CAIS can provide reproducible clinical outcome. Further work will aim at finding the most efficient molecular cues (GFs and homing factors) to enhance chondrocyte outgrowth.

Inducing chondrogenic redifferentiation by combining an engineered C3 exoenzyme and vinylsulfone-modified electrospun PCL fibers

N Lobsiger[1], FA Formica[1], M Zenobi-Wong[1]

[1]*Cartilage Engineering + Regeneration, ETH Zürich, Switzerland*

INTRODUCTION: Cartilage defects are a prevalent pathology in our society and current treatment approaches are limited. We pursue an interdisciplinary approach combining protein engineering and advanced biomaterials. The aim is to create a stable electrospun, nanofibrous 3D scaffold system for controlled release of a cross-linked Rho-inhibiting drug. A bacterial C3 transferase has previously been identified to enhance extracellular cartilage matrix production. However, the wild type protein does not possess a chemical handle that would allow specific cross-linking to a delivery matrix. This chemical modification, used to link the C3 transferase to the PCL scaffold, was added in this project.

METHODS: The C3 exoenzyme (Mw: ~25kDa) was designed to include a cysteine, a MMP-cleavable tag and a cell-penetrating peptide and was expressed in E. Coli (BL21(DE3)). Expression conditions were optimized employing a fluorimetric activity assay based on NAD^+ cleavage. Thereafter bovine chondrocytes (Passage 2) were supplemented with different drug concentrations and effects on both cellular shape (brightfield microscopy) and cartilage matrix deposition were examined.
For electrospinning, a blend of modified and unmodified polycaprolactone (PCL) was used. PCL (~14kDa) was functionalized with a vinyl sulfone (VS) moiety allowing for Michael-addition with molecules containing a thiol-group. In the final step, cross-linking of the protein was performed post-spinning in a TEOA buffer at pH 8. To enlarge the pool of possibilities to tune the release, we employed oxygen plasma treatment to the fiber surface and observed the effect. To allow monitoring of the protein binding/release profile, RhodamineB-labeled BSA was used as a model.

RESULTS: Different variants of functional C3 protein were successfully. We obtained variants showing an activity comparable to the commercially available product (Cytoskeleton, CT04) in the fluorimetric assay, but only effective on cells when added at an around 700x higher concentration. (*Fig. 1)*. For the nanofiber scaffolds, binding of RhoB-BSA correlated with the amount of VS-functionalized PCL (*Fig.2*). The effects of oxygen plasma treatment on the surface and thereby RhoB-BSA binding are under further investigation.

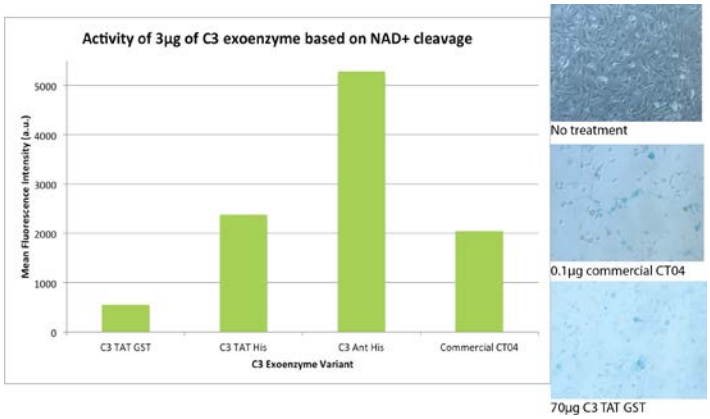

Fig. 1: Graph comparing the activity of different C3 variants with the activity of the commercially available drug CT04. Images with alcian blue staining showing the production of glycosaminoglycans (GAGs) by cells stimulated with C3 exoenzyme.

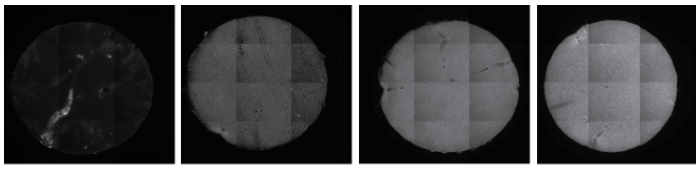

Fig. 2: Images showing the fluorescence intensity of RhoB-BSA cross-linked to PCL fibers. The intensity and therefore the amount of cross-linked RhoB-BSA increases with increasing amounts of VS-functionalized PCL added to a constant amount of non-functionalized PCL.

DISCUSSION & CONCLUSIONS: 3D nanofibers are promising materials for tissue engineering as they structurally mimic the fibrous component of the native ECM. In this work we combine methods of protein engineering with electrospinning. We envision the final result to be a scaffold containing a biologically active drug, which is released in a sustained manner. Due to its versatility, this approach can be extended to other polymers and drugs.

ACKNOWLEDGEMENTS: This work was funded by the Swiss National Science Foundation (Grant 315230_159783 and 315230_143667).

Crosslinking chemistry of hyaluronan-tyramine hydrogels alters mesenchymal stem cell attachment and behaviour

C Loebel[1,2], B Cosgrove[3], M Alini[1], M Zenobi-Wong[2], RL Mauck[3], D Eglin[2]

[1]AO Research Institute, AO Foundation, Davos, CH. [2]ETH Zurich, Switzerland Cartilage Engineering + Regeneration, Department of Health, Science and Technology, [3]University of Pennsylvania, Philadelphia, PA, USA

INTRODUCTION: Given the significance of hydrogels as cell-instructive materials, it is important to understand how their chemical and physical properties direct cell fate. Recently, we introduced visible light crosslinking of tyramine-modified hyaluronan (HA-Tyr) as an alternative to previously established horseradish peroxidase (HRP)/H_2O_2 mediated crosslinking. HA-Tyr provides a broad range of gel mechanics while maintaining bio-functionality (less than 10% HA modification)[1,2]. We hypothesized that given the different crosslinking chemistries and gelation mechanisms, mesenchymal stem cell (MSC) behaviour on these HA-Tyr hydrogels might be differentially modulated.

METHODS: HA-Tyr (6.5% Tyr-substitution) was synthesized as previously described[1]. HA-Tyr films of 7kPa (3.5% w/v) were prepared enzymatic (HRP) (0.68 mM H_2O_2/1 Unit/ml HRP) or singlet-oxygen mediated (EO) (0.02% EosinY, visible light 60 sec), or these gelation mechanisms were combined by sequential crosslinking with 0.34 mM H_2O_2/1 Unit/ml HRP followed by 0.02% EosinY, 20 sec visible light (HRP/EO). These gels were *in-situ* modified with RGD (500µM). Substrates were characterized with proton nuclear magnetic resonance (^{1}H NMR), rheometry and atomic force microscopy (AFM). Juvenile bovine MSCs were plated onto gels (5.000/cm^2), cultured for 4 h and 8 h and then fixed and stained for analysis. For CD44 blocking studies, MSCs were incubated with anti-CD44 before plating. Phalloidin, focal adhesions and YAP (a transcriptional regulator) were visualized by immunofluorescence. Cell area and YAP nuclear localization were quantified using ImageJ[3], and focal adhesions quantified with FAAS[4]. The study was repeated three times and significance determined by ANOVA with Tukey`s post hoc test, $p<0.05$.

RESULTS: ^{1}H NMR analysis showed that low di-tyramine bonds formation was unaffected by the RGD functionalization. Rheometry and AFM demonstrated that both HRP and EO crosslinking mechanisms formed elastic hydrated polymer networks with little stress relaxation. MSC spreading area increased on HRP crosslinked substrates relative to EO matrices (Fig 1). HRP crosslinking led to greater cell focal adhesion length (data not shown) and increased nuclear translocation of YAP compared to EO and HRP/EO gels after 8 h culture (Fig 1).

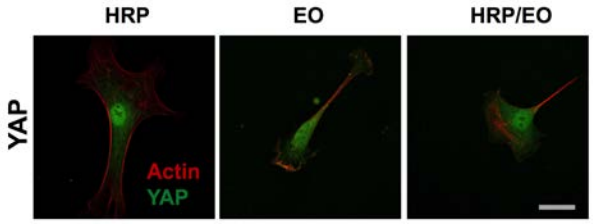

Fig. 1: Actin cytoskeletal organization and YAP nuclear localization of representative MSCs cultured on HRP, EO or HRP/EO crosslinked HA-Tyr hydrogels for 8 h and stained for F-actin (red) and YAP (green), scale bar 25 µm.

DISCUSSION & CONCLUSIONS: The crosslinking chemistry of soft HA-Tyr hydrogels has a substantial impact on MSC behaviour. The presence of EO and visible light did not impair RGD functionality, as confirmed by similar MSC behaviour on HRP/EO crosslinked substrates (Fig 1). CD44 blocking studies suggested that MCS behaviour is mediated by the crosslinking and RGD rather than direct interactions with the HA (data not shown). These findings highlight the importance of considering the crosslinking chemistry of HA hydrogels as an additional cue that may regulate stem cell fate on these engineered cell-instructive materials.

ACKNOWLEDGEMENTS: European Society for Biomaterials (ESB) for the Racquel LeGeros Travel Award (2015, C.L.) and COST Action MP1005 NAMABIO (Grant No.: C11.0126).

Complement activation of artificial liposomes about 100 nm in diameter

S Matviykiv[1], M Buscema[1], S Bugna[1], T Mészáros[2], J Szebeni[2], A Zumbuehl[3], B Müller[1]

[1] *Biomaterials Science Center, Department of Biomedical Engineering, University of Basel, Basel, CH.* [2] *Nanomedicine Research and Education Center, Semmelweis University, Budapest, HU.* [3] *Department of Chemistry, University of Fribourg, Fribourg, CH.*

INTRODUCTION: Cardiovascular diseases are the number one leading cause of mortality in our society underlining the need to ameliorate patient's treatment. One of the therapeutic approaches focuses on nanotherapeutics. Such platform might base on the mechanical activation of liposomes inside blood vessels by shear forces, where the vesicles locally release a vasodilator at the site of a stenosis. The recently discovered mechano-sensitive lentil-shaped liposomes [1] composed of the artificial Pad-PC-Pad (1,3-palmitoylamido- 1,3-deoxy-*sn*-glycero-2-phosphatidyl-choline) belong to such formulations. In order to advance the technology to the bedside, the *in vivo* hypersensitivity towards Pad-PC-Pad has to be tested and compared to the FDA-approved liposomal formulations Doxil [2,3] and AmBisome [4] that are recognized as foreign by the immune system, giving rise to adverse and even lethal effects at certain doses.

METHODS: Pad-PC-Pad was synthetized [1] and liposomes were prepared using the thin-film method [5]. We hydrated the Pad-PC-Pad film with PBS, and extruded at 65 °C through 100 nm membrane polycarbonate filters at a concentration of 20 mg/mL. Dynamic light scattering (DelsaNano C, Beckman Coulter Inc) did not show any liposome aggregation. We tested three human serum samples, labelled F5, F8, F10 using the MicroVue SC5b-9 (Quidel, USA) ELISA kit. After 0, 5, 15, 30 and 45 minutes of incubation, EDTA was added to stop the reaction. Only serum, PBS, and zymosan we incubated for 45 minutes. Each series contained untreated serum and PBS as negative control and zymosan (Sigma-Aldrich, USA) as positive control, respectively. The optical density was measured at a wavelength of 450 nm.

RESULTS: Figure 1 summarizes the results with human sera using ELISA assay. The relative concentration of the SC5b-9 is shown as a percentage of the baseline, calculated as the average of serum only samples. They indicate the same reactivity between three human serum samples. After a lag phase of 30 minutes, Pad-PC-Pad caused a three-fold increase of the complement activation. In contrast to this moderate reaction, zymosan caused an immediate activation more than 90 times higher than the baseline control.

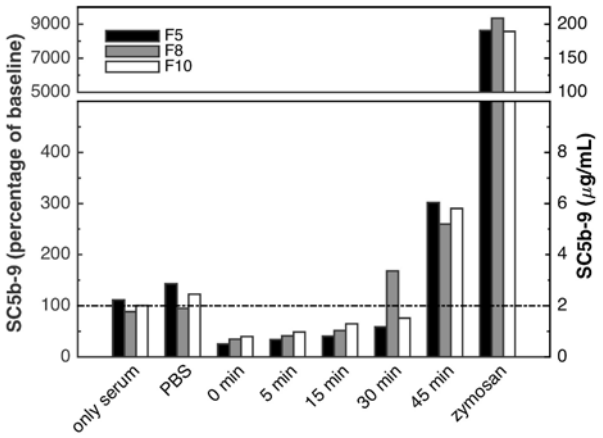

Fig. 1: Surprising lack of complement activation of artificial Pad-PC-Pad liposomes with human sera.

DISCUSSION & CONCLUSIONS: This study explored the *in vitro* complement activation by artificial Pad-PC-Pad phospholipids. Our findings indicate that liposomes do not induce complement activation *in vitro*, unlike the complement activator zymosan that triggered an immediate reaction even at low concentration. Recently, additional studies were conducted [6]. We observed a surprising lack of complement activation both *in vivo* with pigs and *in vitro* with human sera and pig plasma. As a conclusion, Pad-PC-Pad is regarded as a promising phospholipid for future drug delivery applications.

ACKNOWLEDGEMENTS: This work was funded by Swiss National Science Foundation via the program NRP 62 'Smart Materials', and supported by Swiss Government Excellence Scholarships for Foreign Scholars and Artists 2015-2016.

Self- Assembling Peptides a Novel Treatment Strategy to Regenerate Periodontal Ligament

N Meyer[1], F Koch[2], M Hug[3], R Jung[4], S Mathes[1]

[1]*Zurich University of Applied Sciences, ICBC, Tissue Engineering, Wädenswil, Switzerland*
[2]*Institute for Chemistry and Bioanalytics, University of Applied Sciences (FHNW), Switzerland*
[3] *credentis ag, Windisch, Switzerland*
[4]*Clinic of Fixed and Removable Prosthodontics and Dental Material Science, University of Zurich, Zurich, Switzerland*

INTRODUCTION: Periodontal ligament represents a complex tissue structure between the tooth cementum and the alveolar bone. Periodontal ligament is build up by periodontal ligament fibroblasts (PDLF). In periodontal diseases, the ligament is degraded and requires regenerative methods to regenerate the missing tissue.

Enabling the migration of PDLF seems to be the key for a guided regeneration of the periodontal tissue. To achieve this goal a degradable matrix has to be placed into the periodontal gap facilitating the recruitment of precursor cells from the tooth root and surrounding tissue. This matrix requires attachment sites for the cells and has to promote their spreading resulting in de-novo ECM synthesis.

A library of several self-assembling peptides [1](SAP) has been created, which could be transformed from monomeric state to beta sheet structures and fibrils by adjusting pH or salt concentration. This synthetic 3D network is able to serve as the required extracellular matrix (ECM).

METHODS: Cell adhesion, cell morphology and cell proliferation were evaluated to nominate potential SAP´s. Cell proliferation was assessed with human calvarial osteoblasts (HCO) incubated with SAP (15 mg/ml) versus Collagen-Gel (1.5 mg/ml) as positive control. Cell proliferation was measured by the metabolic conversion of PrestoBlue. A newly developed *in vitro* model of a periodontal pocket was used to assess the migration distance of PDLF cells out of the donor compartment.

RESULTS: Currently, two potential SAP candidates leading to stretched actin stress fibres in terms of cell phenotype after adhesion of human primary PDLFs. Cell proliferate up to 14 days with a comparable proliferation rate versus cells cultivated on collagen type 1(control). A migration distance up to 3 mm has been measured with the periodontal pocket model after 7 days cultivation of hPDLF on potential SAP´s.

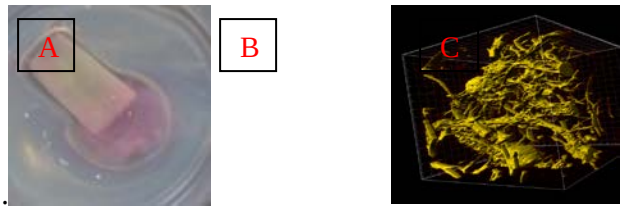

Fig. 1: A) Developed in vitro model of periodontal pocket includes dentin and collagen as a host of PDLF. (B) Measurement of migration distance from donor compartment on SAP coated dentin surfaces (C) Morphology of vital cells by Actin staining.

DISCUSSION & CONCLUSIONS: As periodontitis treatment has emerged to a very important issue the need for uncomplicated and straight forward therapies is obvious. It could be demonstrated that in consideration of the specific characteristics of the natural microenvironment SAP's provide a possible scaffold where cells are able to attach, spread and proliferate into newly tissue. Therefore P11 peptides could be used as a new treatment strategy in periodontal therapy. Within the study we were able to establish an *in vitro* model of the periodontal ligament and first results supported the proof of concept of this approach. Further investigations and subsequent integration of newly developed materials are ongoing and will allow deeper insight in periodontal tissue regeneration.

ACKNOWLEDGEMENTS: We gratefully thank the CTI for project funding.

Development and characterisation of a new bio-ink for 3D bone layer printing as basis for a multilayered osteochondral construct

M Molnar[1], M Müller[1], M Zenobi-Wong[1]

[1] *Cartilage Engineering +Regeneration, ETH Zürich, Zürich, Switzerland*

INTRODUCTION: Current tissue engineering strategies for osteochondral (OC) defects have not yet reproduced characteristics of the native OC interface regarding zonal organization, extracellular matrix (ECM) composition and mechanical properties [l,2]. Here we use 3D bioprinting to assemble a multilayered OC construct (Fig. 1). We developed a cell-free and photocrosslinkable bio-ink consisting of gellan gum methacrylate (GGMA), hyaluronic acid methacrylate (HAMA) and hydroxyapatite (HAP) for printing of the underlying bone layer. The ink aims for osseointegration with the bone and to provide photocrosslinkable moieties to interface the osteolayer to subsequent methacrylated chondral layers. A new synthesis protocol using a biological buffer for gellan gum (GG) methacrylation with glycidyl methacrylate (GMA) was established to facilitate upscaling and reproducibility of GGMA synthesis compared to standard approach where only small quantities of GGMA could be synthesized in a single batch. Further, bio-ink composition and processing was optimized to improve the printability of the ink.

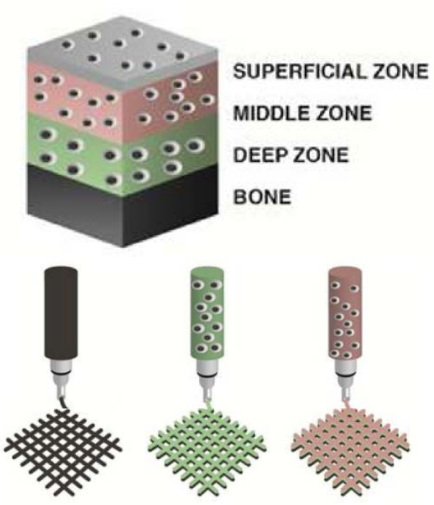

Fig. 1: Layer-by-layer assembly of 3D printed osteochondral construct to mimic native tissue

METHODS: NMR was used to assess the degree of methacrylation of GGMA and HAMA. GGMA was compared with a commercial product (mimsys® G, Irisbioscience) [3] and GGMA synthesized via standard approach. Molar excess of GMA was adjusted to achieve 2% methacrylation of GG. The modified GG was then lyophilized, together with HAMA cryomilled and finally mixed with HAP and water in a planetary centrifugal mixer to obtain a homogenous bio-ink. Rheological measurements enabled comparisons between inks containing GGMA synthesized with the standard and the buffer based synthesis, different HAP contents (15, 20, 25, 30 %) as well as adaptions of processing parameters. Mechanical properties after photocrosslinking of the inks were also investigated.

RESULTS: Synthesis of GGMA utilizing a buffer led to high reproducibility of the desired methacrylation (2 ± 0.4 %). Rheological measurements showed shear-thinning behaviour and a slightly decreased viscosity of the inks when compared with inks containing GGMA synthesized without utilizing a buffer. Viscosity could be controlled by adjusting HAP content or process parameters such as cryomilling of the HAP. We also found the UV-crosslinking of the inks to be fast with final storage moduli in the range of 24 to166 kPa.

DISCUSSION & CONCLUSIONS: GGMA synthesis utilizing a buffer increased production volumes while maintaining a high reproducibility of the degree of methacrylation. Decreased viscosities of inks with the new GGMA synthesis allowed an increase of the HAP content, which could result in better osseointegration. Extrusion force measurements and in-vitro studies on stem cell adhesion and differentiation will be performed in the future to further optimize printability and assess the osteogenic potential of the ink to proceed towards in-vivo models and clinical application.

R

Decellularized cartilage particles and their regenerative potential in combination with an in-situ crosslinkable hydrogel for cartilage repair

A Muhlenbroich[1], E Cavalli[1], N Broguière[1], LA Laurent-Applegate[2], M Zenobi-Wong[1]

[1]*Cartilage Engineering & Regeneration, ETH Zurich, Zurich, CH.* [2] *Department of Musculoskeletal Medicine, University Hospital of Lausanne, Lausanne, CH*

INTRODUCTION: In this study we present a scaffold with bioactive potential for cartilage repair consisting of an enzymatically crosslinkable modified hyaluronic acid (HA) hydrogel and decellularized cartilage particles (DCC). Particles decellularized with a lab own protocol and commercial BioCartilage® particles were loaded with a chondrogenic growth factor and mixed with HA to form stable, injectable, in-situ crosslinkable hydrogels (HA-DCC). When seeded with human epiphyseal chondroprogenitor cells (ECPs), gels stimulated cell proliferation and synthesis of cartilaginous matrix to a higher degree compared to HA-gels without particles when cultured in presence of a growth factor.

METHODS: Bovine articular cartilage was harvested from condyles of calves, croymilled and decellularized with a with a two-step protocol. DCC particles and BioCartilage® were loaded with transforming growth factor beta-3 (TGFβ-3) and were mixed with a 1% (w/v) HA-TG hydrogel together with 15 Mio/ml ECPs. HA-TG is a novel injectable hydrogel made of lysine- and glutamine-modified hyaluronic acid. Factor XIII was added and after activation with thrombin and Ca^{2+} crosslinking was initiated. The gels were cultured in media either with or without TGFβ-3 for 3 weeks for biochemical assays, histological analysis and mechanical testing. Culturing media was analysed with ELISA to determine TGF release.

RESULTS: After culturing, HA+DCC exhibited a significantly higher elastic modulus measured in compression tests than HA gels without particles. The gels increased respectively from 1.04 and 1.61 kPa to 126 and 45 kPa (*Fig.1)*. This was probably due to matrix deposition.

Cell proliferation was investigated by a Picogreen assay. All HA+DCC gels showed up to 5-fold increases of DNA after 3 weeks, whereas gels without particles showed up to a 3-fold increase in DNA.

Histological analysis confirmed deposition of GAGs and collagen II for gels cultured in presence of TGF (media or loaded DCC). No difference was visible between bovine DCC particles and BioCartilage®.

Table 1. Compared groups

	Media	Particles
HA	+TGF	No
HA+DCC	+TGF	normal
HA+DCC^{neg}	No TGF	normal
HA+DCC^{TGF}	No TGF	Loaded with TGF

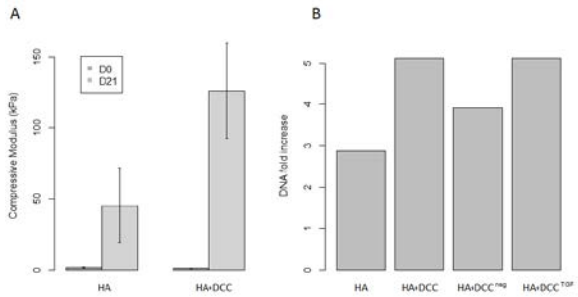

Fig. 1: A) Elastic modulus of HA gels with and w/o DCC at day 0 and 21. B) DNA fold increase after 3 weeks in gels with and w/o DCC.

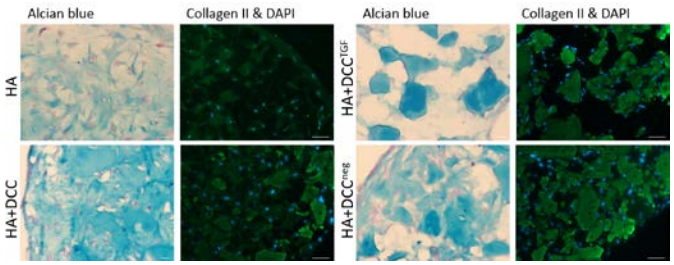

Fig. 2: Histology of matrix components after 3 weeks of culture. Scale bars: 20 µm for alcian blue, 50 µm for collagen II.

DISCUSSION & CONCLUSIONS: DCC particles exhibit a bioactive potential on cells in a hydrogel scaffold. HA is a widely used hydrogel and BioCartilage® a FDA approved clinical product. Combination of both yields an injectable gel presenting a promising alternative to current cartilage defect treatment methods.

ACKNOWLEDGEMENTS: This project was funded by the ETH Foundation (Grant ETH-50 13-1).

Hydrogel-based cell traps for capturing MPCs participating in bone healing and regeneration

P Papageorgiou[1], PS Lienemann[1], S Metzger[1], M Ehrbar[1]

[1]*Laboratory for Cell and Tissue Engineering, Department of Obstetrics, Zurich, Switzerland*

INTRODUCTION: Permanent failure or not proper healing, referred as nonunion, is observed in up to 13% of all tibia fractures. The pathophysiology for nonunions is numerous and includes the insufficient stabilization of fractures, avascular necrosis, infections, osteoporosis, or co-morbidities. While autologous bone grafting is currently the gold standard, bone harvesting requires an additional surgical procedure, with well documented complications. Moreover, the quantity of bone that can be harvested is clearly limited. Alternatively, bone morphogenetic protein (BMP) in combination with materials and cells has been used for the treatment of fractures. However, for such treatments high doses of BMP-2 are required, associated with side effects such as ectopic bone formation and stimulation of cancer cells. Therefore, extensive efforts have been made to develop novel bone-graft substitutes, which consist of natural or synthetic biomaterial scaffolds that more efficiently promote bone regeneration.

Synthetic polymers such as poly (ethylene glycol) PEG provide a blank slate which can be engineered with reproducible properties. Our laboratory has previously described modular designed by transglutaminase factor XIIIa (FXIII)-cross-linked poly (ethylene glycol) PEG-based biomimetic hydrogel which are tailorable in terms of stiffness, proteolytic stability, and presentation of cell adhesion ligands and growth factors [1,2]. Such hydrogels are potent 3D platforms to investigate multiple cellular processes such as proliferation, migration and differentiation under fully controlled ECM-free conditions.

METHODS: Pre-casted PEG-hydrogels were implanted in murine critical-sized (5 mm) calvarial defects for 8 days. Hydrogel infiltrated cells were harvested by collagenase digestion and nucleated cells of non-hematopoietic and non-endothelial lineages were sorted based on the expression of Sca1 and Alcam, as suggested by Nakamura et al. [3].

RESULTS: We report on a PEG-hydrogel based approach to entrap and prospectively isolate Sca1+MPCs from murine healing bone defects. We show that $Sca1^+$MPCs are enriched in the defect area, suggesting their recruitment and/or expansion in a healing environment. Assessment of CFU-F confirms that cells with clonogenic potential are restricted to the prospectively isolated $Sca1^+$ MPC subpopulation. Consistent with the in vitro criteria for MPCs, these cells demonstrated the ability to differentiate into osteoblasts, adipocytes and chondrocytes when cultured under standard specific in vitro differentiation conditions. To determine their *in vivo* differentiation potential, healing-associated MPCs prospectively isolated from transgenic GFP-mice were encapsulated in new PEG-hydrogels implanted for 12 weeks in calvarial defects of wild-type mice. We show that the distribution of the transplanted GFP^+-$Sca1^+$MPCs leads to bone augmentation, with bone nodules formation, whereas the transplanted GFP^+-$Alcam^-$/$Sca1^-$ failed to differentiate, though still present within the defected area.

DISCUSSION & CONCLUSIONS: Together these data indicate that PEG-hydrogel based cell traps can be employed to prospectively isolate MPCs that promote bone augmentation and can be used to further study bone regeneration and formation *in vitro* and *in vivo*.

ACKNOWLEDGEMENTS: This research has received funding from the People Programme (Marie Curie Actions) of the European Union's Seventh Framework Programme FP7/2007-2013/ under REA grant agreement No. 607868 (iTERM).

Development of human tissue engineered cartilaginous grafts in a 3D-model mimicking osteoarthritic conditions *in vivo*

K Pelttari[1], M Mumme[2], A Barbero[1], I Martin[1]

[1] *Department of Biomedicine, University Hospital Basel, University of Basel, Switzerland*
[2] *Clinic for Traumatologic Surgery, University Hospital Basel, Switzerland*

INTRODUCTION: In search for possible treatments of osteoarthritic (OA) cartilage defects, several promising cell-/tissue engineering-based approaches are under investigation[1]. But testing their functional relevance in pre-clinical settings remains challenging - foremost as successful repair strongly relies on interaction of the implanted cells/grafts with the OA-environment. Specifically osteoblasts (OB) of an OA joint were shown to undergo molecular changes altering the interplay between cartilage and subchondral bone, which is believed to play a fundamental role in the onset and development of OA. So far, the interaction between chondrogenic cells and OA-OB has mainly been studied in in vitro co-culture systems enabling to investigate only intercellular communication via soluble factors.

The aim of our study was to investigate the potential of a tissue engineered cartilaginous graft (TEC) generated by human articular chondrocytes to mature and integrate on an OA-like bone compartment in a more physiological setup. Therefore, a culture model consisting of a TEC applied on the top of a bone-component containing OA-OB was developed and its evolution investigated in an in vivo ectopic environment

METHODS: Expanded human articular chondrocytes were labelled with GFP and cultured on Chondro-Gide membranes (Geistlich Pharma AG, 6 mm diameter) for 4 days in medium containing TGF-beta to generate TEC. OB were obtained by outgrowth culture from bone chips harvested from tibial plateaus of patients with OA. OA-OB were seeded on cylindrical ceramic scaffolds (Engipore, 6 mm diameter, 4 mm high) and cultured in osteogenic medium for 4 days. TEC were then combined with the bone-cylinders either with (TEC/OB) or without OB (TEC/-) using fibrin glue (Baxter) prior subcutaneous implantation in nude mice for 4 and 8 weeks. Explanted tissues and corresponding in vitro controls were analyzed (immuno-) histologically to assess the maturation capacity of the TEC and its integrative potential under OA-simulating conditions.

RESULTS: At the time of implantation the TEC did not contain appreciable amounts of glycosaminoglycans (GAG). After 4 weeks, explants and in vitro control tissues consisted of fibro-cartilaginous tissues faintly stained for GAG, but stably integrated to the bone component irrespective of the presence of OB. GFP-positive chondrocytes were identified in pores of the bone compartment suggesting their participation to enable cartilage-bone integration. After 8 weeks in vivo, TEC/OB grafts contained a more mature cartilage layer intensely stained for GAG and a subchondral layer with dense extracellular matrix expressing nuclear pannexin and C-tail connexin (Cx43) and limited amounts of infiltrated inflammatory murine cells. Contrarily, TEC/- were massively infiltrated by inflammatory cells both in the bone and in the cartilage layer that did not express GAG.

DISCUSSION & CONCLUSIONS: We demonstrated that TEC can mature and become functionally integrated with a ceramic bone compartment only in case OB - even if obtained from OA joints - were present. Future investigations will be required to identify the mechanisms by which OB can mediate this evolution.

ACKNOWLEDGEMENTS: Funded by SNSF No. 310030_149614, SNSF PMPDP3_151396/1

Hydrogels made from cartilage-mimetic sulfated alginate polymers via di-tyramine bond formation show increased stability and adhesion to cartilage

T Stauber[1], E Öztürk[1], C Loebel[2], D Eglin[2], M Zenobi-Wong[1]

[1] Cartilage Engineering + Regeneration, ETH Zurich, CH. [2] AO Research Institute, AO Foundation, Davos, CH.

INTRODUCTION: Autologous chondrocyte implantation (ACI) is a promising cell-based strategy for cartilage repair, but requires a high cell number and thus 2D expansion. Unfortunately, this leads to de-differentiation along with loss of chondrogenic phenotype. Recently, sulfated alginate hydrogels have been shown to increase proliferation of chondrocytes in 3D as well as preventing their de-differentiation by promoting FGF signalling[1]. However, the reversibility of the ionic crosslinking and the non-adhesiveness of alginate should be addressed for clinical translation of sulfated alginate in cartilage repair. Here, we modified alginate sulfate with tyramine groups to enable enzymatic crosslinking of the material as well as adhesion to the cartilage tissue.

METHODS: Alginate (Alg) and alginate sulfate (AlgS) with low and high sulfation degrees (AlgS low: 0.17, AlgS high: 0.59 sulfates/monomer) were used. The polymers were modified with tyramine groups using 4-(4,6-Dimethoxy-1,3,5-triazin-2-yl)-4-methyl morpholinium chloride (DMTMM) as previously reported[2]. Aliquots were taken after 24h and 72h and molar degree of substitution (DSmol) was determined with UV-vis and ^{1}H NMR spectroscopy. For the crosslinking, polymers were mixed with tyrosinase (20 kU/ml). To test the bond strengths between the hydrogel and native cartilage, gels were made in cartilage explant rings and push-out tests were performed. Then, bovine chondrocytes were encapsulated in the sulfated and tyraminated alginate gels (ASTA) and viability was assessed after one week.

RESULTS: Tyramination of alginate and alginate sulfate was successful and the DSmol was found to depend on the duration of synthesis and correlate with the sulfation degree of the alginates (Fig.1).

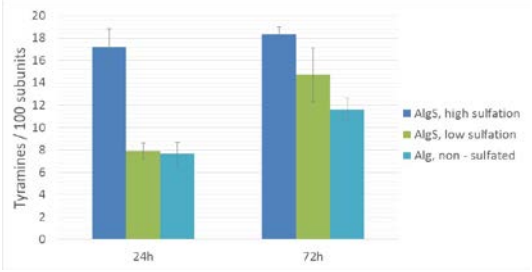

Figure 1: Molar degree of tyramine substitution in different reaction conditions

In the push-out test, the tyramine modified and enzymatically crosslinked hydrogels showed stronger binding to native cartilage compared to ionically crosslinked alginate sulfate gels (Fig. 2).

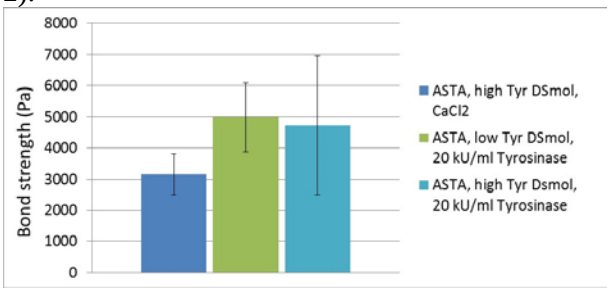

Figure 2: Bond strength of enzymatically / ionically crosslinked alginate sulfate gels to native cartilage

The bovine chondrocytes encapsulated in ASTA hydrogels showed good viability after one week and the gels did not show any sign of degradation or instability in culture.

DISCUSSION & CONCLUSIONS: Here we demonstrate the modification of alginate and alginate sulfate with tyramine groups with tunable degree of substitution. Furthermore, we show that the tyramine-modified polymers could crosslink with tyrosinase to yield mechanically stable hydrogels with adhesion to native cartilage rings. ASTA hydrogels exhibit good biocompatibility with high viability of encapsulated chondrocytes. On-going studies investigate the chondrogenic re-differentiation and proliferation of human chondrocytes within ASTA hydrogels. Future studies will explore the stability of ASTA hydrogels and cartilage matrix formation *in vivo* with subcutaneous implantation in mice.

ACKNOWLEDGEMENTS: This project was funded by SNF (315230_159783).

Diamond-like carbon layers enriched with chromium as a potential biomaterial for osteogenic differentiation of human mesenchymal stem cells

M Travnickova[1], E Filova[1], L Bacakova[1], M Jelinek[2], J Zemek[2], J Houdkova[2], J Remsa[2]

[1]*Department of Biomaterials and Tissue Engineering, Institute of Physiology of the Czech Academy of Sciences, Prague, Czech Republic.* [2]*Department of Optical and Biophysical Systems, Institute of Physics of the Czech Academy of Sciences, Prague, Czech Republic.*

INTRODUCTION: In recent times, diamond-like carbon (DLC) layers seem to be promising coatings of implants for bone tissue engineering. There are many modifications of DLC films that are widely studied. Some chromium-doped DLC layers were observed to reduce internal stress, and improve stability of the superficial layers [1]. Human mesenchymal stem cells (hMSCs) are known to have a potential to differentiate into bone tissue.

METHODS: The samples of DLC layers doped with chromium were prepared; the content of Cr was as follows: 0, 1, 2, 4, and 12 at%, referred as 92, 93, 94, 95, 96, respectively. As control materials, glass coverslip (Glass) and tissue culture polystyrene (PS) were used. Prior cell seeding, the samples were sterilized in 70% ethanol**.** The hMSCs were seeded in a density of 5000 cells/cm^2 and cultivated in α-MEM medium with 15% fetal bovine serum. Glycerolphosphate, dexamethasone, and ascorbic acid were added on day 3 after seeding. The osteogenic medium was replaced three times a week. The metabolic activity of the cells was measured by resazurin assay on day 1, 3, 7, and 14 after seeding. The cell spreading area was measured from microphotographs of the cells immunostained for vinculin using Atlas Tescan software on day 1 after seeding. On days 7 and 14, the cells were fixed by 4% paraformaldehyde and immunocytochemically stained for markers of osteogenic differentiation, i.e. type I collagen and osteocalcin. The fluorescence intensity was measured from 5 microphotographs of each sample using Fluorescent Image Analyser software.

RESULTS: Cell spreading area was similar on all samples on day 1 after seeding. However, vinculin-containing focal adhesions plaques were best observable on samples 95 and 96. The metabolic activity of the cells, measured by resazurin, increased in time course of the culture as the cells were proliferating. On day 1 and 3, high cell metabolic activity was found on 92, Glass and PS samples. On day 7 and 14, high metabolic activity was measured mainly on samples 96 (day 7), or 95 (day 14) compared to Glass and PS. The fluorescence intensity of early osteogenic marker type I collagen, measured on day 7, was highest on sample 96, and on sample 93 on day 14. The fluorescence intensity of late osteogenic marker osteocalcin was highest on PS on day 7 and on sample 93 on day 14. Between days 7 and 14, an increase in fluorescence intensity of both osteocalcin and type I collagen on every sample was observed.

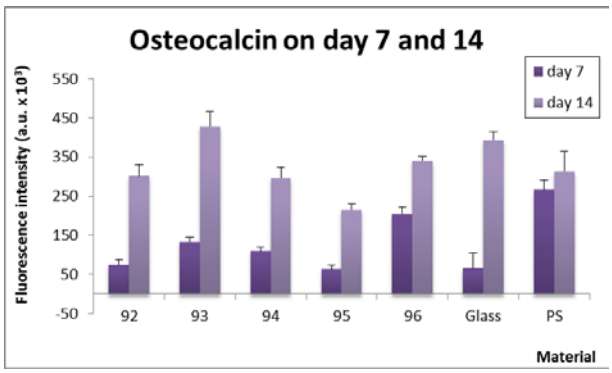

Fig. 1: The fluorescence intensity of osteocalcin in hMSC cultured on samples 92, 93, 94, 95, 96, Glass, and PS on day 7 and 14

DISCUSSION & CONCLUSIONS: We proved that the hMSCs adhered, proliferated and differentiated into osteoblasts on Cr-doped DLC layers as well as on control glass and PS samples. The cell proliferation was higher on all Cr-doped DLC layers than on control samples. The samples 93 and 96 seem to be the most suitable for osteogenic differentiation from all tested Cr-doped DLC samples.

ACKNOWLEDGEMENTS: Supported by the Grant Agency of the Czech Republic, grant No. P108/12/G108 and No. 15-05864S, BIOCEV – "Biotechnology and Biomedicine Centre of the Academy of Sciences and Charles University" project (CZ.1.05/1.1.00/02.0109), funded by the European Regional Development Fund, and the National Programme for Sustainability II (grant LQ 1604).

Cell-laden electrospun hybrid membrane to mimic native blood barrier

L Weidenbacher[1,2], A Mertgen[1,2], A Abrishamkar[1,3], M Rottmar[1], K Maniura-Weber[1], RM Rossi[1], G Fortunato[1]

[1]*Empa, Swiss Federal Laboratories for Materials Science and Technology, St. Gallen, CH*
[2]*ETH Zurich, Department of Health Science and Technology, Zurich, CH*
[3]*ETH Zurich, Department of Chemistry and Applied Biosciences Zurich, CH*

INTRODUCTION: Formation of blood clots on the inner surface of ventricular assist devices can cause fatal complications for patients. In nature, the endothelium intimately regulates a range of physiological vascular functions including the prevention of thrombosis. The aim of this project is to develop a non-thrombotic hyperelastic membrane for blood propulsion devices inspired by nature's design of the blood vessel structure. For this, we are developing cytocompatible fibrous polymer networks incorporating smooth muscle cells (SMC) and endothelial cells (EC) on top to mimic the native blood-tissue interface. Furthermore, novel concepts to enable targeted and stable long-term adhesion of these two cell types to the polymer network are developed in the frame of this biomimetic approach.

METHODS: 3D networks made of polymeric fibers and smooth muscle cells are created by a simultaneous process of electrospinning and cell spraying. Polymers such as poly(vinylidene fluoride-co-hexafluoropropylene) and Poly ethylene-co-vinyl alcohol were chosen for this approach due to their reported blood compatibility and mechanical properties. C2C12 murine skeletal myoblasts were electro-sprayed with selected voltages followed by incubation in differentiation medium.The influence of cell spraying on viability as well as on the cellular phenotype was investigated via Live/Dead assays and immunohistochemical stainings. To protect the cells from the solvents used for electrospinning, they were encapsulated in gelatin employing a droplet-based microfluidic setting.

RESULTS: Live/Dead staining as well as microscopic analysis indicate that there is no negative effect on viability as well as the expression of the characteristic phenotype of C2C12 cells. Formation of myotubes could be observed after cell spraying with different voltages up to 15 kV (Fig. 1). Gelatin encapsulation of fluorescently labelled C2C12 cells resulted in the formation of homogeneous cell-capsules with most of the gelatin capsules carrying at least one cell (Fig. 2). Adjusting the channel size and the flow parameters on the microfluidic chip, the size of the capsules could be controlled ranging from ~50-150µm. Importantly, cell encapsulation had no negative effect on viability.

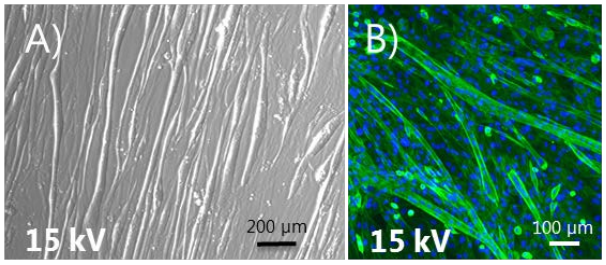

Fig. 1: C2C12 cells after the cell spraying process imaged by A) bright-field microscopy and B) confocal microscopy after staining for actin (green) and nuclei (blue).

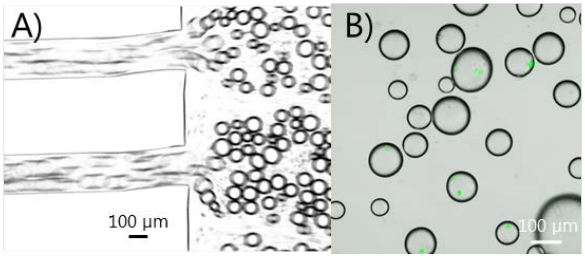

Fig. 2: Cell-laden gelatin capsules A) produced by microfluidics and B) imaged by confocal microscopy. Cells are shown in green.

DISCUSSION & CONCLUSIONS: The results of the cell electro-spraying experiments as well as the cell encapsulation show great potential to combine cells with tailored polymeric structures. Complex 3D structures with SMCs homogenously distributed in the polymer network and ECs covering the top surface are the envisioned goal of this approach. To optimize and guide cell adhesion, we will study the feasibility of binding cell specific adhesion molecules to the network. For spatial targeted adhesion we will create gradients of these molecules covalently immobilized throughout the membrane.

ACKNOWLEDGEMENTS: This work is part of the Zurich Heart project of Hochschulmedizin Zürich.

Oxidative passivation of Ti for dental implants characterized by ec-pen

FM Weiss[1], F Schmidli[2], M Jungo[1], B Müller[1]

[1] *Biomaterials Science Center, University of Basel, Switzerland;* [2] *School of Dental Medicine, University of Basel, Switzerland*

INTRODUCTION: Titanium and its alloys are ubiquitous and indispensable for medical implants. Due to their protective native or man-made oxide layer they are usually inert to corrosion. Once the oxide layer is damaged the titanium itself is prone to corrosion. Corroding Ti implants may induce inflammatory reactions and negatively influence their functionality. Thus, it is a major concern to understand under which circumstances the oxide film is formed or dissolved. A method for such an analysis is an electrochemistry technique termed electrochemical impedance spectroscopy (EIS). Here, a special ESI setup is applied termed ec-pen. This setup is designed to measure corrosion *in vivo* as well as *ex vivo*, cp. Fig 1. It has been used in dentistry for more than ten years. In this presentation, the impact of milieu on changes of the passivation layer is addressed.

METHODS: Containing a working electrode (WE) and a reference electrode (RE) both immersed into the electrolyte (lactic acid 10.01 g/L – sodium chloride 5.8 g/L in distilled H_2O), enclosed in a reservoir, the ec-pen is a compact mean for electrochemical impedance studies. For measurements the pen's tip and a counter electrode (CE) are pressed against the Ti specimen, here Ti, grade 4. The samples were exposed to either ambient conditions, Ringer solution (B. Braun Melsungen AG, Germany) or artificial saliva (citric acid 47.6 M, Na citrate 47.6 M, NaCl 42,8 M, KSCN 2.6 M) for increasing time intervals before measurement. More detailed description of the experimental setup and functionality has been discussed previously [1-4].

RESULTS: A simple parallel RC circuit served as model for data analysis. The evaluated data show that the titanium oxidation is favoured in artificial saliva and Ringer solution compared to ambient atmosphere. The times obtained for half maximum values of the phase shift using the Michaelis-Menten fit are (54.5 ± 4.1) s for artificial saliva, (51.6 ± 3.3) s for Ringer solution and (280 ± 40) s for ambient atmosphere. The maximum values of the phase shift corresponds to (73.6 ± 1.6), (76.6 ± 1.0), and (68.3 ± 3.9) degrees, respectively, indicating significant variations in the thickness of passivation layers formed.

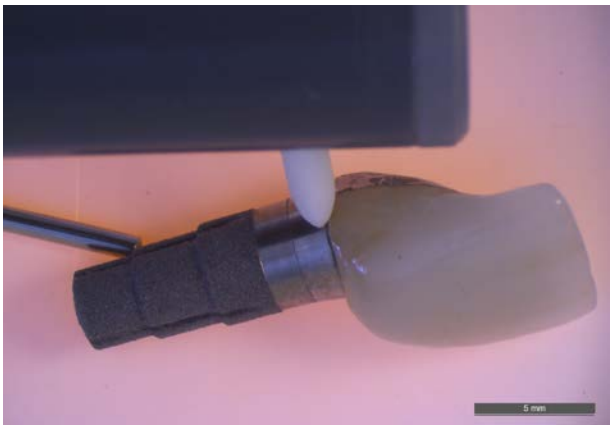

Fig. 1: The ex vivo measurement of a Ti implant with a ceramic crown attached using the ec-pen.

Table 1. The results depend on contact area and location [5].

	Impedance [Ω cm^2]	Phase [degree]
Tip 90° rel. to surface	354 ± 119	50 ± 6
Tip 45° rel. to surface	206 ± 65	48 ± 10

DISCUSSION & CONCLUSIONS: The results demonstrate that the oxidative passivation of Ti is massively influenced by the milieu present in oral cavity. The error bars are derived from the ec-pen's sensitivity taking into account the contact area issues and the dimensions of the meniscus of the electrolyte [5]. Thus, the obtained data have to be further evaluated. The limitation of the present study relates to restrictions on three milieus. Currently, a study with a broader scope to reveal the passivation mechanisms in detail is in planning stage.

Improvement of the porcine *ex vivo* model for adrenergic and muscarinic signalling in smooth muscle

S. Bachmann[1], C Betschart[2], AP Simões-Wüst[1]

[1] *Department of Obstetrics, University Hospital Zurich.* [2] *Department of Gynaecology, University Hospital Zurich.*

INTRODUCTION: The ability to perform functional contractions in response to physiological stimuli is crucial for engineered smooth muscle[1]. Here we present an experimental set-up to measure smooth muscle contractility that is easy to handle and requires only minimal amounts of material. The aim is to test inhibitory effects of adrenergic and muscarinic substances on depolarisation-induced contractions in an *ex vivo* porcine model.

METHODS: Porcine bladders were obtained from the local slaughterhouse. Muscle strips (ca. 3 x 5 mm^2) were taken from the bladder body, freed from the adjacent epithelium and fixed in the chamber. Vehicle controls (DMSO, water) were included in all experiments.

1) Depolarisation-induced contractions were achieved by incubating the strips with 124 mM KCl. Effects of treatment with isoprenaline, a non-specific beta agonist (1 microM; n=10) and BRL37344, a beta3 agonist (1 microM; n=5) on a subsequent contraction were investigated. To characterise inhibitory effects on depolarisation-induced contractions, strips were treated sequentially as follows: twice with KCl to induce contractions, once with the test substance (treatment) and again with KCl. Data of the third contraction were compared with the average of the two first ones (100%).

2) Contractions induced by muscarinic-stimulation were triggered by adding bethanechol up to 10 mM. Effects of treatment with oxybutynin, a muscarinic antagonist (0.1 microM; n=3), on a subsequent contraction were investigated. To investigate effects on the contractions induced by bethanechol-stimulation, different strips were treated either with oxybutynin or with the corresponding vehicle, and thereafter stimulated with bethanechol. In each experiment, the contraction induced after treatment with vehicle was taken as 100%.

In an attempt to reduce the inter-strip variability, bethanechol-induced contractions were compared with additional KCl-contractions.

RESULTS: 1) In the depolarization experiments, vehicle controls revealed moderate but highly reproducible force increases (typically up to 120% of initial). In all cases, KCl-induced contractions were highly reversible. Both beta agonists led to a statistically significant decrease in contraction force relatively to vehicle treated trips (isoprenaline and BRL37344 down to 76% and to 94% of initial, respectively).

2) Bethanechol-stimulation could be prevented by treatment with oxybutynin (down to 34% of the value obtained in control strips). This type of this experimental design was however associated with low reproducibility and throughput. Further results revealed a direct proportionality between the strength of bethanechol versus KCl-induced contractions (factor: 2).

DISCUSSION & CONCLUSIONS: Our data confirm previous work showing that bladder smooth muscle small strips react *in vitro* to depolarisation and to muscarinic stimulation as well as to adrenergic-induced relaxation. Standardising the data on muscarinic stimulation relatively to a previous depolarisation-induced contraction should lead to higher reproducibility.

A comparable model should be adequate to test the contractility of engineered smooth muscle strips. In an initial step, part of the *ex vivo* material might be partially replaced by engineered smooth muscle tissue.

ACKNOWLEDGEMENTS: Ms. A. Dolder is gratefully acknowledged for excellent technical assistance.

An in-situ crosslinkable, adhesive scaffold for cartilage repair: *in vitro* and *in vivo* characterization

E Cavalli[1], N Broguiere[1], LA Applegate[2], M Zenobi-Wong[1]

[1]*Cartilage Engineering + Regeneration, ETH Zürich, Zürich, Switzerland,* [2]*Department of Musculoskeletal Medicine, University Hospital of Lausanne, Switzerland*

INTRODUCTION: In this study we present a novel biomimetic hydrogel for cartilage repair. It is based on a modified hyaluronic acid (HA-TG) that can be crosslinked with the activated transglutaminase (TG) factor XIII. The hydrogel is injectable with a crosslinking time of less than 2 minutes and strongly adheres to cartilage tissue. When seeded with human epiphyseal chondroprogenitor cells (ECPs), this hydrogel is able to promote cell proliferation and cartilaginous matrix deposition. HA-TG demonstrated to be stable and to support cell maturation in vivo in a subcutaneous model.

METHODS: Lysine-modified hyaluronic acid (HA-lys) and glutamine-modified hyaluronic acid (HA-glu) were synthetized according to a recently developed protocol and mixed with 15 mio/ml ECPs. Gels were investigated both alone and in a bovine ex-vivo explant model. The scaffolds were cultured for 3 weeks in chondrogenic media and then implanted subcutaneously in nude mice. Gene expression and mechanical testing were evaluated at the beginning of the culture and after 3 weeks of in vitro culture, while histological analysis and push-out testing were conducted at the time of implantation and after additional 6 weeks.

RESULTS: After 3 weeks of culturing, the cells in the hydrogels expressed up to 100,000 fold increase in collagen type 2 and up to 10 fold aggrecan expression compared to cells in 2D (*Figure 1*). This resulted in a dramatic increase in mechanical properties in the softer gels: from the initial 2, 6 and 9 kPa to 250, 25 and 10 kPa (1, 2 and 3% HA-XIII gels respectively) at 3 weeks.
Adhesive properties of the gels were investigated by push-out test and showed initial bond strength 4 times higher than fibrin glue. After 3 weeks of culture of the hydrogel/ECPS within bovine cartilage explants, the bond strength increased to 6 kPa likely due to matrix production and remodelling. HA-TG gels were stable for 6 weeks in vivo, prevented vascular ingrowth and supported the construct maturation reaching 160 kPa in bond strength (*Figure 2*).

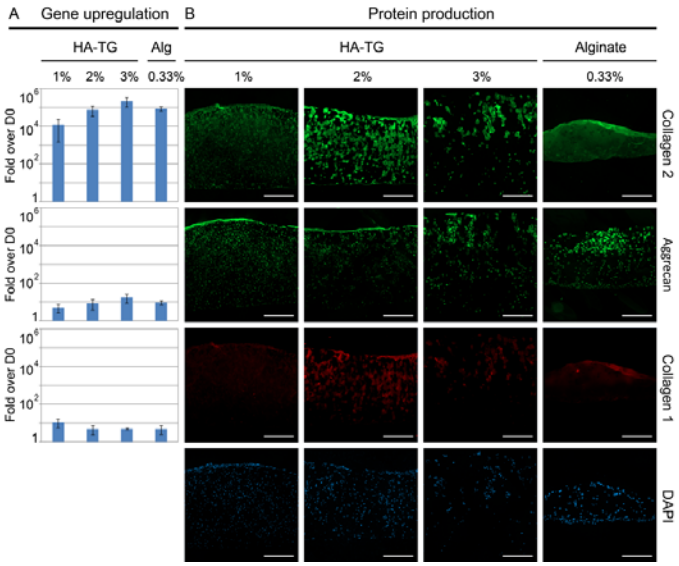

Figure 1: Gene expression (A) and protein production (B) of HA-TG gels after 3 week of in vitro culture. Scale bar: 500µm.

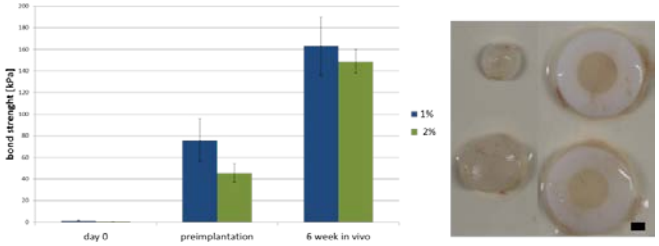

Figure 2: Bond strength of HA-TG gels to bovine cartilage explants after crosslinking, after 3 weeks of in vitro clture and after 6 more weeks in vivo. Macroscopic images of 1% (top row) and 2% (bottom row) gels after 6 weeks in vivo. Scale bar: 2mm.

DISCUSSION & CONCLUSIONS: Due to its adhesive properties, injectable potential and in vivo stability, this novel scaffold represents a promising alternative to the current cartilage repair techniques.

ACKNOWLEDGEMENTS: This project was funded by the ETH Foundation (Grant ETH-50 13-1).